



A search for top-squark pair production, in final states containing a top quark, a charm quark and missing transverse momentum, using the 139 fb^{-1} of pp collision data collected by the ATLAS detector

The ATLAS Collaboration

This paper presents a search for top-squark pair production in final states with a top quark, a charm quark and missing transverse momentum. The data were collected with the ATLAS detector during LHC Run 2 and correspond to an integrated luminosity of 139 fb^{-1} of proton–proton collisions at a centre-of-mass energy of $\sqrt{s} = 13 \text{ TeV}$. The analysis is motivated by an extended Minimal Supersymmetric Standard Model featuring a non-minimal flavour violation in the second- and third-generation squark sector. The top squark in this model has two possible decay modes, either $\tilde{t}_1 \rightarrow c\tilde{\chi}_1^0$ or $\tilde{t}_1 \rightarrow t\tilde{\chi}_1^0$, where the $\tilde{\chi}_1^0$ is undetected. The analysis is optimised assuming that both of the decay modes are equally probable, leading to the most likely final state of $tc + E_T^{\text{miss}}$. Good agreement is found between the Standard Model expectation and the data in the search regions. Exclusion limits at 95% CL are obtained in the $m(\tilde{t}_1)$ vs $m(\tilde{\chi}_1^0)$ plane and, in addition, limits on the branching ratio of the $\tilde{t}_1 \rightarrow t\tilde{\chi}_1^0$ decay as a function of $m(\tilde{t}_1)$ are also produced. Top-squark masses of up to 800 GeV are excluded for scenarios with light neutralinos, and top-squark masses up to 600 GeV are excluded in scenarios where the neutralino and the top squark are almost mass degenerate.

Contents

1	Introduction	2
2	ATLAS detector	3
3	Data and simulated event samples	4
4	Event reconstruction	5
5	Analysis strategy	7
6	Systematic uncertainties	13
7	Results	15
8	Conclusion	24

1 Introduction

The Standard Model (SM) of particle physics is one of the most comprehensively tested theories of nature, yielding predictions that agree with a wide range of experimental measurements. However, several aspects of nature remain unexplained by this model despite its success. Amongst them, the experimental mass of the Higgs boson and the possible existence of a non-baryonic component of the universe, called dark matter (DM) [1, 2], pose some of the most important open questions in current particle physics.

Supersymmetry (SUSY) [3–8] is one of the most flexible frameworks extending beyond the SM that can provide answers to the above questions. By introducing a scalar supersymmetric partner for every chiral component of the standard model fermions,¹ it can mitigate large radiative corrections to the Higgs boson mass. These naturalness arguments favour light states for the supersymmetric partners of the top quark, the \tilde{t}_L and \tilde{t}_R . The two top squark states mix to yield mass eigenstates \tilde{t}_1 and \tilde{t}_2 , by convention the former being the lightest. Moreover, in R -parity-conserving supersymmetric models [9], supersymmetric partners are produced in pairs, and the lightest supersymmetric particle (LSP) is stable, providing a viable DM candidate. This LSP is generally assumed to be lightest neutralino ($\tilde{\chi}_1^0$).

Searches for the top squark at the LHC experiments have set stringent limits on these particles [10–17], imposing constraints on the \tilde{t}_1 mass in the Minimal Supersymmetric Standard Model (MSSM) at the order of 1 TeV, in scenarios where R -parity and flavour are conserved. Extensions of the MSSM can propose scenarios where flavour is not conserved, resulting in looser constraints. In this paper, a non-minimal flavour violation (MFV) extension of the MSSM is considered, as described in Ref. [18]. In this framework, the second-generation and third-generation right-handed squark sectors can mix and the mixing is quantified through the mixing angle (θ_{tc}). As a consequence of this mixing, the mass eigenstate \tilde{t}_1 is a combination of the gauge eigenstates of the second- and third-generation squarks and can decay into a charm quark and a neutralino in addition to decaying into a top quark and a neutralino, as shown in Figure 1. This search focuses on signals containing on-shell top quarks produced in the final state, thus signals with a mass

¹ For a generic fermion f , with chiral components f_L and f_R , two scalar fields exist (named respectively \tilde{f}_L and \tilde{f}_R).

splitting between the top squark and the neutralino ($\Delta m(\tilde{t}_1, \tilde{\chi}_1^0)$) of at least 175 GeV, and it considers a scan of the branching ratio for $\tilde{t}_1 \rightarrow c\tilde{\chi}_1^0/t\tilde{\chi}_1^0$. Only final states with hadronically decaying top quarks are considered in the analysis. The advancement of charm-tagging techniques has opened the exploration of charm particle final states. Those techniques are used in this paper to define a selection predominantly sensitive to events with a top-quark and a charm-quark, allowing a first exploration of this signature at the LHC. Final results are derived by performing model-dependent and model-independent profile likelihood fits, which respectively evaluate the presence of a SUSY signal or a generic one.

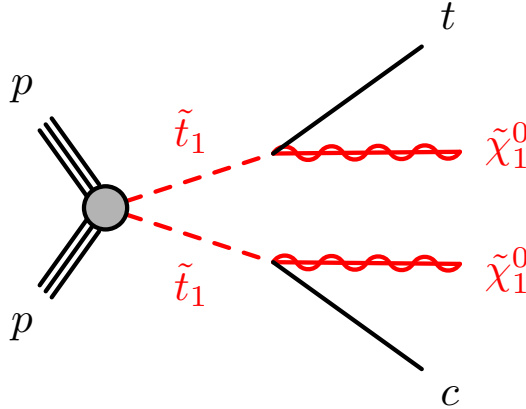


Figure 1: Signal diagram for \tilde{t}_1 pair production showing the two possible decay modes of the \tilde{t}_1 . Decays into pairs of top quarks or charm quarks are also taken into account.

2 ATLAS detector

The ATLAS detector [19] at the LHC covers nearly the entire solid angle around the collision point.² It consists of an inner tracking detector surrounded by a thin superconducting solenoid, electromagnetic and hadronic calorimeters, and a muon spectrometer incorporating three large superconducting air-core toroidal magnets.

The inner-detector system (ID) is immersed in a 2 T axial magnetic field and provides charged-particle tracking in the range $|\eta| < 2.5$. The high-granularity silicon pixel detector covers the vertex region and typically provides four measurements per track, the first hit generally being in the insertable B-layer (IBL) installed before Run 2 [20, 21]. It is followed by the SemiConductor Tracker (SCT), which usually provides eight measurements per track. These silicon detectors are complemented by the transition radiation tracker (TRT), which enables radially extended track reconstruction up to $|\eta| = 2.0$. The TRT also provides electron identification information based on the fraction of hits (typically 30 in total) above a higher energy-deposit threshold corresponding to transition radiation.

² ATLAS uses a right-handed coordinate system with its origin at the nominal interaction point (IP) in the centre of the detector and the z -axis along the beam pipe. The x -axis points from the IP to the centre of the LHC ring, and the y -axis points upwards. Polar coordinates (r, ϕ) are used in the transverse plane, ϕ being the azimuthal angle around the z -axis. The pseudorapidity is defined in terms of the polar angle θ as $\eta = -\ln \tan(\theta/2)$ and is equal to the rapidity $y = \frac{1}{2} \ln \left(\frac{E+p_z c}{E-p_z c} \right)$ in the relativistic limit. Angular distance is measured in units of $\Delta R \equiv \sqrt{(\Delta y)^2 + (\Delta \phi)^2}$.

The calorimeter system covers the pseudorapidity range $|\eta| < 4.9$. Within the region $|\eta| < 3.2$, electromagnetic calorimetry is provided by barrel and endcap high-granularity lead/liquid-argon (LAr) calorimeters, with an additional thin LAr presampler covering $|\eta| < 1.8$ to correct for energy loss in material upstream of the calorimeters. Hadronic calorimetry is provided by the steel/scintillator-tile calorimeter, segmented into three barrel structures within $|\eta| < 1.7$, and two copper/LAr hadronic endcap calorimeters. The solid angle coverage is completed with forward copper/LAr and tungsten/LAr calorimeter modules optimised for electromagnetic and hadronic energy measurements respectively.

The muon spectrometer (MS) comprises separate trigger and high-precision tracking chambers measuring the deflection of muons in a magnetic field generated by the superconducting air-core toroidal magnets. The field integral of the toroids ranges between 2.0 and 6.0 T m across most of the detector. Three layers of precision chambers, each consisting of layers of monitored drift tubes, cover the region $|\eta| < 2.7$, complemented by cathode-strip chambers in the forward region, where the background is highest. The muon trigger system covers the range $|\eta| < 2.4$ with resistive-plate chambers in the barrel, and thin-gap chambers in the endcap regions.

The luminosity is measured mainly by the LUCID-2 [22] detector that records Cherenkov light produced in the quartz windows of photomultipliers located close to the beam pipe.

Events are selected by the first-level trigger system implemented in custom hardware, followed by selections made by algorithms implemented in software in the high-level trigger [23]. The first-level trigger accepts events from the 40 MHz bunch crossings at a rate below 100 kHz, which the high-level trigger further reduces in order to record complete events to disk at about 1 kHz.

A software suite [24] is used in data simulation, in the reconstruction and analysis of real and simulated data, in detector operations, and in the trigger and data acquisition systems of the experiment.

3 Data and simulated event samples

The proton–proton collision data analysed in this paper were collected between 2015 and 2018 at a centre-of-mass energy of 13 TeV with a 25 ns proton bunch crossing interval. Multiple pp interactions occur per bunch crossing (pile-up), with a measured average of approximately 34 interactions. Application of beam, detector, and data-quality criteria [25] result in a total integrated luminosity of 139 fb^{-1} . The uncertainty in the combined 2015–2018 integrated luminosity is 1.7% [26], obtained using the LUCID-2 detector [22] for the primary luminosity measurements and cross-checked by a suite of other systems.

This analysis searches for signatures with a significant missing transverse momentum (\vec{p}_T^{miss}). This \vec{p}_T^{miss} is calculated as the negative sum of all reconstructed objects and a “soft-term” composed of all tracks associated with the primary vertex but not matched to any reconstructed object. The magnitude of this \vec{p}_T^{miss} is the missing transverse energy, denoted as E_T^{miss} . Due to the presence of two $\tilde{\chi}_1^0$ which don’t interact with the detector in the final state considered in this analysis, events are required to satisfy a E_T^{miss} trigger [23, 27] and to present an offline reconstructed E_T^{miss} exceeding 250 GeV [27] in order to ensure the full efficiency of the trigger. To aid with the estimate of some of the SM background processes, events are also selected using single-lepton triggers [28, 29] with corresponding offline thresholds above 27 GeV used to ensure the lepton triggers are also fully efficient.

Samples of Monte Carlo (MC) simulated events are used to model the SUSY signal and background processes in the analysis. The SUSY signal models were generated with MADGRAPH5_AMC@NLO 2.8.1 [30] at

leading order (LO) in QCD using the NNPDF3.0NLO [31] set of parton distribution functions (PDFs) and interfaced with PYTHIA 8.244 [32] using the A14 set of tuned parameters (‘tune’) [33] with NNPDF2.3LO for the parton showering and hadronisation, and with EVTGEN 1.7.0 [34] for the modelling of heavy flavour hadron decays. The samples were normalised using the cross-section calculations at next-to-next-to-leading order (NNLO) in the strong coupling constant, adding the resummation of soft gluon emission at next-to-next-to-leading-logarithmic (NNLL) accuracy [35–37]. The signal samples were generated with both possible decays $\tilde{t}_1 \rightarrow t\tilde{\chi}_1^0$ and $\tilde{t}_1 \rightarrow c\tilde{\chi}_1^0$ occurring with equal probability. This allows a branching-ratio (BR) scan to be performed by applying a reweighting procedure based upon the number of generated signal events of each decay-type.

The SM backgrounds considered in this analysis are: Z + jets production; W + jets production; $t\bar{t}$ production; single-top-quark production; $t\bar{t}$ production in association with electroweak bosons ($t\bar{t} + V$); multi-top and top rare processes (tWZ , tZ); and multi-boson production (VV). The events were simulated using different MC generator programs depending on the process. Details of the generators, PDF set and tune used for each process are listed in Table 1.

For all the generated samples, the response of the detector was modelled with the full ATLAS detector simulation [38] based on GEANT4 [39]. All simulated events were overlaid with multiple pp collisions simulated with PYTHIA 8.186 using the A3 tune [40] and the NNPDF2.3LO PDF set [41]. The MC samples were generated with variable levels of pile-up in three campaigns which were reweighted to match the actual distribution of the mean number of interactions observed in data in 2015–2018.

Table 1: Summary of the simulated background samples. ‘ME’ stands for matrix-element, ‘PS’ for parton shower and ‘UE’ for underlying event.

Process	ME event generator and order	ME PDF	PS and hadronisation	UE tune	Cross-section calculation
V +jets ($V = W/Z$)	SHERPA 2.2.1 [42], NLO	NNPDF3.0NNLO [31]	SHERPA	Default	NNLO [43]
Multi-boson	SHERPA 2.2.1 or 2.2.2 [44], NLO	NNPDF3.0NNLO	SHERPA	Default	NLO
$t\bar{t}$	POWHEG Box [45], NLO	NNPDF3.0NLO	PYTHIA 8.230	A14	NNLO+NNLL [46, 47]
Single-top	POWHEG Box, NLO	NNPDF3.0NLO	PYTHIA 8.230	A14	NNLO+NNLL [48–50]
$t\bar{t} + V$	AMC@NLO 2.3.3, NLO	NNPDF3.0NLO	PYTHIA 8.210	A14	NLO
tWZ , tZ	AMC@NLO 2.3.3, NLO	NNPDF3.0NLO	PYTHIA 8.230	A14	NLO
ttt , $t\bar{t}\bar{t}$	AMC@NLO 2.3.3, NLO	NNPDF3.1NLO	PYTHIA 8.230	A14	NLO

4 Event reconstruction

The analysis uses standard ATLAS reconstruction techniques with the object selections used to define small- R jets, large- R jets, leptons (e, μ), top- and b -tagged jets reported in Table 2. A loose set of requirements on the properties of the candidate objects is used to define ‘‘baseline’’ objects. The baseline requirements for each physics object are shown in the second column of Table 2. The physics objects used to define selections and calculate kinematic variables are required to satisfy tighter selections, referred to as the ‘‘signal’’ requirements, and are presented in the third column of Table 2. Baseline objects are used to estimate the E_T^{miss} , previously mentioned in Section 3. A quality criterion for the matching of topological cell clusters [51] in the electromagnetic calorimeter to electrons is also imposed in events containing electrons with $|\eta| \in [1.37, 1.52]$ in data recorded during 2015 and 2016.

After the baseline objects are defined, an overlap removal procedure is applied to prevent double-counting of tracks and energy depositions associated with overlapping jets, electrons and muons. The procedure

applies the following actions to the event. First, baseline electrons are discarded if they share a track in the inner detector with a baseline muon. Next, any jet within a distance $\Delta R = \sqrt{(\Delta y)^2 + (\Delta\phi)^2} = 0.2$ of a baseline electron is discarded and the electron is retained, if the jet is *not* identified as a b -tagged jet, otherwise the jet is kept instead. Similarly, any jet satisfying $N_{\text{trk}} < 3$ (where N_{trk} refers to the number of tracks with $p_T > 500$ MeV that are associated with the jet) within $\Delta R < 0.2$ of a baseline muon is discarded and the muon is retained. Finally, baseline electrons or muons within a distance $\Delta R < 0.4$ of any remaining jet are discarded.

For charm tagging, a non-standard, analysis-specific c -tagging algorithm, denoted DL1r_c , was optimised. It is based on the DL1r algorithm used for b -tagging [52] that provides three probabilities of a jet to be coming from the hadronisation of a b -quark (b -jet), a c -quark (c -jet) or a lighter quark/gluon (l -jet). These three probabilities are combined in a similar manner as in the b -tagging algorithm, but with tuned parameters optimised to identify jets containing c -hadrons. To avoid ambiguities in identifying a jet as both a c - or b -jet, priority is given to b -tagged jets. Namely the two tagging algorithms, DL1r and DL1r_c , are run in sequence with the b -tagging algorithm taking precedence, and if a jet is classified as a b -jet, it is no longer considered as an input to the c -tagging algorithm. This technique is referred to as *c -tagging with b -veto* technique and is very helpful to avoid a large rate of b -jets misidentified as c -jets. The chosen working point for the b -tagging algorithm is the 77% working point, which corresponds to an identification efficiency of 77% for b -jets and a misidentification rate of 20% for c -jets and 0.9% for light flavour jets. The working point selected for the c -tagging algorithm (including the effect of the b -veto) corresponds to a 20% c -jet efficiency, with rejection factors of 29 for b -jets and 57 for light-jets, evaluated on simulated $t\bar{t}$ events. Similarities in the decay chain of hadronically decaying τ -leptons and c -hadrons lead to a significant misidentification efficiency of τ -leptons as charm jets of the order of 15%. Due to this, dedicated kinematic variables are defined at event level to reject events containing hadronic τ -leptons, as described in Section 5. The DNN top tagger [53] is used to identify large- R jets which arise from top quark decays. The 80% efficiency working point is used and it is valid for top-tagged jets with masses in the 40–600 GeV range and p_T between 350 and 2500 GeV. Large- R jets outside these validity ranges are not identified as arising from a top quark.

Scale factors are applied to account for differences between data and simulation for the trigger, reconstruction, identification, and isolation efficiencies. In the case of the charm tagging algorithm used in this analysis, dedicated scale factors and uncertainties were derived using the same techniques as used for b -tagging algorithms [52]. The resulting scale factors correct for differences between data and simulation in its c -jet efficiency and in its b -jet and light-jet misidentification rate. In the p_T range between 20 and 250 GeV, the c -jet correction factors are found to be mostly compatible with unity, with systematic uncertainties ranging from 17% at low p_T (< 65 GeV) to a few % for higher- p_T jets. The b -jet correction and light-jet factors are also found to be compatible with unity, with uncertainties ranging from 7% to 5% between 20 and 250 GeV for b -jets and around 13% for all light-jets. For jets with $p_T > 250$ GeV, the correction is assumed constant and an additional systematic uncertainty due to the extrapolation is derived using MC simulation, with the uncertainty increasing up to 30% for charm and bottom jets with p_T of 3 TeV.

Table 2: Overview of the baseline and signal physics object definitions. The impact parameter along the beam direction and the significance of the transverse impact parameter are denoted by $z_0 \sin \theta$ and $|d_0/\sigma_{d_0}|$, respectively. Similarly, p_T , η , and m are the transverse momentum, pseudorapidity and mass, respectively, for each physics object. WP is the considered working point for each jet tagger, corresponding to the listed selection efficiency.

Physics object	Baseline requirements	Additional signal requirements
Electrons	Loose likelihood-based selection [54] $ z_0 \sin \theta < 0.5 \text{ mm}$ $ \eta < 2.47$ $p_T > 4.5 \text{ GeV}$	Tight likelihood-based selection [54] $p_T > 10 \text{ GeV}$ Isolation ‘Loose’ ($p_T > 200 \text{ GeV}$ ‘HighPtCaloOnly’) [54] $ d_0/\sigma_{d_0} < 5$
Muons	Medium identification [55] $ \eta < 2.7$ $p_T > 4 \text{ GeV}$	$p_T > 10 \text{ GeV}$ Isolation ‘Loose_VarRad’ [55] $ d_0/\sigma_{d_0} < 3$
Small- R jets	Particle-flow anti- k_t $R=0.4$ [51, 56–58] $p_T > 20 \text{ GeV}$ $ \eta < 2.8$	Jet vertex tagger > 0.5 and $ \eta < 2.4$ [59] or $p_T > 60 \text{ GeV}$
Large- R jets	LCTopo trimmed $R=1.0$ [60] $p_T \geq 200 \text{ GeV}$ $ \eta < 2.0$	
E_T^{miss}		Tight WP [61]
Top-tagged jets		DNN top tagger [53] 80% efficiency WP $p_T \in [350, 2500] \text{ GeV}$ $m \in [40, 600] \text{ GeV}$
b -tagged jets		DL1r tagger [52] 77% efficiency WP
c -tagged jets		DL1r _c tagger 20% efficiency WP

5 Analysis strategy

The kinematic properties of the SUSY signal under consideration are heavily dependent upon the mass splitting $\Delta m(\tilde{t}_1, \tilde{\chi}_1^0)$. Generally, the parameter space can be split into three main regions: the “bulk” region, with large $\Delta m(\tilde{t}_1, \tilde{\chi}_1^0)$; the “intermediate” region where the top squark and neutralino are relatively close in mass; and, finally, the “compressed” region, where the mass splitting is such that the top quark from the \tilde{t}_1 decay is produced just on-shell ($\Delta m(\tilde{t}_1, \tilde{\chi}_1^0) \approx m_t$).

The general analysis strategy is to define Signal Regions (SRs) which target different regions of the SUSY signal phase-space by placing selections on particle multiplicities and kinematic variables. Control Regions (CRs) are then defined with negligible signal contamination and enriched in the main backgrounds present in the SRs. These CRs are orthogonal to the SRs. A likelihood fit is performed where normalisation factors for the main backgrounds are calculated in the CRs and extrapolated to estimate the contributions of these backgrounds in the SRs. Finally, Validation Regions (VRs) are defined, again, non-overlapping with the SRs and the CRs, to investigate the modelling of the backgrounds and confirm the normalisation factor can be extrapolated to the SRs.

Many kinematic variables are employed in the definition of the SRs to isolate the SUSY signals and to

reject events arising from the SM background. In addition to selections on the number of b -tagged jets ($N_{b\text{-jets}}$), c -tagged jets ($N_{c\text{-jets}}$), large- R jets compatible with arising from a top quark ($N_{\text{tops}}^{\text{DNN}}$), $E_{\text{T}}^{\text{miss}}$, and selections on the transverse momentum of the jets ($p_{\text{T}(j/b/c)}$), more complex variables are used, and are described below.

- $\Delta\phi(j_{1-4}, E_{\text{T}}^{\text{miss}})_{\text{min}}, \Delta\phi(j_{1-3}, E_{\text{T}}^{\text{miss}})_{\text{min}}$:

The minimum difference in azimuthal angle between any of the leading four (j_{1-4}) or three (j_{1-3}) jets and the $E_{\text{T}}^{\text{miss}}$. In regions with zero lepton this variable removes the contribution from multi-jet processes which arise from jet mismeasurement leading to “fake” $E_{\text{T}}^{\text{miss}}$ in the final state.

- $m_{\text{T}}(c, E_{\text{T}}^{\text{miss}})_{\text{min}}, m_{\text{T}}(b, E_{\text{T}}^{\text{miss}})_{\text{min}}$:

The minimum value of the transverse mass calculated between any of the c -tagged (b -tagged) jets and the missing transverse momentum vector. The transverse mass (m_{T}) is defined as:

$$m_{\text{T}} = \sqrt{2p_{\text{T}}(c/b)E_{\text{T}}^{\text{miss}}(1 - \cos \Delta\phi(c/b, E_{\text{T}}^{\text{miss}}))}.$$

In $t\bar{t}$ events, these variables present kinematic end-points at truth-level around the mass of the top quark and the W -boson, which is exploited to reduce the $t\bar{t}$ background.

- $m_{\text{T}}(c, E_{\text{T}}^{\text{miss}})_{\text{max}}, m_{\text{T}}(b, E_{\text{T}}^{\text{miss}})_{\text{max}}$:

The maximum value of the transverse mass when calculated between any of the c -tagged (b -tagged) jets and the missing transverse momentum vector. These variables are used to enhance the signal against the $t\bar{t}$ background, as the $t\bar{t}$ background tends to have lower values than the signal.

- $m_{\text{T}}(j, E_{\text{T}}^{\text{miss}})_{\text{close}}$:

The transverse mass calculated between the jet closest in azimuthal angle to the missing transverse momentum vector and the missing transverse momentum vector itself. This variable is used in conjunction with the $\Delta\phi$ variables to remove the contributions from multijet processes with “fake” $E_{\text{T}}^{\text{miss}}$.

- $E_{\text{T}}^{\text{miss}}$ Sig:

The global $E_{\text{T}}^{\text{miss}}$ significance, calculated including the parameterisations of all objects, defined as:

$$E_{\text{T}}^{\text{miss}} \text{ Sig} = \sqrt{\frac{|\vec{p}_{\text{T}}^{\text{miss}}|^2}{\sigma_{\text{L}}^2(1-\rho_{\text{LT}}^2)}}.$$

Here σ_{L} is the summed momentum resolution of all the objects entering the $E_{\text{T}}^{\text{miss}}$ calculation in the direction parallel to the $\vec{p}_{\text{T}}^{\text{miss}}$ direction (longitudinal direction), while ρ_{LT} is the correlation factor between this longitudinal resolution and the total momentum resolution in the transverse direction to $\vec{p}_{\text{T}}^{\text{miss}}$. This variable is used to discriminate between events where the $E_{\text{T}}^{\text{miss}}$ arises from invisible particles in the final state and events where the $E_{\text{T}}^{\text{miss}}$ arises from poorly measured particles [62].

- $m_{\text{T}2}(j_{R=1.0}^b, c)$:

The transverse mass variable [63], a generalisation of the transverse mass for the case in which two semi-invisibly decaying particles are pair-produced, defined as:

$$m_{\text{T}2}(\vec{p}_{\text{T}}^1, \vec{p}_{\text{T}}^2, \vec{p}_{\text{T}}^{\text{miss}}) = \min_{\vec{q}_{\text{T}}^1 + \vec{q}_{\text{T}}^2 = \vec{p}_{\text{T}}^{\text{miss}}} \{\max[m_{\text{T}}(\vec{p}_{\text{T}}^1, \vec{q}_{\text{T}}^1), m_{\text{T}}(\vec{p}_{\text{T}}^2, \vec{q}_{\text{T}}^2)]\}.$$

This generalization assumes that two visible particles, each reconstructed as one of the objects defined in Section 4, and two invisible particles, reconstructed as E_T^{miss} , are produced. A minimization is then performed on the transverse mass of the combinations between the two visible particles and all the possible transverse momenta configurations of the two invisible particles, denoted as \vec{q}_T^1 and \vec{q}_T^2 , consistent with the observed E_T^{miss} . In this analysis, the two visible objects in the decay, with transverse momentum denoted as \vec{p}_T^1 and \vec{p}_T^2 , are: a large- R jet in the event containing a b -tagged jet ($\Delta\phi(j_{R=1.0}^b, b) < 1.0$); and a c -tagged small- R jet. If, in a given event, there is more than one large- R jet containing a b -tagged jet, or more than one c -tagged jet, the large- R jet and c -jet with the highest \vec{p}_T are used in the calculation. No top-tagging requirement is imposed on the b -tagged large- R jet. This allows the use of this variable in the definition of all regions across the analysis, regardless if those regions require events with a top-tagged jet or not. For the high-mass \tilde{t}_1 signal this variable is expected to extend to large values, whereas for the $t\bar{t}$ background this variable should dramatically drop-off at the top quark mass.

- m_{eff} :

The effective mass, the scalar sum of the transverse momenta of all jets in the event and the E_T^{miss} , defined as:

$$m_{\text{eff}} = \sum_{i=0}^{N_{\text{jets}}} p_T(j_i) + E_T^{\text{miss}}.$$

Generally, for the signal scenarios considered, the m_{eff} extends to high values, compared to the SM backgrounds which generally have lower values of m_{eff} .

Four orthogonal sets of SRs were designed to target the different areas of parameter space, with SRA targeting the bulk region, SRB and SRC targeting the intermediate region, and SRD targeting the compressed region. Due to general similarities between the kinematics of the bulk and intermediate regions, SRA, SRB and SRC have generally similar selections and primarily differ based upon the usage of the $m_{T2}(j_{R=1.0}^b, c)$ variable and the number of top-tagged jets present in the event. Due to the similarity between the SRA, SRB, and SRC regions, common CRs are used to predict the main SM backgrounds, and common VRs are used to validate the background modelling. The kinematic properties of the SRD region are significantly different, with a selection requiring the presence of initial-state radiation (ISR) to boost the sparticle system, providing enough E_T^{miss} to satisfy the trigger selection. All SRs require that events contain zero leptons, at least one b -tagged jet, at least one c -tagged jet, and high E_T^{miss} .

The full selections used to define the A-, B-, and C-type regions are summarized in Table 3. Commonalities among these regions include specific selections based on large values of E_T^{miss} , E_T^{miss} significance, and $m_T(c, E_T^{\text{miss}})_{\text{min}}$ between the c -tagged jet and the E_T^{miss} . SRA is kept orthogonal to the SRB region using the number of top-tagged large- R jets ($N_{\text{tops}}^{\text{DNN}}(R = 1.0)$), with SRA requiring at least one top-tagged jet whereas SRB requires exactly zero top-tagged jets. The SRA and SRC regions are orthogonal due to the selection on $m_{T2}(j_{R=1.0}^b, c)$. The SRB and SRC regions are also orthogonal due to the selection on $N_{\text{tops}}^{\text{DNN}}(R = 1.0)$, with SRB requiring zero top-tagged jets whereas SRC requires at least one.

In the parameter space targeted by the SRA region, very large values of $m_{T2}(j_{R=1.0}^b, c)$ are expected. To enhance sensitivity to these signals when performing the model dependent interpretation, a multi-bin fit is performed, and two bins of $m_{T2}(j_{R=1.0}^b, c)$ are used: $[450, 575]$ and ≥ 575 GeV. For the intermediate region of parameter space, lower values of $m_{T2}(j_{R=1.0}^b, c)$ are expected, so, instead, sensitivity can be enhanced by performing a multi-bin fit in the $m_T(j, E_T^{\text{miss}})_{\text{close}}$ variable. The SRB region is split into three orthogonal regions in the $m_T(j, E_T^{\text{miss}})_{\text{close}}$ variable: $[100, 150]$, $[150, 400]$ and ≥ 450 GeV. SRC uses a similar strategy, however, with a finer granularity of $m_T(j, E_T^{\text{miss}})_{\text{close}}$ bins: $[100, 150]$, $[150, 300]$,

[300, 500], and ≥ 500 GeV. When performing the model-independent fit, the same lower bounds are used for the SRA, SRB, and SRC regions as in the model-dependent fit, however, the upper bounds on the bins are removed, allowing for more general regions than those used for the model-dependent interpretation.

The largest background contribution in SRA, SRB, and SRC originates from $Z + \text{jets}$ events, followed by single-top quark (‘single-top’) or $W + \text{jets}$ events. Due to the stringent requirement in E_T^{miss} significance and $\Delta\phi(j_{1-4}, E_T^{\text{miss}})_{\text{min}}$, the multijet background is negligible. Common CRs are used to estimate the main backgrounds for both of the SRA and SRB regions, with a single VR used to validate the background estimate strategy. CRs requiring two leptons (2L) are used to extract a normalisation factor for the $Z + \text{jets}$ background. In these regions the leptons are subtracted from \vec{p}_T^{miss} , and are used as a proxy for neutrinos mimicking the $Z \rightarrow \nu\nu$ decay. This ‘‘lepton-corrected’’ E_T^{miss} is denoted by $E_{T,\ell\ell}^{\text{miss}}$ and in the 2L regions is used when calculating all kinematic variables. The CRZAC region is used to normalise the $Z + \text{jets}$ process in both of the SRA and SRC regions (as both of the regions require one top-tagged large- R jet). The CRZB region is used to estimate the $Z + \text{jets}$ background in the SRB region, where the presence of a top-tagged large- R jet is explicitly vetoed. A CR requiring exactly one lepton (1L), denoted CRstAC, is used to estimate the single-top contribution in the SRA and SRC regions by specifically requiring the presence of one top-tagged large- R jet in the event. Due to the subdominant contribution of other potential SM backgrounds, no further CRs are defined, and rather the contributions from these processes are estimated directly from simulation. A single 0L VR, denoted VRZABC, is used to validate the modelling of the $Z + \text{jets}$ background in all three SRs. This 0L selection is inclusive relative to the number of top-tagged jets in the event, and hence can be used to validate the modelling across all SRA, SRB, and SRC regions.

Table 3: Analysis selections for the A-, B-, and C-type regions associated with the SRs targeting the bulk and intermediate signal mass scenarios respectively. Selections denoted by an * are split into multiple bins (for the SR considered) when the model-dependent fit is performed and the selection shown in the table is the lower-bound on the selection used for the given region. ‘SFOS’ indicates that the selected leptons are required to have the same flavour and opposite-sign electric charges, such that they are compatible with the decay of a Z boson. More information about the fit strategy is provided in the text.

Variable	SRA	SRB	SRC	VRZABC	CRstAC	CRZB	CRZAC
Trigger	E_T^{miss} Trigger					1L Trigger	
Baseline & signal leptons	= 0				= 1 ($p_T \geq 30$ GeV)	= 2 SFOS ($p_T \geq 30$ GeV)	
E_T^{miss} [GeV]	≥ 250	≥ 300	≥ 250	≥ 250	≥ 250	≤ 150	
$E_{T,\ell\ell}^{\text{miss}}$ [GeV]	–					≥ 250	
$(N_{b\text{-jets}}, N_{c\text{-jets}})$	$(\geq 1, \geq 1)$ (Leading jet is either b -tagged or c -tagged)						
N_{jets}	≥ 3	≥ 5	≥ 3	[3, 8]	≥ 3	≥ 5	≥ 3
$p_T(j_1)$ [GeV]	≥ 50					≥ 20	
$\Delta\phi(j_{1-4}, E_{T,\ell\ell}^{\text{miss}})_{\text{min}}$	≥ 0.4				–		
$m_{\ell\ell}$ [GeV]	–					[76, 106]	
$m_T(c, E_T^{\text{miss}})_{\text{min}}$ [GeV]	≥ 200				≥ 300	≥ 150	–
$m_T(c, E_{T,\ell\ell}^{\text{miss}})_{\text{min}}$ [GeV]	–					≥ 150	
$N_{\text{tops}}^{\text{DNN}}$ ($R = 1.0$)	≥ 1	= 0	≥ 1	–	≥ 1	= 0	≥ 1
$p_T(b_1)$ [GeV]	≥ 20	≥ 20	≥ 100	≥ 20	≥ 20	≥ 20	
$p_T(c_1)$ [GeV]	≥ 20	≥ 100	≥ 100	≤ 200	≥ 20	≥ 20	
$p_T(j_2)$ [GeV]	≥ 20	≥ 100	≥ 20	≥ 20	≥ 20	≥ 20	
$p_T(j_4)$ [GeV]	–	≥ 50	–	–	–	–	
$m_T(c, E_T^{\text{miss}})_{\text{max}}$ [GeV]	–	≥ 400	–	≤ 400	–	≥ 400	–
$m_T(b, E_T^{\text{miss}})_{\text{max}}$ [GeV]	–	[200, 700]	–	≥ 200	–	≥ 200	–
$m_T(b, E_T^{\text{miss}})_{\text{min}}$ [GeV]	≥ 200				≥ 300	≥ 200	–
$m_T(j, E_T^{\text{miss}})_{\text{close}}$ [GeV]	≥ 100	≥ 100 *		≥ 150	≥ 200	–	
E_T^{miss} Sig	≥ 18	≥ 10	≥ 17	[15, 17]	[12, 22]	≥ 10	≥ 17
$m_{T2}(j_{R=1.0}^b, c)$ [GeV]	≥ 450 *	≥ 150	[200, 450]	–	≥ 200	–	

Due to the small mass difference between the \tilde{t} and $\tilde{\chi}_1^0$ targeted, the kinematics in the SRD region are dramatically different from the other SRs. An ISR-like selection, requiring additional jet activity, is used to “boost” the sparticle system providing the large E_T^{miss} to satisfy the trigger selection. The full selections used to define all D-type regions are summarized in Table 4.

Generally, the selections for the SRD region follow a standard ISR-like selection with a high- p_T leading-jet which is not b - or c -tagged. Due to the similarity of the signal with the main SM backgrounds of $t\bar{t}$ and V + jets, a dedicated multi-class neural network (NN) was developed to isolate the signal against these two main backgrounds.

The NN [64] is defined using the PyTorch library [65] to identify signal events which contain the mixed $tc + E_T^{\text{miss}}$ decay, $t\bar{t}$, and V +jets. To avoid issues due to the finite size of the training dataset, this NN is trained using events which satisfy a looser 0L ISR-like selection (which is a baseline for the SRD definition) and uses a total of 44 low-level variables³ to produce three output scores according to the likelihood for a given event to be signal-like, $t\bar{t}$ -like or V + jets-like. Binary scores were also considered to separate signal and background events, but they were found to be suboptimal compared to the considered three output scores. A dedicated hyperparameter optimisation is performed with a “leaky ReLU” activation function [66] and the model is optimized by minimising a cross-entropy loss function. The key variables found to be useful by the NN are E_T^{miss} , the b -jet multiplicity, and the p_T of the two leading jets. A “leaky ReLU” activation function is also applied to the final layer of the NN leading to an output which is a set of scores per event for the three categories mentioned above. The signal score (“NN signal score”) is later used to define SRD. The V + jets (“ V + jets score”) score is implemented in the W + jets CR defined below, to enhance the W + jets contribution. As defining a region enhanced in $t\bar{t}$ is comparatively simple in the parameter space targeted, the output corresponding to $t\bar{t}$ events is unused.

In the parameter space targeted by SRD, large values of m_{eff} are expected. When considering the model-dependent interpretation, a 2D binning in both m_{eff} and $m_T(j, E_T^{\text{miss}})_{\text{close}}$ is employed to further enhance sensitivity to the signal. The binning in m_{eff} is as follows: SRD750, [750, 1000]; SRD1000, [1000, 1250]; SRD1250, [1250, 1500]; SRD1500, [1500, 1750]; SRD1750, [1750, 2000]; and SRD2000, ≥ 2000 GeV. The four lowest m_{eff} bins are further subdivided using the $m_T(j, E_T^{\text{miss}})_{\text{close}}$ variable: SRD750 is split into four bins [0, 100], [100, 200], [200, 300], and ≥ 300 GeV; SRD1000 is split into three bins [0, 100], [100, 200], ≥ 200 GeV; and both SRD1250 and SRD1500 are split into two bins of [0, 100] and ≥ 100 GeV. In a similar manner to the SRA and SRB regions, when performing the model-independent fit, the lower bound of the m_{eff} selections are used, with the upper bounds removed. For the SRD750 and SRD1000 regions the $m_T(j, E_T^{\text{miss}})_{\text{close}}$ selection is increased to ≥ 200 GeV, whereas for the remaining SRD regions, it is removed.

The multijet background is also negligible in the SRD region, its main backgrounds being $t\bar{t}$, W +jets, and Z +jets. Three dedicated CRs are defined to estimate the backgrounds from these processes. The CRZZ region is a 2L region where (as in the CRZAC and CRZB regions) the leptons are subtracted from the E_T^{miss} calculation and mimic neutrinos from the Z boson decay, and the lepton-corrected $E_{T,\ell\ell}^{\text{miss}}$ is used in all calculations. To constrain W + jets and $t\bar{t}$, single-lepton CRs are used (CRWD and CRtD respectively), which are orthogonal due to the $N_{b\text{-jets}}$ selections used. In these 1L regions, the lepton is added to the jet collection to mimic the scenario where a hadronic- τ in the zero-lepton selection is misreconstructed as a jet. Additionally, to ensure a region pure in the W + jets process, the output V + jets score of the NN classifier is used. A common 0L VR, denoted VRD, is defined requiring the NN score in the range [0.0, 0.5]. It is

³ The $p_T, \eta, \Delta\phi(j, E_T^{\text{miss}})$ and flavour of the 6 jets of the event with the highest- p_T ; the $p_T, \eta, \Delta\phi(j, E_T^{\text{miss}})$ of the 2 highest- p_T b -tagged and c -tagged jets of the event; the jet, b -jet and c -jet multiplicities; and the E_T^{miss} .

thus orthogonal to the SR, for which the NN score is required to be ≥ 0.75 , and is then used to validate the extrapolation of the three main backgrounds.

As mentioned in Section 3, the $t\bar{t}$ background is modelled at NLO using POWHEG BOX [45]. A mismodelling of the top quark p_T distribution was observed for these simulated samples [67, 68]. The top quark p_T is highly correlated with the m_{eff} distribution used in the D-regions, thus CRttD and VRD regions are also binned in m_{eff} in order to respectively correct and validate the $t\bar{t}$ background prediction in the m_{eff} -binned SRD. For CRttD, three bins in m_{eff} are considered: CRttD750, [750, 1000] GeV; CRttD1000, [1000, 1250] GeV; and CRttD1250, ≥ 1250 GeV. The lack of statistical precision at high- m_{eff} prevents applying a finer binning at high- m_{eff} . This is compensated by a finer binning in the VRD region: VRD750, [750, 1000]; VRD1000, [1000, 1250]; VRD1250, [1250, 1500]; VRD1500, [1500, 1750] and VRD1750 ≥ 1750 GeV. This latter bin also includes a $E_T^{\text{miss}} < 600$ GeV requirement to minimize a possible signal contamination.

Table 4: Analysis selections for the D-type regions associated with the SR which targets compressed signal scenarios. Selections denoted by * are split into multiple bins when the fitting procedure is performed and the selection shown in the table is the lower-bound on the selection used for the given region. More information about the fit strategy is provided in the text.

Variable	SRD	CRttD	CRWD	CRZD	VRD
Trigger	E_T^{miss} Trigger			1L Trigger	E_T^{miss} Trigger
Number of baseline & signal leptons	= 0	= 1 ($p_T \geq 30$ GeV)		= 2 ($p_T \geq 30$ GeV)	= 0
E_T^{miss} [GeV]	≥ 250			≤ 100	≥ 250
$E_{T,\ell\ell}^{\text{miss}}$ [GeV]	-			≥ 250	-
N_{jets}	≥ 3 (Leading jet not b - or c -tagged)				
$N_{c\text{-jets}}$	≥ 1				
$N_{b\text{-jets}}$	≥ 1	≥ 2	= 1	≥ 1	≥ 1
$m_T(c, E_T^{\text{miss}})_{\text{min}}$ [GeV]	≥ 100	≥ 150		≥ 100	≥ 100
$p_T(j_1)$ [GeV]	≥ 100				
$p_T(j_4)$ [GeV]	≥ 30				
E_T^{miss} Sig	≥ 6				
$\Delta\phi(j_{1-3}, E_T^{\text{miss}})_{\text{min}}$	≥ 0.3			-	≥ 0.3
$\Delta\phi(j_{1-3}, E_{T,\ell\ell}^{\text{miss}})_{\text{min}}$	-			≥ 0.3	-
m_T [GeV]	-	≥ 30	[30, 120]	-	-
NN V + jets score	-	≥ 0		-	-
$\Delta R(j_1, j_2)$	≥ 1.0				
$\Delta R(b_1, l_1)$	-	≥ 1.8		-	-
$m_{\ell\ell}$ [GeV]	-			[76, 106]	-
NN signal score	≥ 0.75	≥ 0.0			[0, 0.5]
m_{eff} [GeV]	≥ 750 *	≥ 750 *	-		≥ 750 *

6 Systematic uncertainties

This analysis considers several sources of uncertainty, of both experimental and theoretical nature, that affect the prediction of the SM background and the SUSY signal in all channels.

The jet energy scale and resolution uncertainties (for both the small- R and large- R jets) are derived as a function of the jet p_T , η , and flavour, using a combination of data and simulated events, as detailed in Refs. [69]. These uncertainties also take into account the different pile-up conditions during the four years of data-taking.

Uncertainties in the correction factors for the b - and c -tagging identification efficiencies are applied to the simulated event samples. The corrections are extracted from dedicated flavour-enriched samples in data [70–72]. An additional term is included to extrapolate the measured uncertainties to the high- p_T region of interest. This term is calculated from simulated events by considering variations on the quantities affecting the b -tagging performance, such as the impact parameter resolution, percentage of poorly measured tracks, description of the detector material, and track multiplicity per jet. The dominant effect on the uncertainty when extrapolating to high- p_T is related to the different tagging efficiency when smearing the track impact parameters based on the resolution measured in data and simulation.

Uncertainties connected with the lepton reconstruction and identification are included in the fit, and they are found to have a negligible impact. All uncertainties in the final-state object reconstruction are propagated to the reconstruction of the E_T^{miss} , including an additional term taking into account uncertainties in the scale and resolution of the soft term.

The uncertainties related to the modelling of the SM background processes using MC simulation are taken into account. The modelling uncertainties are assumed to be correlated between different SRs but are uncorrelated between the different processes considered. Uncertainties related to the modelling of the $t\bar{t}$ and single-top processes arise due to the choice of hard-scattering generator and the matching scheme, and these uncertainties are evaluated by comparing the nominal samples with an alternative generator (MadGraph5_aMC@NLO). The uncertainty due to the choice of PS and hadronisation model is calculated by comparing the nominal sample with a sample produced with Powheg interfaced to HERWIG 7 [73, 74]. Variations of the renormalisation and factorisation scales, the initial- and final-state radiation parameters and PDF sets are also considered [75]. Specifically for the single-top process, a systematic uncertainty corresponding to the interference term between single-top and $t\bar{t}$ events (at NLO) is applied by comparing the nominal sample, generated with the diagram removal (DR) scheme, with a dedicated sample generated with the diagram subtraction (DS) scheme [76]. The modelling uncertainties related to the Z + jets and W + jets processes are evaluated using the 7-point renormalisation and factorisation scale variations [77], varying these scales by factors of 0.5 and 2. The matrix element matching and the resummation scales are also varied by 0.5 and 2. A conservative 100% uncertainty is applied to Z + jets events containing both a true b - and c -quark in the final state. For rare backgrounds that are not normalised in any region (multi-boson, $t\bar{t}V$ and $t + X$), a conservative 30% uncertainty is applied, covering the difference between the theory prediction for these subprocesses and their measured cross-section by ATLAS plus one standard deviation [78–83]. Similarly, an uncertainty of 5% is applied on $t\bar{t}$ and W + jets processes in regions A, B and C, an uncertainty of 30% is applied to single-top processes in the D-regions, and an uncertainty of 10% is applied to $t\bar{t}$ Z processes in all regions as these backgrounds are not normalized in any region. For the SUSY signal scenarios, systematic uncertainties are also calculated by varying the factorisation and renormalisation scales, the ISR parameters, and the choice of PDF. The maximum uncertainty for any signal mass scenario is found to be 20%.

The breakdown of the systematic uncertainties in the post-fit background prediction is shown in Figure 2. The contributions are split by model-dependent SR. The total uncertainty shown is not simply the sum in quadrature of the individual uncertainties due to correlations between the components resulting from the fit. In the A-type regions, the dominant uncertainty arises from the experimental uncertainties of the large- R jets, driven by the relatively high- p_T large- R jets in this region of parameter space. In the B-type

and C-type regions, the main contribution is from the small- R jet uncertainties due to the tight selections on the leading b - and leading c -jet p_T . In the D-type regions, the main uncertainty is the uncertainty in the background normalisation parameters, as, in comparison to the other SRs, the CRDs and SRD are kinematically much closer. This generally results in a reduction of the impact of the uncertainties in the SRs, absorbed by the normalization parameters of the background, leaving the uncertainty from the background normalisation in the CRs as the dominant systematic uncertainty. The statistical uncertainties on the MC also contribute to the total uncertainty of the background, particularly in SRA, SRB and SRC due to the tight selection criteria of these regions.

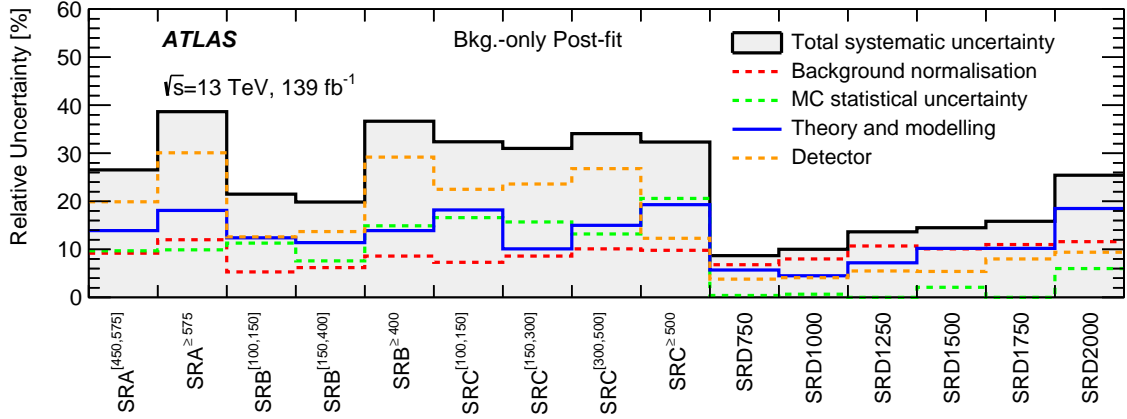


Figure 2: Summary of the systematic uncertainties affecting the background yields in the SRs after the likelihood fit to data (‘Post-fit’). The “Detector” category contains all detector-related systematic uncertainties. The “Background normalisation” represents the uncertainty in the fitted normalisation factors, including the available data event counts in the CRs. The “Theory and modelling” represents the theoretical uncertainties of the modelling of the SM background processes. The individual uncertainties may not sum (in quadrature) to the total uncertainty due to correlations between the different components. Each superscript stands for the limits of each bin defined for the corresponding SR as presented in Section 5. For instance, $SRA^{[450,575]}$ refers to events in the SRA region with $m_{T2}(j_{R=1,0}^b, c) \in [450, 575]$ GeV.

7 Results

The presence of supersymmetric signals is explored by performing multi-bin fits that maximize a likelihood function, $\mathcal{L}(\mu, \theta)$, constructed as a product of Poisson probabilities for all bins considered in the search. This likelihood depends on a parameter of interest $\mu_{\text{sig}} = \sigma^{\text{fit}}/\sigma^{\text{theory}}$, defined as the ratio of the fitted signal cross-section being tested (σ^{fit}) and its theoretical prediction (σ^{theory}). The effects of many sources of systematic uncertainty in both the signal and background yields are included when performing the likelihood fit through the introduction of nuisance parameters that impact the expectation values of the poissonian terms for each CR and SR bin. The nuisance parameters are described by Gaussian probability density functions, with the standard deviations on the functions corresponding to a specific experimental or theoretical modelling uncertainty. The preferred value of each nuisance parameter is determined as a part of the likelihood fit. Unconstrained normalization parameters (μ_{bkg}) are also defined to adjust the background

predictions in the kinematic regime probed by this search. The fits performed do not significantly alter or constrain the nuisance parameter values relative to the fit input.

Three likelihood fits are performed: the “background-only” fit, which corrects the SM background prediction in all regions of the analysis by performing a fit only in the CRs and applying the resulting normalisation parameters to the SM prediction in the VRs and SRs; the “model-dependent” fit, which uses both of the CRs and SRs to evaluate the confidence-levels (CLs) for a specific signal hypothesis; and the “model-independent” fit, which is used to calculate the p -value of the SM-only hypothesis [84], again, using both the CRs and the SRs.

When performing the background-only fit, the CRs are used in the likelihood, and the fitted background estimate is then compared with the observed yields in the VRs and SRs. A single fit is performed using the associated CRs for the A, B, C, and D regions. The SM processes which do not have an associated CR are derived from the MC prediction, but they are allowed to vary within their own uncertainties in the fit. Concerning the A, B, and C regions, there are two unconstrained normalisation parameters, for the $Z + \text{jets}$ and single-top backgrounds. For the D regions, there are five unconstrained normalisation parameters, one for $W + \text{jets}$, one for $Z + \text{jets}$, and three normalisations (split over the different m_{eff} bins corresponding to the SRs) for the $t\bar{t}$ background. Due to the different phase-space targeted by the SRD region, the normalisation factors calculated from the ABC regions are applied solely to the ABC regions, and similarly for the D regions. The top panel of Figure 3 presents the pre-fit agreement between the data and the SM predictions in the CRs, which is subsequently used to estimate the background normalization parameters shown in the bottom panel. These normalisations are mostly consistent with unity, aside from the single-top normalisation. A relatively large uncertainty is also found for the single-top normalisation, driven by the comparison between the DR and DS calculation schemes. As the single-top background is sub-dominant and is a relatively small contribution to the SRs in comparison to the $Z + \text{jets}$ background, the single-top normalisation and associated uncertainty is not of great concern.

Generally, good agreement is observed between data and post-fit background in all VRs, which is shown in Figure 4. The statistical significance [85] of the deviations between the observed data and the post-fit SM is also evaluated in all VRs, showing a maximum deviation of less than 2σ , confirming the good modelling of the main background provided by the fit strategy. Finally, Figures 5 and 6 present the post-fit SM yields and observed data in the SRs using the selections and the bins for the model-dependent fit defined in Section 5. The largest background contribution in the SRA and SRB regions is $Z + \text{jets}$, followed by single-top. There are deviations from the SM prediction in the fit to the SRs, with a largest deviation of 2σ , generally corresponding to the SRs which contain the tightest $m_{T2}(j_{R=1,0}^b, c)$ selections. The dominant background in the SRD regions is $t\bar{t}$, followed by $V + \text{jets}$ and then single-top production. The post-fit SM is in very good agreement with the data with a largest deficit of 1.8σ in the SRD1500 high- $m_T(j, E_T^{\text{miss}})_{\text{close}}$ bin.

Figures 7 and 8 present a selection of key kinematic variables in the SRs, where the arrow shown denotes where the selection on that variable is applied in the relevant region. The $\sim 2\sigma$ discrepancies in the SRA and SRC regions are already present in these distributions. For the SRB and SRD selections, it is seen that generally there is good agreement between the post-fit SM prediction and the observed data.

The model-dependent fit takes into account the contribution of the specific signal model that is being considered in all CRs and SRs to derive 95% CL exclusion limits on the SUSY signal scenarios. These limits are obtained by performing a combined fit to all SRs, i.e. SRA, SRB, SRC and SRD, increasing the sensitivity to the SUSY signal models considered by using the orthogonal bins as described in Section 5. The result of this combined fit is presented in Figure 9, where the $\text{BR}(\tilde{\tau}_1 \rightarrow t + \tilde{\chi}_1^0) = 0.5$ is chosen, as this

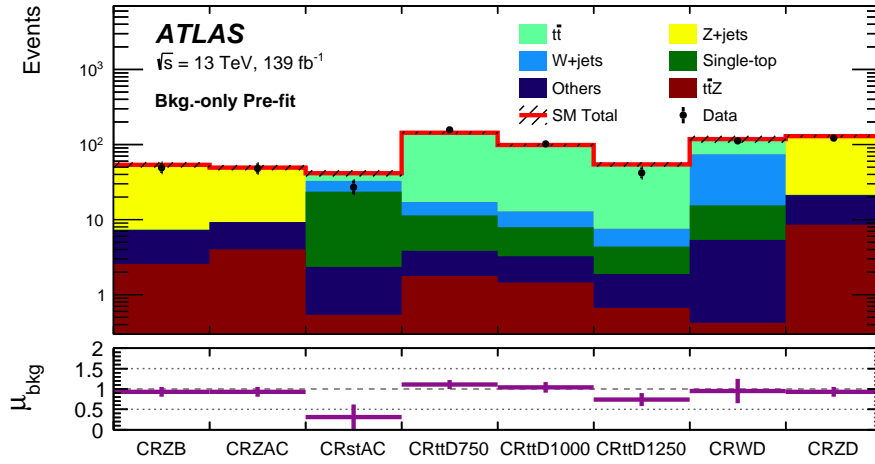


Figure 3: Control region data and SM prediction yields before performing the background-only fit (top-panel) and the obtained normalisations after performing the background-only fit (bottom panel). Generally, the normalisation parameters are found to be consistent with unity. Both systematic and statistical uncertainties are considered in the uncertainty band. The μ_{bkg} label represents the normalisation parameter for the SM background calculated from the relevant CR, for example in CRZB, μ_{bkg} represents the normalisation for the $Z + \text{jets}$ background.

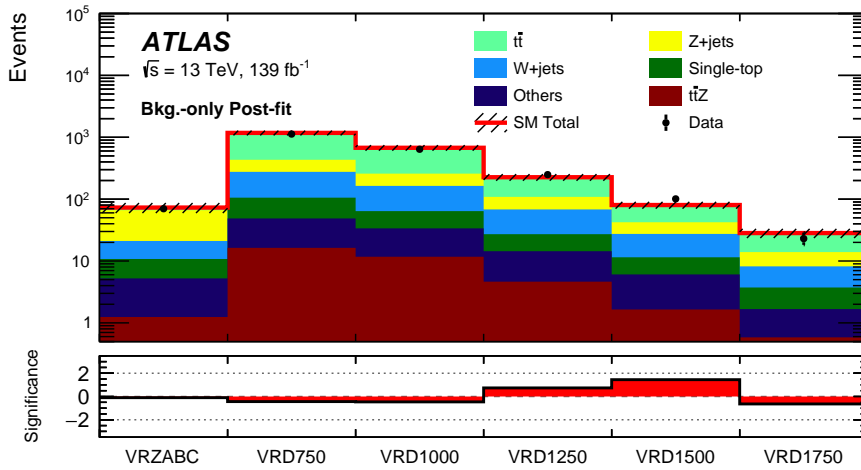


Figure 4: Validation region yields and statistical significance [85], derived from the background-only fit. The post-fit VR yields are found to be consistent within 2σ of the observed data. Both systematic and statistical uncertainties are considered in the uncertainty band.

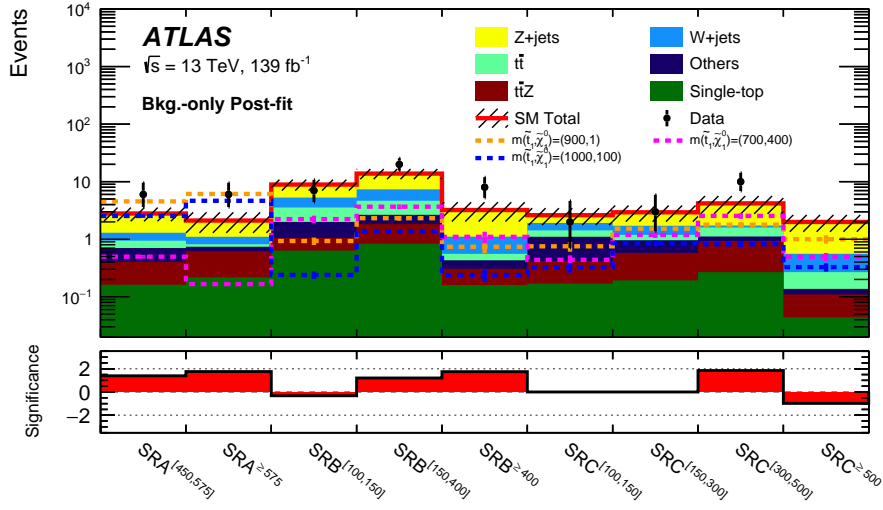


Figure 5: Background-only post-fit SM yields and statistical significance in the model-dependent SRA, SRB, and SRC selections. The largest deviation between the post-fit expectation and the observed data is close to 2σ in three regions. Both systematic and statistical uncertainties are considered in the uncertainty band. The pre-fit contribution for representative signal scenarios in each analysis region is shown for illustrative purposes.

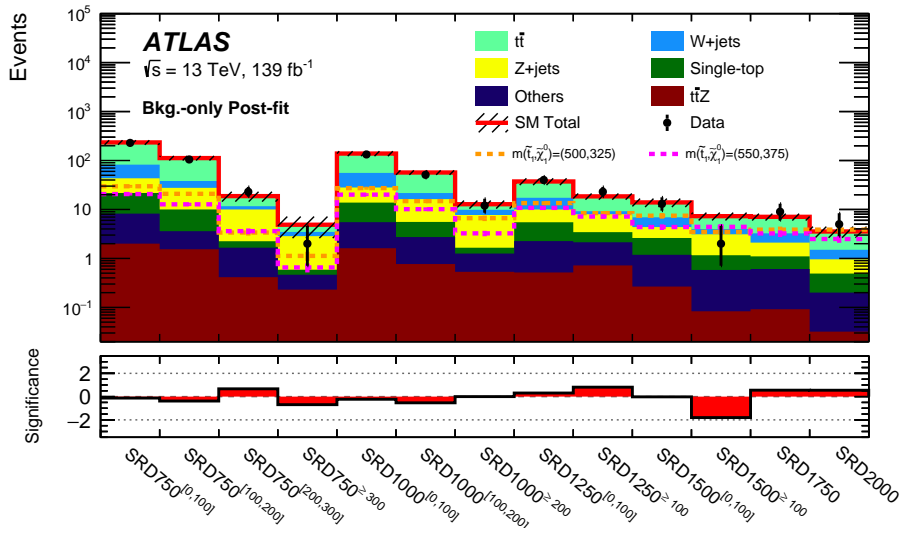


Figure 6: Background-only post-fit SM yields and statistical significance in the model-dependent SRD selections. The largest deviation between the post-fit expectation and the observed data is a 1.8σ deficit in the SRD1500 with $m_T(j, E_T^{\text{miss}})_{\text{close}} \geq 100$ GeV. Both systematic and statistical uncertainties are considered in the uncertainty band. The pre-fit contribution for representative signal scenarios in each analysis region is shown for illustrative purposes.

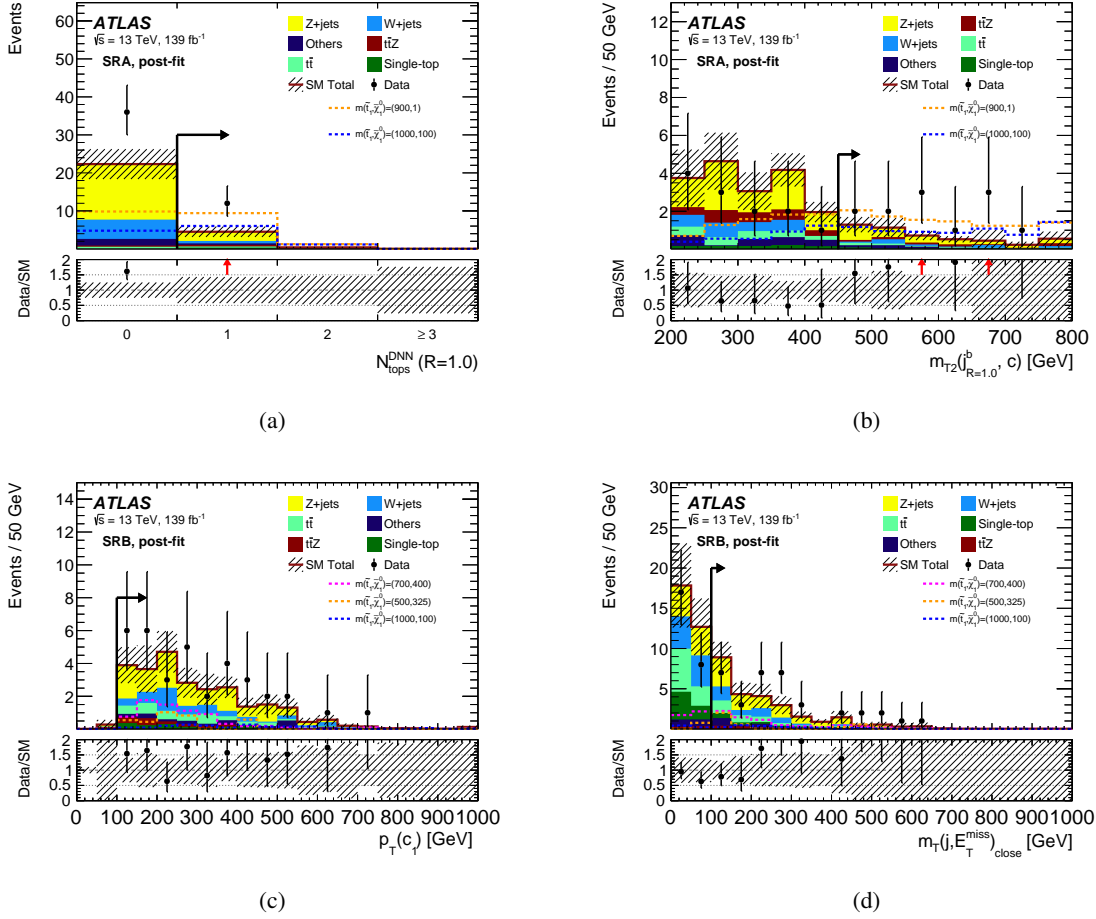


Figure 7: A selection of kinematic distributions in SRA and SRB, presented without the associated SR selection applied to the variable under consideration: (a) presents $N_{\text{tops}}^{\text{DNN}}$ in SRA; (b) $m_{T2}(j_{R=1.0}^b, c)$ in SRA; (c) $p_{T1}(c_1)$ in SRB; (d) $m_T(j, E_T^{\text{miss}})_{\text{close}}$ in SRB. The selection applied on the given variable is represented by the arrow. The right-most bin in each histogram contains the overflow entries. The expected distributions for representative signal scenarios in each analysis region are shown for illustrative purposes.

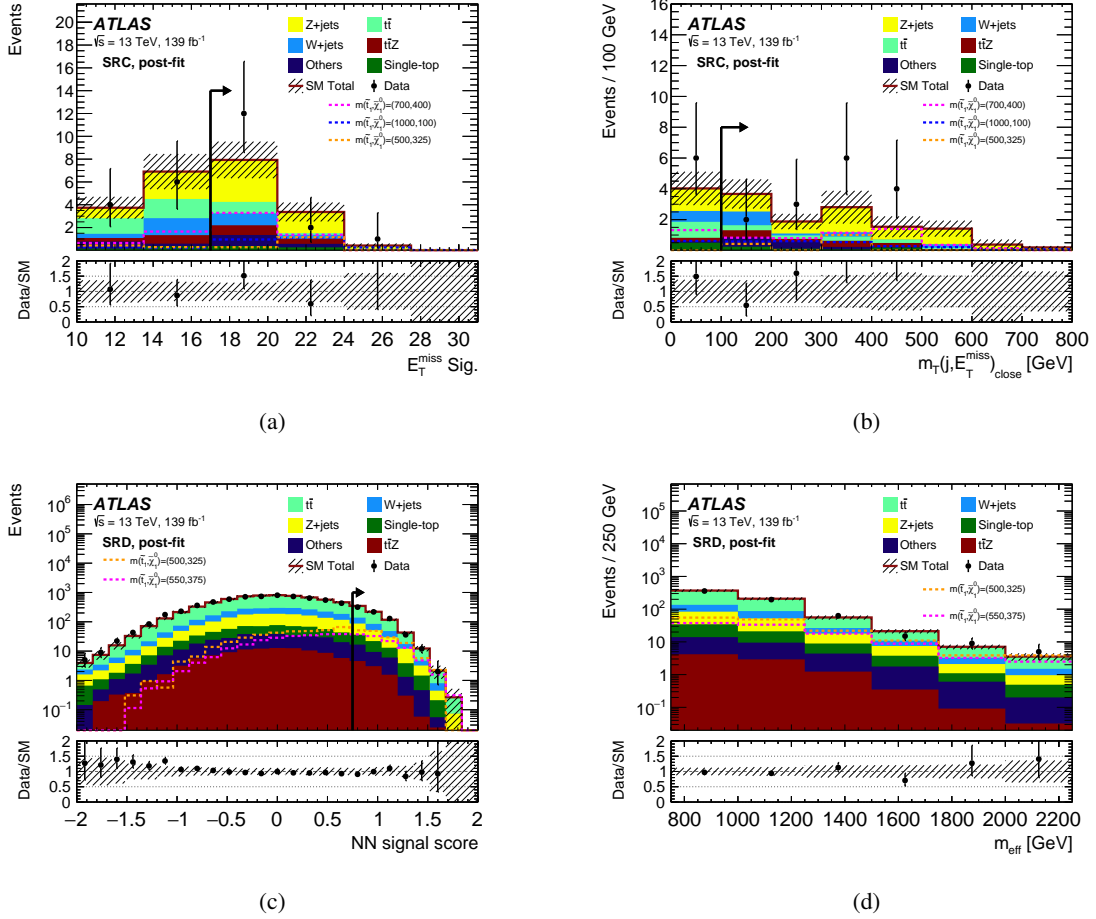


Figure 8: A selection of kinematic distributions in SRC and SRD, presented without the associated SR selection applied to the variable under consideration (except for the SRD m_{eff} distribution at the bottom right plot): (a) $E_T^{\text{miss}} \text{ Sig}$ in SRC; (b) $m_T(j, E_T^{\text{miss}})_{\text{close}}$ in SRC; (c) NN signal score in SRD; (d) m_{eff} in SRD. The selection applied on the given variable is represented by the arrow. The right-most bin in each histogram contains the overflow entries. The expected distributions for representative signal scenarios in each analysis region are shown for illustrative purposes.

scenario gives the maximal number of $tc + E_T^{\text{miss}}$ events. The effect of the 1.8σ over-fluctuation of data in the A and C regions is clearly observed. Despite this, an exclusion up to 800 GeV on top-squark masses is observed for a massless neutralino. In the compressed region, top-squark masses up to 600 GeV are excluded. Figure 10 presents an alternative interpretation, where the neutralino mass is fixed to 1 GeV and the BR of the $\tilde{t}_1 \rightarrow t + \tilde{\chi}_1^0$ decay is allowed to vary between zero and one. As expected, the maximal sensitivity in this interpretation is obtained for $\text{BR}(\tilde{t}_1 \rightarrow t + \tilde{\chi}_1^0) = 0.5$. A relatively high sensitivity is still found as the BR moves to 1 for the $\tilde{t}_1 \rightarrow t + \tilde{\chi}_1^0$ decay, primarily arising from the identification of c -jets from W boson decays. In this scenario, for $\text{BR}(\tilde{t}_1 \rightarrow t + \tilde{\chi}_1^0) \geq 0.5$, top-squark masses are excluded up to 800 GeV, whereas in the case where $\text{BR}(\tilde{t}_1 \rightarrow t + \tilde{\chi}_1^0) = 0$, the mass exclusion is reduced to 600 GeV.

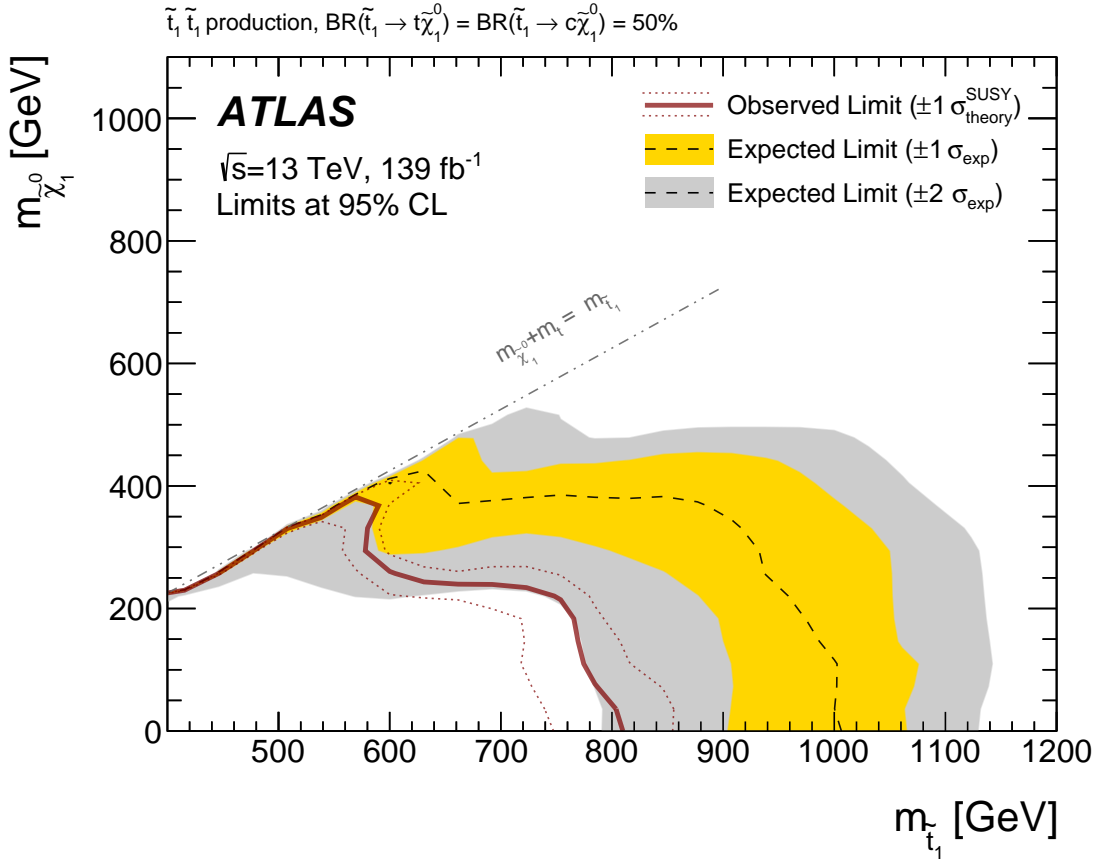


Figure 9: Exclusion limits at the 95% CL in the $m(\tilde{t}_1) - m(\tilde{\chi}_1^0)$ plane, assuming $\text{BR}(\tilde{t}_1 \rightarrow t + \tilde{\chi}_1^0) = 0.5$. The dashed line, yellow band, and grey band present the expected limit, $\pm 1\sigma$ uncertainty, and $\pm 2\sigma$ uncertainty respectively. The solid red line presents the observed upper limit on the signal cross-section. The dashed red lines present the observed upper limit if the signal cross-section is varied by $\pm 1\sigma$ of its predicted theoretical uncertainty.

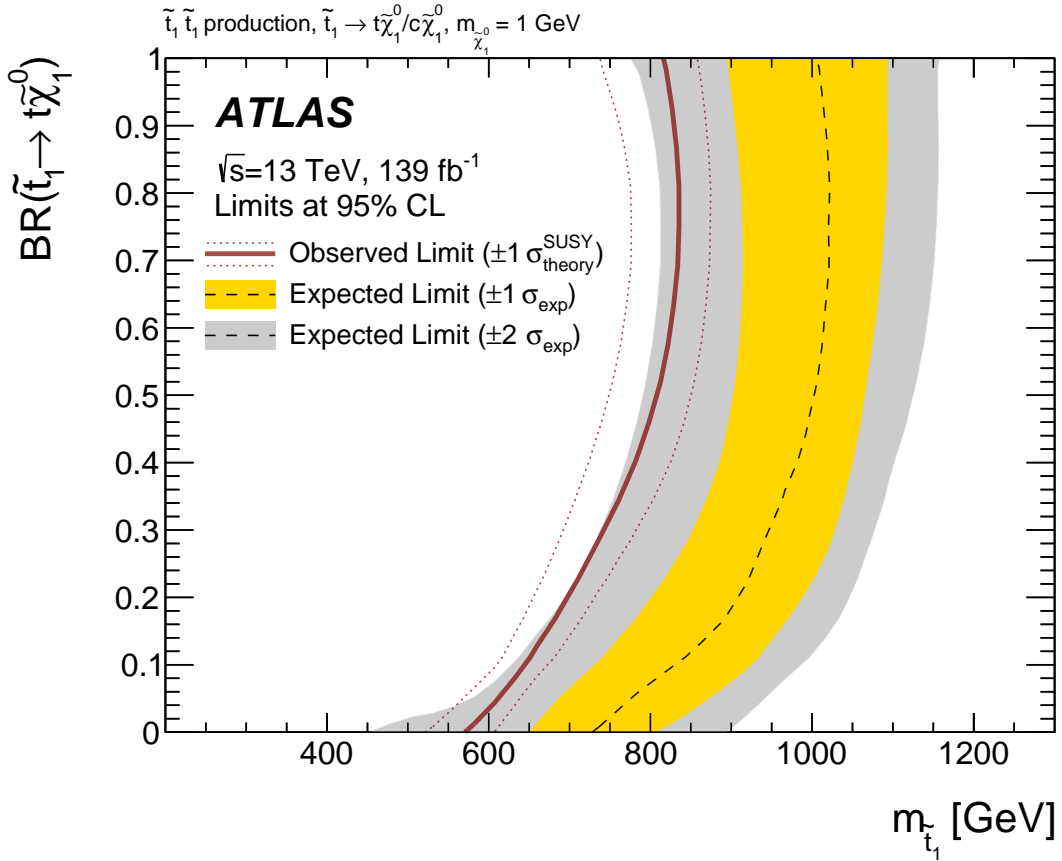


Figure 10: Exclusion limits at the 95% CL in the $m(\tilde{t}_1)$, $\text{BR}(\tilde{t}_1 \rightarrow t + \tilde{\chi}_1^0)$ plane, assuming $m(\tilde{\chi}_1^0) = 1 \text{ GeV}$. The dashed line, yellow band, and grey band present the expected limit, $\pm 1\sigma$ uncertainty, and $\pm 2\sigma$ uncertainty respectively. The solid red line presents the observed upper limit on the signal cross-section. The dashed red lines present the observed upper limit if the signal cross-section is varied by $\pm 1\sigma$ of its predicted theoretical uncertainty.

The model-independent fit is performed by including the signal regions with an inclusive binning to maximise the general sensitivity to new phenomena, as previously discussed. A profile-likelihood-ratio statistic is used with a signal strength of μ_{sig} assumed to contribute only to the SR, and is used to assess the p -value of the background-only hypothesis, and to extract observed and expected 95% confidence level (CL) limits on the number of signal events (S_{obs}^{95} and S_{exp}^{95} respectively). The 95% CL limit on the observed visible cross-section ($\epsilon\sigma_{\text{obs}}^{95}$, where ϵ denotes the efficiency times acceptance) is calculated by dividing S_{obs}^{95} by the total integrated luminosity. Table 5 presents these results for the inclusive SRs. The calculated p -values (and thus model-independent limits) generally reflect the 1.8σ differences between the observed and expected yields in the SRs.

Table 5: 95% CL upper limits on the visible cross-section ($\langle \epsilon\sigma \rangle_{\text{obs}}^{95}$) and on the number of signal events (S_{obs}^{95}). The third column (S_{exp}^{95}) shows the 95% CL upper limit on the number of signal events, given the expected number (and $\pm 1\sigma$ shifts of the expectation) of background events. The last two columns indicate the CL_B value, which provides a measure of compatibility of the observed data with the 95% CL signal strength hypothesis relative to the fluctuations of the background, and the discovery p -value (p_0) together with its corresponding Gaussian significance (Z), which measures compatibility of the observed data with the background-only (zero signal strength) hypothesis relative to fluctuations of the background.

Signal region	$\langle \epsilon\sigma \rangle_{\text{obs}}^{95}$ [fb]	S_{obs}^{95}	S_{exp}^{95}	CL_B	p_0 (Z)
SRA ($m_{T2}(j_{R=1.0}^b, c) \geq 450$ GeV)	0.10	14.4	$8.4_{-1.9}^{+3.5}$	0.94	0.02 (2.1)
SRA ($m_{T2}(j_{R=1.0}^b, c) \geq 575$ GeV)	0.07	9.4	$5.8_{-1.2}^{+2.9}$	0.89	0.04 (1.7)
SRB ($m_T(j, E_T^{\text{miss}})_{\text{close}} \geq 100$ GeV)	0.17	24.1	$16.8_{-5.2}^{+7.0}$	0.85	0.09 (1.3)
SRB ($m_T(j, E_T^{\text{miss}})_{\text{close}} \geq 150$ GeV)	0.16	22.8	$13.2_{-3.6}^{+5.5}$	0.95	0.03 (1.9)
SRB ($m_T(j, E_T^{\text{miss}})_{\text{close}} \geq 400$ GeV)	0.08	11.3	$6.5_{-1.6}^{+3.1}$	0.92	0.04 (1.8)
SRC ($m_T(j, E_T^{\text{miss}})_{\text{close}} \geq 100$ GeV)	0.09	12.6	$9.6_{-2.1}^{+4.2}$	0.76	0.22 (0.76)
SRC ($m_T(j, E_T^{\text{miss}})_{\text{close}} \geq 150$ GeV)	0.09	11.9	$8.7_{-1.9}^{+3.9}$	0.81	0.15 (1.0)
SRC ($m_T(j, E_T^{\text{miss}})_{\text{close}} \geq 300$ GeV)	0.08	11.0	$7.8_{-1.7}^{+3.6}$	0.83	0.13 (1.1)
SRC ($m_T(j, E_T^{\text{miss}})_{\text{close}} \geq 500$ GeV)	0.02	2.5	$4.0_{-1.4}^{+2.4}$	0.13	0.50 (0.00)
SRD ($m_{\text{eff}} \geq 750$ GeV, $m_T(j, E_T^{\text{miss}})_{\text{close}} \geq 200$ GeV)	0.15	20.4	$18.5_{-5.1}^{+8.4}$	0.58	0.50 (0.00)
SRD ($m_{\text{eff}} \geq 1000$ GeV, $m_T(j, E_T^{\text{miss}})_{\text{close}} \geq 200$ GeV)	0.10	13.9	$13.7_{-5.7}^{+3.5}$	0.52	0.50 (0.00)
SRD ($m_{\text{eff}} \geq 1250$ GeV)	0.30	41	37_{-11}^{+12}	0.60	0.50 (0.00)
SRD ($m_{\text{eff}} \geq 1500$ GeV)	0.09	12.9	$14.6_{-4.1}^{+6.3}$	0.36	0.50 (0.00)
SRD ($m_{\text{eff}} \geq 1750$ GeV)	0.09	12.1	$9.1_{-1.9}^{+3.9}$	0.77	0.20 (0.84)
SRD ($m_{\text{eff}} \geq 2000$ GeV)	0.05	7.3	$5.6_{-1.2}^{+3.0}$	0.70	0.26 (0.64)

8 Conclusion

This paper presented a first search for \tilde{t}_1 pair production leading to signatures with mixed final state containing a top-quark, a charm-quark and missing transverse momentum. Signal regions are defined based on recent top- and charm-tagging techniques developed by the ATLAS Collaboration. Neural networks are also used to increase the discrimination of backgrounds for compressed signal scenarios, traditionally difficult to probe. The SM background prediction is corrected in dedicated control regions and verified in validation regions, both depleted of signal contributions but representative of the kinematics of the SRs.

A multi-bin profile likelihood fit is performed to assess the agreement of the signal and SM predictions against data. No significant deviations are observed from the expected background prediction. The largest deviation reaches a significance of 1.8σ in the SRs targeting the bulk and intermediate region of parameter space. In the optimal scenario for this analysis, where the branching ratios for the $\tilde{t}_1 \rightarrow t + \tilde{\chi}_1^0$ and $\tilde{t}_1 \rightarrow c + \tilde{\chi}_1^0$ are equal, an exclusion on the top-squark masses up to 800 GeV is found for light neutralinos. In the compressed region, considering the same branching ratio scenario, top-squark masses up to 600 GeV are excluded. These constitute the first results to date at the LHC on a search for BSM physics in this final-state signature.

Acknowledgements

We thank CERN for the very successful operation of the LHC and its injectors, as well as the support staff at CERN and at our institutions worldwide without whom ATLAS could not be operated efficiently.

The crucial computing support from all WLCG partners is acknowledged gratefully, in particular from CERN, the ATLAS Tier-1 facilities at TRIUMF/SFU (Canada), NDGF (Denmark, Norway, Sweden), CC-IN2P3 (France), KIT/GridKA (Germany), INFN-CNAF (Italy), NL-T1 (Netherlands), PIC (Spain), RAL (UK) and BNL (USA), the Tier-2 facilities worldwide and large non-WLCG resource providers. Major contributors of computing resources are listed in Ref. [86].

We gratefully acknowledge the support of ANPCyT, Argentina; YerPhI, Armenia; ARC, Australia; BMWFW and FWF, Austria; ANAS, Azerbaijan; CNPq and FAPESP, Brazil; NSERC, NRC and CFI, Canada; CERN; ANID, Chile; CAS, MOST and NSFC, China; Minciencias, Colombia; MEYS CR, Czech Republic; DNRf and DNSRC, Denmark; IN2P3-CNRS and CEA-DRF/IRFU, France; SRNSFG, Georgia; BMBF, HGF and MPG, Germany; GSRI, Greece; RGC and Hong Kong SAR, China; ISF and Benozziyo Center, Israel; INFN, Italy; MEXT and JSPS, Japan; CNRST, Morocco; NWO, Netherlands; RCN, Norway; MEiN, Poland; FCT, Portugal; MNE/IFA, Romania; MESTD, Serbia; MSSR, Slovakia; ARRS and MIZŠ, Slovenia; DSI/NRF, South Africa; MICINN, Spain; SRC and Wallenberg Foundation, Sweden; SERI, SNSF and Cantons of Bern and Geneva, Switzerland; MOST, Taipei; TENMAK, Türkiye; STFC, United Kingdom; DOE and NSF, United States of America.

Individual groups and members have received support from BCKDF, CANARIE, CRC and DRAC, Canada; CERN-CZ, PRIMUS 21/SCI/017 and UNCE SCI/013, Czech Republic; COST, ERC, ERDF, Horizon 2020, ICSC-NextGenerationEU and Marie Skłodowska-Curie Actions, European Union; Investissements d’Avenir Labex, Investissements d’Avenir Idex and ANR, France; DFG and AvH Foundation, Germany; Herakleitos, Thales and Aristeia programmes co-financed by EU-ESF and the Greek NSRF, Greece; BSF-NSF and MINERVA, Israel; Norwegian Financial Mechanism 2014-2021, Norway; NCN and NAWA, Poland; La Caixa Banking Foundation, CERCA Programme Generalitat de Catalunya and PROMETEO and GenT

Programmes Generalitat Valenciana, Spain; Göran Gustafssons Stiftelse, Sweden; The Royal Society and Leverhulme Trust, United Kingdom.

In addition, individual members wish to acknowledge support from Chile: Agencia Nacional de Investigación y Desarrollo (FONDECYT 1190886, FONDECYT 1210400, FONDECYT 1230987); China: National Natural Science Foundation of China (NSFC - 12175119, NSFC 12275265, NSFC-12075060); Czech Republic: PRIMUS Research Programme (PRIMUS/21/SCI/017); European Union: European Research Council (ERC - 948254), Horizon 2020 Framework Programme (MUCCA - CHIST-ERA-19-XAI-00), Italian Center for High Performance Computing, Big Data and Quantum Computing (ICSC, NextGenerationEU), Marie Skłodowska-Curie Actions (EU H2020 MSC IF GRANT NO 101033496); France: Agence Nationale de la Recherche (ANR-20-CE31-0013, ANR-21-CE31-0013, ANR-21-CE31-0022), Investissements d'Avenir Idex (ANR-11-LABX-0012), Investissements d'Avenir Labex (ANR-11-LABX-0012); Germany: Baden-Württemberg Stiftung (BW Stiftung-Postdoc Eliteprogramme), Deutsche Forschungsgemeinschaft (DFG - CR 312/5-1); Italy: Istituto Nazionale di Fisica Nucleare (FELLINI G.A. n. 754496, ICSC, NextGenerationEU); Japan: Japan Society for the Promotion of Science (JSPS KAKENHI JP21H05085, JSPS KAKENHI JP22H01227, JSPS KAKENHI JP22H04944); Netherlands: Netherlands Organisation for Scientific Research (NWO Veni 2020 - VI.Veni.202.179); Norway: Research Council of Norway (RCN-314472); Poland: Polish National Agency for Academic Exchange (PPN/PPO/2020/1/00002/U/00001), Polish National Science Centre (NCN 2021/42/E/ST2/00350, NCN OPUS nr 2022/47/B/ST2/03059, NCN UMO-2019/34/E/ST2/00393, UMO-2020/37/B/ST2/01043, UMO-2021/40/C/ST2/00187); Slovenia: Slovenian Research Agency (ARIS grant J1-3010); Spain: BBVA Foundation (LEO22-1-603), Generalitat Valenciana (Artemisa, FEDER, IDIFEDER/2018/048), La Caixa Banking Foundation (LCF/BQ/PI20/11760025), Ministry of Science and Innovation (MCIN & NextGenEU -PCI2022-135018-2, MICIN & FEDER -PID2021-125273NB, RYC2019-028510-I, RYC2020-030254-I, RYC2021-031273-I), PROMETEO and GenT Programmes Generalitat Valenciana (CIDEGENT/2019/023, CIDEGENT/2019/027); Sweden: Swedish Research Council (VR 2018-00482, VR 2022-03845, VR 2022-04683, VR grant 2021-03651), Knut and Alice Wallenberg Foundation (KAW 2017.0100, KAW 2018.0157, KAW 2018.0458, KAW 2019.0447); Switzerland: Swiss National Science Foundation (SNSF - PCEFP2_194658); United Kingdom: Leverhulme Trust (Leverhulme Trust RPG-2020-004); United States of America: Neubauer Family Foundation.

References

- [1] H. Goldberg, *Constraint on the Photino Mass from Cosmology*, [Phys. Rev. Lett. **50** \(1983\) 1419](#),
Erratum: [Phys. Rev. Lett. **103** \(2009\) 099905](#).
- [2] J. Ellis, J. Hagelin, D. V. Nanopoulos, K. Olive, and M. Srednicki,
Supersymmetric relics from the big bang, [Nucl. Phys. B **238** \(1984\) 453](#).
- [3] Y. Golfand and E. Likhtman,
Extension of the Algebra of Poincare Group Generators and Violation of P Invariance,
[JETP Lett. **13** \(1971\) 323](#), [[Pisma Zh. Eksp. Teor. Fiz. **13** \(1971\) 452](#)].
- [4] D. Volkov and V. Akulov, *Is the neutrino a goldstone particle?*, [Phys. Lett. B **46** \(1973\) 109](#).
- [5] J. Wess and B. Zumino, *Supergauge transformations in four dimensions*,
[Nucl. Phys. B **70** \(1974\) 39](#).
- [6] J. Wess and B. Zumino, *Supergauge invariant extension of quantum electrodynamics*,
[Nucl. Phys. B **78** \(1974\) 1](#).
- [7] S. Ferrara and B. Zumino, *Supergauge invariant Yang-Mills theories*, [Nucl. Phys. B **79** \(1974\) 413](#).
- [8] A. Salam and J. Strathdee, *Super-symmetry and non-Abelian gauges*, [Phys. Lett. B **51** \(1974\) 353](#).
- [9] G. R. Farrar and P. Fayet, *Phenomenology of the production, decay, and detection of new hadronic states associated with supersymmetry*, [Phys. Lett. B **76** \(1978\) 575](#).
- [10] ATLAS Collaboration, *Search for a scalar partner of the top quark in the all-hadronic $t\bar{t}$ plus missing transverse momentum final state at $\sqrt{s} = 13$ TeV with the ATLAS detector*,
[Eur. Phys. J. C **80** \(2020\) 737](#), arXiv: [2004.14060 \[hep-ex\]](#).
- [11] ATLAS Collaboration, *Search for squarks and gluinos in final states with same-sign leptons and jets using 139 fb^{-1} of data collected with the ATLAS detector*, [JHEP **06** \(2020\) 046](#),
arXiv: [1909.08457 \[hep-ex\]](#).
- [12] ATLAS Collaboration,
Search for new phenomena with top quark pairs in final states with one lepton, jets, and missing transverse momentum in pp collisions at $\sqrt{s} = 13$ TeV with the ATLAS detector,
[JHEP **04** \(2021\) 174](#), arXiv: [2012.03799 \[hep-ex\]](#).
- [13] ATLAS Collaboration, *Search for new phenomena in events with two opposite-charge leptons, jets and missing transverse momentum in pp collisions at $\sqrt{s} = 13$ TeV with the ATLAS detector*,
[JHEP **04** \(2021\) 165](#), arXiv: [2102.01444 \[hep-ex\]](#).
- [14] CMS Collaboration, *Combined searches for the production of supersymmetric top quark partners in proton–proton collisions at $\sqrt{s} = 13$ TeV*, [Eur. Phys. J. C **81** \(2021\) 970](#),
arXiv: [2107.10892 \[hep-ex\]](#).
- [15] CMS Collaboration, *Search for supersymmetry in final states with two or three soft leptons and missing transverse momentum in proton–proton collisions at $\sqrt{s} = 13$ TeV*, [JHEP **04** \(2022\) 091](#),
arXiv: [2111.06296 \[hep-ex\]](#).
- [16] CMS Collaboration, *Search for top squarks in the four-body decay mode with single lepton final states in proton–proton collisions at $\sqrt{s} = 13$ TeV*, [JHEP **06** \(2023\) 060](#),
arXiv: [2301.08096 \[hep-ex\]](#).
- [17] CMS Collaboration, *Search for top squark pair production in a final state with at least one hadronically decaying tau lepton in proton–proton collisions at $\sqrt{s} = 13$ TeV*, [JHEP **07** \(2023\) 110](#),
arXiv: [2304.07174 \[hep-ex\]](#).

- [18] A. Chakraborty et al., *Flavour-violating decays of mixed top-charm squarks at the LHC*, *Eur. Phys. J. C* **78** (2018) 844, arXiv: [1808.07488 \[hep-ph\]](#).
- [19] ATLAS Collaboration, *The ATLAS Experiment at the CERN Large Hadron Collider*, *JINST* **3** (2008) S08003.
- [20] ATLAS Collaboration, *ATLAS Insertable B-Layer: Technical Design Report*, ATLAS-TDR-19; CERN-LHCC-2010-013, 2010, URL: <https://cds.cern.ch/record/1291633>, Addendum: ATLAS-TDR-19-ADD-1; CERN-LHCC-2012-009, 2012, URL: <https://cds.cern.ch/record/1451888>.
- [21] B. Abbott et al., *Production and integration of the ATLAS Insertable B-Layer*, *JINST* **13** (2018) T05008, arXiv: [1803.00844 \[physics.ins-det\]](#).
- [22] G. Avoni et al., *The new LUCID-2 detector for luminosity measurement and monitoring in ATLAS*, *JINST* **13** (2018) P07017.
- [23] ATLAS Collaboration, *Performance of the ATLAS trigger system in 2015*, *Eur. Phys. J. C* **77** (2017) 317, arXiv: [1611.09661 \[hep-ex\]](#).
- [24] ATLAS Collaboration, *The ATLAS Collaboration Software and Firmware*, ATL-SOFT-PUB-2021-001, 2021, URL: <https://cds.cern.ch/record/2767187>.
- [25] ATLAS Collaboration, *ATLAS data quality operations and performance for 2015–2018 data-taking*, *JINST* **15** (2020) P04003, arXiv: [1911.04632 \[physics.ins-det\]](#).
- [26] ATLAS Collaboration, *Luminosity determination in pp collisions at $\sqrt{s} = 13$ TeV using the ATLAS detector at the LHC*, ATLAS-CONF-2019-021, 2019, URL: <https://cds.cern.ch/record/2677054>.
- [27] ATLAS Collaboration, *Performance of the missing transverse momentum triggers for the ATLAS detector during Run-2 data taking*, *JHEP* **08** (2020) 080, arXiv: [2005.09554 \[hep-ex\]](#).
- [28] ATLAS Collaboration, *Performance of the ATLAS muon triggers in Run 2*, *JINST* **15** (2020) P09015, arXiv: [2004.13447 \[physics.ins-det\]](#).
- [29] ATLAS Collaboration, *Performance of electron and photon triggers in ATLAS during LHC Run 2*, *Eur. Phys. J. C* **80** (2020) 47, arXiv: [1909.00761 \[hep-ex\]](#).
- [30] J. Alwall et al., *The automated computation of tree-level and next-to-leading order differential cross sections, and their matching to parton shower simulations*, *JHEP* **07** (2014) 079, arXiv: [1405.0301 \[hep-ph\]](#).
- [31] NNPDF Collaboration, R. D. Ball, et al., *Parton distributions for the LHC run II*, *JHEP* **04** (2015) 040, arXiv: [1410.8849 \[hep-ph\]](#).
- [32] T. Sjöstrand et al., *An introduction to PYTHIA 8.2*, *Comput. Phys. Commun.* **191** (2015) 159, arXiv: [1410.3012 \[hep-ph\]](#).
- [33] ATLAS Collaboration, *ATLAS Pythia 8 tunes to 7 TeV data*, ATL-PHYS-PUB-2014-021, 2014, URL: <https://cds.cern.ch/record/1966419>.
- [34] D. J. Lange, *The EvtGen particle decay simulation package*, *Nucl. Instrum. Meth. A* **462** (2001) 152.
- [35] W. Beenakker, M. Krämer, T. Plehn, M. Spira, and P. Zerwas, *Stop production at hadron colliders*, *Nucl. Phys. B* **515** (1998) 3, arXiv: [hep-ph/9710451](#).

- [36] W. Beenakker et al., *Supersymmetric top and bottom squark production at hadron colliders*, *JHEP* **08** (2010) 098, arXiv: [1006.4771 \[hep-ph\]](#).
- [37] W. Beenakker et al., *Squark and gluino hadroproduction*, *Int. J. Mod. Phys. A* **26** (2011) 2637, arXiv: [1105.1110 \[hep-ph\]](#).
- [38] ATLAS Collaboration, *The ATLAS Simulation Infrastructure*, *Eur. Phys. J. C* **70** (2010) 823, arXiv: [1005.4568 \[physics.ins-det\]](#).
- [39] S. Agostinelli et al., *GEANT4 – a simulation toolkit*, *Nucl. Instrum. Meth. A* **506** (2003) 250.
- [40] ATLAS Collaboration, *The Pythia 8 A3 tune description of ATLAS minimum bias and inelastic measurements incorporating the Donnachie–Landshoff diffractive model*, ATL-PHYS-PUB-2016-017, 2016, URL: <https://cds.cern.ch/record/2206965>.
- [41] NNPDF Collaboration, R. D. Ball, et al., *Parton distributions with LHC data*, *Nucl. Phys. B* **867** (2013) 244, arXiv: [1207.1303 \[hep-ph\]](#).
- [42] T. Gleisberg et al., *Event generation with SHERPA 1.1*, *JHEP* **02** (2009) 007, arXiv: [0811.4622 \[hep-ph\]](#).
- [43] S. Catani, L. Cieri, G. Ferrera, D. de Florian, and M. Grazzini, *Vector Boson Production at Hadron Colliders: A Fully Exclusive QCD Calculation at Next-to-Next-to-Leading Order*, *Phys. Rev. Lett.* **103** (2009) 082001, arXiv: [0903.2120 \[hep-ph\]](#).
- [44] E. Bothmann et al., *Event generation with Sherpa 2.2*, *SciPost Phys.* **7** (2019) 034, arXiv: [1905.09127 \[hep-ph\]](#).
- [45] S. Alioli, P. Nason, C. Oleari, and E. Re, *A general framework for implementing NLO calculations in shower Monte Carlo programs: the POWHEG BOX*, *JHEP* **06** (2010) 043, arXiv: [1002.2581 \[hep-ph\]](#).
- [46] M. Cacciari, M. Czakon, M. Mangano, A. Mitov, and P. Nason, *Top-pair production at hadron colliders with next-to-next-to-leading logarithmic soft-gluon resummation*, *Phys. Lett. B* **710** (2012) 612, arXiv: [1111.5869 \[hep-ph\]](#).
- [47] M. Czakon and A. Mitov, *Top++: A program for the calculation of the top-pair cross-section at hadron colliders*, *Comput. Phys. Commun.* **185** (2014) 2930, arXiv: [1112.5675 \[hep-ph\]](#).
- [48] N. Kidonakis, *Next-to-next-to-leading-order collinear and soft gluon corrections for t-channel single top quark production*, *Phys. Rev. D* **83** (2011) 091503, arXiv: [1103.2792 \[hep-ph\]](#).
- [49] N. Kidonakis, *Two-loop soft anomalous dimensions for single top quark associated production with a W^- or H^-* , *Phys. Rev. D* **82** (2010) 054018, arXiv: [1005.4451 \[hep-ph\]](#).
- [50] N. Kidonakis, *Next-to-next-to-leading logarithm resummation for s-channel single top quark production*, *Phys. Rev. D* **81** (2010) 054028, arXiv: [1001.5034 \[hep-ph\]](#).
- [51] ATLAS Collaboration, *Topological cell clustering in the ATLAS calorimeters and its performance in LHC Run 1*, *Eur. Phys. J. C* **77** (2017) 490, arXiv: [1603.02934 \[hep-ex\]](#).
- [52] ATLAS Collaboration, *ATLAS flavour-tagging algorithms for the LHC Run 2 pp collision dataset*, *Eur. Phys. J. C* **83** (2023) 681, arXiv: [2211.16345 \[physics.data-an\]](#).

- [53] ATLAS Collaboration, *Performance of top-quark and W-boson tagging with ATLAS in Run 2 of the LHC*, *Eur. Phys. J. C* **79** (2019) 375, arXiv: [1808.07858 \[hep-ex\]](#).
- [54] ATLAS Collaboration, *Electron and photon performance measurements with the ATLAS detector using the 2015–2017 LHC proton–proton collision data*, *JINST* **14** (2019) P12006, arXiv: [1908.00005 \[hep-ex\]](#).
- [55] ATLAS Collaboration, *Muon reconstruction and identification efficiency in ATLAS using the full Run 2 pp collision data set at $\sqrt{s} = 13$ TeV*, *Eur. Phys. J. C* **81** (2021) 578, arXiv: [2012.00578 \[hep-ex\]](#).
- [56] M. Cacciari, G. P. Salam, and G. Soyez, *The anti- k_t jet clustering algorithm*, *JHEP* **04** (2008) 063, arXiv: [0802.1189 \[hep-ph\]](#).
- [57] M. Cacciari, G. P. Salam, and G. Soyez, *FastJet user manual*, *Eur. Phys. J. C* **72** (2012) 1896, arXiv: [1111.6097 \[hep-ph\]](#).
- [58] ATLAS Collaboration, *Jet reconstruction and performance using particle flow with the ATLAS Detector*, *Eur. Phys. J. C* **77** (2017) 466, arXiv: [1703.10485 \[hep-ex\]](#).
- [59] ATLAS Collaboration, *Performance of pile-up mitigation techniques for jets in pp collisions at $\sqrt{s} = 8$ TeV using the ATLAS detector*, *Eur. Phys. J. C* **76** (2016) 581, arXiv: [1510.03823 \[hep-ex\]](#).
- [60] ATLAS Collaboration, *In situ calibration of large-radius jet energy and mass in 13 TeV proton–proton collisions with the ATLAS detector*, *Eur. Phys. J. C* **79** (2019) 135, arXiv: [1807.09477 \[hep-ex\]](#).
- [61] ATLAS Collaboration, *Performance of missing transverse momentum reconstruction with the ATLAS detector using proton–proton collisions at $\sqrt{s} = 13$ TeV*, *Eur. Phys. J. C* **78** (2018) 903, arXiv: [1802.08168 \[hep-ex\]](#).
- [62] ATLAS Collaboration, *Object-based missing transverse momentum significance in the ATLAS Detector*, ATLAS-CONF-2018-038, 2018, URL: <https://cds.cern.ch/record/2630948>.
- [63] C. G. Lester and D. J. Summers, *Measuring masses of semi-invisibly decaying particle pairs produced at hadron colliders*, *Phys. Lett. B* **463** (1999) 99, arXiv: [hep-ph/9906349](#).
- [64] I. H. Witten, E. Frank, M. A. Hall, and C. J. Pal, “Chapter 10 - Deep learning”, *Data Mining (Fourth Edition)*, ed. by I. H. Witten, E. Frank, M. A. Hall, and C. J. Pal, Fourth Edition, Morgan Kaufmann, 2017 417, ISBN: 978-0-12-804291-5, URL: <https://www.sciencedirect.com/science/article/pii/B9780128042915000106>.
- [65] A. Paszke et al., “PyTorch: An Imperative Style, High-Performance Deep Learning Library”, *Advances in Neural Information Processing Systems* **32**, Curran Associates, Inc., 2019 8024, URL: <http://papers.nips.cc/paper/9015-pytorch-an-imperative-style-high-performance-deep-learning-library.pdf>.
- [66] A. L. Maas, “Rectifier Nonlinearities Improve Neural Network Acoustic Models”, 2013, URL: <https://api.semanticscholar.org/CorpusID:16489696>.

- [67] ATLAS Collaboration, *Measurement of the $t\bar{t}$ production cross-section in the lepton+jets channel at $\sqrt{s} = 13$ TeV with the ATLAS experiment*, *Phys. Lett. B* **810** (2020) 135797, arXiv: [2006.13076 \[hep-ex\]](#).
- [68] ATLAS Collaboration, *Inclusive and differential cross-sections for dilepton $t\bar{t}$ production measured in $\sqrt{s} = 13$ TeV pp collisions with the ATLAS detector*, *JHEP* **07** (2023) 141, arXiv: [2303.15340 \[hep-ex\]](#).
- [69] ATLAS Collaboration, *Jet energy scale and resolution measured in proton–proton collisions at $\sqrt{s} = 13$ TeV with the ATLAS detector*, *Eur. Phys. J. C* **81** (2021) 689, arXiv: [2007.02645 \[hep-ex\]](#).
- [70] ATLAS Collaboration, *ATLAS b -jet identification performance and efficiency measurement with $t\bar{t}$ events in pp collisions at $\sqrt{s} = 13$ TeV*, *Eur. Phys. J. C* **79** (2019) 970, arXiv: [1907.05120 \[hep-ex\]](#).
- [71] ATLAS Collaboration, *Measurement of the c -jet mistagging efficiency in $t\bar{t}$ events using pp collision data at $\sqrt{s} = 13$ TeV collected with the ATLAS detector*, *Eur. Phys. J. C* **82** (2022) 95, arXiv: [2109.10627 \[hep-ex\]](#).
- [72] ATLAS Collaboration, *Calibration of the light-flavour jet mistagging efficiency of the b -tagging algorithms with Z +jets events using 139fb^{-1} of ATLAS proton–proton collision data at $\sqrt{s} = 13$ TeV*, *Eur. Phys. J. C* **83** (2023) 728, arXiv: [2301.06319 \[hep-ex\]](#).
- [73] M. Bähr et al., *Herwig++ physics and manual*, *Eur. Phys. J. C* **58** (2008) 639, arXiv: [0803.0883 \[hep-ph\]](#).
- [74] J. Bellm et al., *Herwig 7.0/Herwig++ 3.0 release note*, *Eur. Phys. J. C* **76** (2016) 196, arXiv: [1512.01178 \[hep-ph\]](#).
- [75] ATLAS Collaboration, *Improvements in $t\bar{t}$ modelling using NLO+PS Monte Carlo generators for Run 2*, ATL-PHYS-PUB-2018-009, 2018, URL: <https://cds.cern.ch/record/2630327>.
- [76] S. Frixione, E. Laenen, P. Motylinski, C. White, and B. R. Webber, *Single-top hadroproduction in association with a W boson*, *JHEP* **07** (2008) 029, arXiv: [0805.3067 \[hep-ph\]](#).
- [77] E. Bothmann, M. Schönherr, and S. Schumann, *Reweighting QCD matrix-element and parton-shower calculations*, *Eur. Phys. J. C* **76** (2016) 590, arXiv: [1606.08753 \[hep-ph\]](#).
- [78] ATLAS Collaboration, *Measurements of the inclusive and differential production cross sections of a top-quark-antiquark pair in association with a Z boson at $\sqrt{s} = 13$ TeV with the ATLAS detector*, *Eur. Phys. J. C* **81** (2021) 737, arXiv: [2103.12603 \[hep-ex\]](#).
- [79] ATLAS Collaboration, *Observation of the associated production of a top quark and a Z boson in pp collisions at $\sqrt{s} = 13$ TeV with the ATLAS detector*, *JHEP* **07** (2020) 124, arXiv: [2002.07546 \[hep-ex\]](#).
- [80] ATLAS Collaboration, *Measurements of $W^+W^- + \geq 1$ jet production cross-sections in pp collisions at $\sqrt{s} = 13$ TeV with the ATLAS detector*, *JHEP* **06** (2021) 003, arXiv: [2103.10319 \[hep-ex\]](#).
- [81] ATLAS Collaboration, *Measurement of the $t\bar{t}Z$ and $t\bar{t}W$ cross sections in proton–proton collisions at $\sqrt{s} = 13$ TeV with the ATLAS detector*, *Phys. Rev. D* **99** (2019) 072009, arXiv: [1901.03584 \[hep-ex\]](#).

- [82] ATLAS Collaboration, *Observation of electroweak production of two jets and a Z-boson pair*, *Nature Phys.* **19** (2023) 237, arXiv: [2004.10612 \[hep-ex\]](#).
- [83] ATLAS Collaboration, *Measurements of differential cross-sections in four-lepton events in 13 TeV proton–proton collisions with the ATLAS detector*, *JHEP* **07** (2021) 005, arXiv: [2103.01918 \[hep-ex\]](#).
- [84] M. Baak et al., *HistFitter software framework for statistical data analysis*, *Eur. Phys. J. C* **75** (2015) 153, arXiv: [1410.1280 \[hep-ex\]](#).
- [85] R. D. Cousins, J. T. Linnemann, and J. Tucker, *Evaluation of three methods for calculating statistical significance when incorporating a systematic uncertainty into a test of the background-only hypothesis for a Poisson process*, *Nucl. Instrum. Meth. A* **595** (2008) 480, arXiv: [physics/0702156 \[physics.data-an\]](#).
- [86] ATLAS Collaboration, *ATLAS Computing Acknowledgements*, ATL-SOFT-PUB-2023-001, 2023, URL: <https://cds.cern.ch/record/2869272>.

The ATLAS Collaboration

G. Aad ¹⁰², B. Abbott ¹²⁰, K. Abeling ⁵⁵, N.J. Abicht ⁴⁹, S.H. Abidi ²⁹, A. Aboulhorma ^{35e}, H. Abramowicz ¹⁵¹, H. Abreu ¹⁵⁰, Y. Abulaiti ¹¹⁷, B.S. Acharya ^{69a,69b,m}, C. Adam Bourdarios ⁴, L. Adamczyk ^{86a}, S.V. Addepalli ²⁶, M.J. Addison ¹⁰¹, J. Adelman ¹¹⁵, A. Adiguzel ^{21c}, T. Adye ¹³⁴, A.A. Affolder ¹³⁶, Y. Afik ³⁶, M.N. Agaras ¹³, J. Agarwala ^{73a,73b}, A. Aggarwal ¹⁰⁰, C. Agheorghiesei ^{27c}, A. Ahmad ³⁶, F. Ahmadov ^{38,y}, W.S. Ahmed ¹⁰⁴, S. Ahuja ⁹⁵, X. Ai ^{62a}, G. Aielli ^{76a,76b}, A. Aikot ¹⁶³, M. Ait Tamlihat ^{35e}, B. Aitbenchikh ^{35a}, I. Aizenberg ¹⁶⁹, M. Akbiyik ¹⁰⁰, T.P.A. Åkesson ⁹⁸, A.V. Akimov ³⁷, D. Akiyama ¹⁶⁸, N.N. Akolkar ²⁴, S. Aktas ^{21a}, K. Al Houry ⁴¹, G.L. Alberghi ^{23b}, J. Albert ¹⁶⁵, P. Albicocco ⁵³, G.L. Albouy ⁶⁰, S. Alderweireldt ⁵², Z.L. Alegria ¹²¹, M. Aleksa ³⁶, I.N. Aleksandrov ³⁸, C. Alexa ^{27b}, T. Alexopoulos ¹⁰, F. Alfonsi ^{23b}, M. Algren ⁵⁶, M. Alhroob ¹²⁰, B. Ali ¹³², H.M.J. Ali ⁹¹, S. Ali ¹⁴⁸, S.W. Alibocus ⁹², M. Aliev ¹⁴⁵, G. Alimonti ^{71a}, W. Alkakhki ⁵⁵, C. Allaire ⁶⁶, B.M.M. Allbrooke ¹⁴⁶, J.F. Allen ⁵², C.A. Allendes Flores ^{137f}, P.P. Allport ²⁰, A. Aloisio ^{72a,72b}, F. Alonso ⁹⁰, C. Alpigiani ¹³⁸, M. Alvarez Estevez ⁹⁹, A. Alvarez Fernandez ¹⁰⁰, M. Alves Cardoso ⁵⁶, M.G. Alviggi ^{72a,72b}, M. Aly ¹⁰¹, Y. Amaral Coutinho ^{83b}, A. Ambler ¹⁰⁴, C. Amelung ³⁶, M. Amerl ¹⁰¹, C.G. Ames ¹⁰⁹, D. Amidei ¹⁰⁶, S.P. Amor Dos Santos ^{130a}, K.R. Amos ¹⁶³, V. Ananiev ¹²⁵, C. Anastopoulos ¹³⁹, T. Andeen ¹¹, J.K. Anders ³⁶, S.Y. Andreev ^{47a,47b}, A. Andreatta ^{71a,71b}, S. Angelidakis ⁹, A. Angerami ^{41,ab}, A.V. Anisenkov ³⁷, A. Annovi ^{74a}, C. Antel ⁵⁶, M.T. Anthony ¹³⁹, E. Antipov ¹⁴⁵, M. Antonelli ⁵³, F. Anulli ^{75a}, M. Aoki ⁸⁴, T. Aoki ¹⁵³, J.A. Aparisi Pozo ¹⁶³, M.A. Aparo ¹⁴⁶, L. Aperio Bella ⁴⁸, C. Appelt ¹⁸, A. Apyan ²⁶, N. Aranzabal ³⁶, S.J. Arbiol Val ⁸⁷, C. Arcangeletti ⁵³, A.T.H. Arce ⁵¹, E. Arena ⁹², J-F. Arguin ¹⁰⁸, S. Argyropoulos ⁵⁴, J.-H. Arling ⁴⁸, O. Arnaez ⁴, H. Arnold ¹¹⁴, G. Artoni ^{75a,75b}, H. Asada ¹¹¹, K. Asai ¹¹⁸, S. Asai ¹⁵³, N.A. Asbah ⁶¹, K. Assamagan ²⁹, R. Astalos ^{28a}, S. Atashi ¹⁶⁰, R.J. Atkin ^{33a}, M. Atkinson ¹⁶², H. Atmani ^{35f}, P.A. Atlasiddha ¹²⁸, K. Augsten ¹³², S. Auricchio ^{72a,72b}, A.D. Auriol ²⁰, V.A. Austrup ¹⁰¹, G. Avolio ³⁶, K. Axiotis ⁵⁶, G. Azuelos ^{108,af}, D. Babal ^{28b}, H. Bachacou ¹³⁵, K. Bachas ^{152,p}, A. Bachi ³⁴, F. Backman ^{47a,47b}, A. Badea ⁶¹, T.M. Baer ¹⁰⁶, P. Bagnaia ^{75a,75b}, M. Bahmani ¹⁸, D. Bahner ⁵⁴, A.J. Bailey ¹⁶³, V.R. Bailey ¹⁶², J.T. Baines ¹³⁴, L. Baines ⁹⁴, O.K. Baker ¹⁷², E. Bakos ¹⁵, D. Bakshi Gupta ⁸, V. Balakrishnan ¹²⁰, R. Balasubramanian ¹¹⁴, E.M. Baldin ³⁷, P. Balek ^{86a}, E. Ballabene ^{23b,23a}, F. Balli ¹³⁵, L.M. Baltes ^{63a}, W.K. Balunas ³², J. Balz ¹⁰⁰, E. Banas ⁸⁷, M. Bandieramonte ¹²⁹, A. Bandyopadhyay ²⁴, S. Bansal ²⁴, L. Barak ¹⁵¹, M. Barakat ⁴⁸, E.L. Barberio ¹⁰⁵, D. Barberis ^{57b,57a}, M. Barbero ¹⁰², M.Z. Barel ¹¹⁴, K.N. Barends ^{33a}, T. Barillari ¹¹⁰, M-S. Barisits ³⁶, T. Barklow ¹⁴³, P. Baron ¹²², D.A. Baron Moreno ¹⁰¹, A. Baroncelli ^{62a}, G. Barone ²⁹, A.J. Barr ¹²⁶, J.D. Barr ⁹⁶, L. Barranco Navarro ^{47a,47b}, F. Barreiro ⁹⁹, J. Barreiro Guimarães da Costa ^{14a}, U. Barron ¹⁵¹, M.G. Barros Teixeira ^{130a}, S. Barsov ³⁷, F. Bartels ^{63a}, R. Bartoldus ¹⁴³, A.E. Barton ⁹¹, P. Bartos ^{28a}, A. Basan ¹⁰⁰, M. Baselga ⁴⁹, A. Bassalat ^{66,b}, M.J. Basso ^{156a}, C.R. Basson ¹⁰¹, R.L. Bates ⁵⁹, S. Batlamous ^{35e}, J.R. Batley ³², B. Batool ¹⁴¹, M. Battaglia ¹³⁶, D. Battulga ¹⁸, M. Baunce ^{75a,75b}, M. Bauer ³⁶, P. Bauer ²⁴, L.T. Bazzano Hurrell ³⁰, J.B. Beacham ⁵¹, T. Beau ¹²⁷, J.Y. Beaucamp ⁹⁰, P.H. Beauchemin ¹⁵⁸, F. Becherer ⁵⁴, P. Bechtel ²⁴, H.P. Beck ^{19,o}, K. Becker ¹⁶⁷, A.J. Beddall ⁸², V.A. Bednyakov ³⁸, C.P. Bee ¹⁴⁵, L.J. Beamster ¹⁵, T.A. Beermann ³⁶, M. Begalli ^{83d}, M. Begel ²⁹, A. Behera ¹⁴⁵, J.K. Behr ⁴⁸, J.F. Beirer ³⁶, F. Beisiegel ²⁴, M. Belfkir ¹⁵⁹, G. Bella ¹⁵¹, L. Bellagamba ^{23b}, A. Bellerive ³⁴, P. Bellos ²⁰, K. Beloborodov ³⁷, D. Bencheikroun ^{35a}, F. Bendebba ^{35a}, Y. Benhammou ¹⁵¹, M. Benoit ²⁹, J.R. Bensinger ²⁶, S. Bentvelsen ¹¹⁴, L. Beresford ⁴⁸,

M. Beretta ⁵³, E. Bergeaas Kuutmann ¹⁶¹, N. Berger ⁴, B. Bergmann ¹³², J. Beringer ^{17a},
G. Bernardi ⁵, C. Bernius ¹⁴³, F.U. Bernlochner ²⁴, F. Bernon ^{36,102}, A. Berrocal Guardia ¹³,
T. Berry ⁹⁵, P. Berta ¹³³, A. Berthold ⁵⁰, I.A. Bertram ⁹¹, S. Bethke ¹¹⁰, A. Betti ^{75a,75b},
A.J. Bevan ⁹⁴, N.K. Bhalla ⁵⁴, M. Bhamjee ^{33c}, S. Bhatta ¹⁴⁵, D.S. Bhattacharya ¹⁶⁶,
P. Bhattarai ¹⁴³, V.S. Bhopatkar ¹²¹, R. Bi ^{29,ai}, R.M. Bianchi ¹²⁹, G. Bianco ^{23b,23a}, O. Biebel ¹⁰⁹,
R. Bielski ¹²³, M. Biglietti ^{77a}, M. Bindi ⁵⁵, A. Bingul ^{21b}, C. Bini ^{75a,75b}, A. Biondini ⁹²,
C.J. Birch-sykes ¹⁰¹, G.A. Bird ^{20,134}, M. Birman ¹⁶⁹, M. Biros ¹³³, S. Biryukov ¹⁴⁶,
T. Bisanz ⁴⁹, E. Bisceglie ^{43b,43a}, J.P. Biswal ¹³⁴, D. Biswas ¹⁴¹, A. Bitadze ¹⁰¹, K. Bjørke ¹²⁵,
I. Bloch ⁴⁸, A. Blue ⁵⁹, U. Blumenschein ⁹⁴, J. Blumenthal ¹⁰⁰, G.J. Bobbink ¹¹⁴,
V.S. Bobrovnikov ³⁷, M. Boehler ⁵⁴, B. Boehm ¹⁶⁶, D. Bogavac ³⁶, A.G. Bogdanchikov ³⁷,
C. Bohm ^{47a}, V. Boisvert ⁹⁵, P. Bokan ⁴⁸, T. Bold ^{86a}, M. Bomben ⁵, M. Bona ⁹⁴,
M. Boonekamp ¹³⁵, C.D. Booth ⁹⁵, A.G. Borbély ⁵⁹, I.S. Bordulev ³⁷, H.M. Borecka-Bielska ¹⁰⁸,
G. Borissov ⁹¹, D. Bortoletto ¹²⁶, D. Boscherini ^{23b}, M. Bosman ¹³, J.D. Bossio Sola ³⁶,
K. Bouaouda ^{35a}, N. Bouchhar ¹⁶³, J. Boudreau ¹²⁹, E.V. Bouhova-Thacker ⁹¹, D. Boumediene ⁴⁰,
R. Bouquet ¹⁶⁵, A. Boveia ¹¹⁹, J. Boyd ³⁶, D. Boye ²⁹, I.R. Boyko ³⁸, J. Bracinik ²⁰,
N. Brahimy ^{62d}, G. Brandt ¹⁷¹, O. Brandt ³², F. Braren ⁴⁸, B. Brau ¹⁰³, J.E. Brau ¹²³,
R. Brenner ¹⁶⁹, L. Brenner ¹¹⁴, R. Brenner ¹⁶¹, S. Bressler ¹⁶⁹, D. Britton ⁵⁹, D. Britzger ¹¹⁰,
I. Brock ²⁴, G. Brooijmans ⁴¹, W.K. Brooks ^{137f}, E. Brost ²⁹, L.M. Brown ¹⁶⁵, L.E. Bruce ⁶¹,
T.L. Bruckler ¹²⁶, P.A. Bruckman de Renstrom ⁸⁷, B. Brüers ⁴⁸, A. Bruni ^{23b}, G. Bruni ^{23b},
M. Bruschi ^{23b}, N. Bruscinò ^{75a,75b}, T. Buanes ¹⁶, Q. Buat ¹³⁸, D. Buchin ¹¹⁰, A.G. Buckley ⁵⁹,
O. Bulekov ³⁷, B.A. Bullard ¹⁴³, S. Burdin ⁹², C.D. Burgard ⁴⁹, A.M. Burger ⁴⁰,
B. Burghgrave ⁸, O. Burlayenko ⁵⁴, J.T.P. Burr ³², C.D. Burton ¹¹, J.C. Burzynski ¹⁴²,
E.L. Busch ⁴¹, V. Büscher ¹⁰⁰, P.J. Bussey ⁵⁹, J.M. Butler ²⁵, C.M. Buttar ⁵⁹,
J.M. Butterworth ⁹⁶, W. Buttinger ¹³⁴, C.J. Buxo Vazquez ¹⁰⁷, A.R. Buzykaev ³⁷,
S. Cabrera Urbán ¹⁶³, L. Cadamuro ⁶⁶, D. Caforio ⁵⁸, H. Cai ¹²⁹, Y. Cai ^{14a,14e}, Y. Cai ^{14c},
V.M.M. Cairo ³⁶, O. Cakir ^{3a}, N. Calace ³⁶, P. Calafiura ^{17a}, G. Calderini ¹²⁷, P. Calfayan ⁶⁸,
G. Callea ⁵⁹, L.P. Caloba ^{83b}, D. Calvet ⁴⁰, S. Calvet ⁴⁰, T.P. Calvet ¹⁰², M. Calvetti ^{74a,74b},
R. Camacho Toro ¹²⁷, S. Camarda ³⁶, D. Camarero Munoz ²⁶, P. Camarri ^{76a,76b},
M.T. Camerlingo ^{72a,72b}, D. Cameron ³⁶, C. Camincher ¹⁶⁵, M. Campanelli ⁹⁶, A. Camplani ⁴²,
V. Canale ^{72a,72b}, A. Canesse ¹⁰⁴, J. Cantero ¹⁶³, Y. Cao ¹⁶², F. Capocasa ²⁶, M. Capua ^{43b,43a},
A. Carbone ^{71a,71b}, R. Cardarelli ^{76a}, J.C.J. Cardenas ⁸, F. Cardillo ¹⁶³, G. Carducci ^{43b,43a},
T. Carli ³⁶, G. Carlino ^{72a}, J.I. Carlotto ¹³, B.T. Carlson ^{129,q}, E.M. Carlson ^{165,156a},
L. Carminati ^{71a,71b}, A. Carnelli ¹³⁵, M. Carnesale ^{75a,75b}, S. Caron ¹¹³, E. Carquin ^{137f},
S. Carrá ^{71a}, G. Carratta ^{23b,23a}, F. Carrio Argos ^{33g}, J.W.S. Carter ¹⁵⁵, T.M. Carter ⁵²,
M.P. Casado ^{13,i}, M. Caspar ⁴⁸, F.L. Castillo ⁴, L. Castillo Garcia ¹³, V. Castillo Gimenez ¹⁶³,
N.F. Castro ^{130a,130e}, A. Catinaccio ³⁶, J.R. Catmore ¹²⁵, V. Cavaliere ²⁹, N. Cavalli ^{23b,23a},
V. Cavasinni ^{74a,74b}, Y.C. Cekmecelioglu ⁴⁸, E. Celebi ^{21a}, F. Celli ¹²⁶, M.S. Centonze ^{70a,70b},
V. Cepaitis ⁵⁶, K. Cerny ¹²², A.S. Cerqueira ^{83a}, A. Cerri ¹⁴⁶, L. Cerrito ^{76a,76b}, F. Cerutti ^{17a},
B. Cervato ¹⁴¹, A. Cervelli ^{23b}, G. Cesarini ⁵³, S.A. Cetin ⁸², D. Chakraborty ¹¹⁵, J. Chan ¹⁷⁰,
W.Y. Chan ¹⁵³, J.D. Chapman ³², E. Chapon ¹³⁵, B. Chargeishvili ^{149b}, D.G. Charlton ²⁰,
M. Chatterjee ¹⁹, C. Chauhan ¹³³, S. Chekanov ⁶, S.V. Chekulaev ^{156a}, G.A. Chelkov ^{38,a},
A. Chen ¹⁰⁶, B. Chen ¹⁵¹, B. Chen ¹⁶⁵, H. Chen ^{14c}, H. Chen ²⁹, J. Chen ^{62c}, J. Chen ¹⁴²,
M. Chen ¹²⁶, S. Chen ¹⁵³, S.J. Chen ^{14c}, X. Chen ^{62c,135}, X. Chen ^{14b,ae}, Y. Chen ^{62a},
C.L. Cheng ¹⁷⁰, H.C. Cheng ^{64a}, S. Cheong ¹⁴³, A. Cheplakov ³⁸, E. Cheremushkina ⁴⁸,
E. Cherepanova ¹¹⁴, R. Cherkaoui El Moursli ^{35e}, E. Cheu ⁷, K. Cheung ⁶⁵, L. Chevalier ¹³⁵,
V. Chiarella ⁵³, G. Chiarelli ^{74a}, N. Chiedde ¹⁰², G. Chiodini ^{70a}, A.S. Chisholm ²⁰,
A. Chitan ^{27b}, M. Chitishvili ¹⁶³, M.V. Chizhov ³⁸, K. Choi ¹¹, A.R. Chomont ^{75a,75b},

Y. Chou [id](#)¹⁰³, E.Y.S. Chow [id](#)¹¹³, T. Chowdhury [id](#)^{33g}, K.L. Chu [id](#)¹⁶⁹, M.C. Chu [id](#)^{64a}, X. Chu [id](#)^{14a,14e},
 J. Chudoba [id](#)¹³¹, J.J. Chwastowski [id](#)⁸⁷, D. Cieri [id](#)¹¹⁰, K.M. Ciesla [id](#)^{86a}, V. Cindro [id](#)⁹³, A. Ciocio [id](#)^{17a},
 F. Cirotto [id](#)^{72a,72b}, Z.H. Citron [id](#)^{169,k}, M. Citterio [id](#)^{71a}, D.A. Ciubotaru^{27b}, A. Clark [id](#)⁵⁶, P.J. Clark [id](#)⁵²,
 C. Clarry [id](#)¹⁵⁵, J.M. Clavijo Columbie [id](#)⁴⁸, S.E. Clawson [id](#)⁴⁸, C. Clement [id](#)^{47a,47b}, J. Clercx [id](#)⁴⁸,
 Y. Coadou [id](#)¹⁰², M. Cobal [id](#)^{69a,69c}, A. Coccaro [id](#)^{57b}, R.F. Coelho Barrue [id](#)^{130a},
 R. Coelho Lopes De Sa [id](#)¹⁰³, S. Coelli [id](#)^{71a}, A.E.C. Coimbra [id](#)^{71a,71b}, B. Cole [id](#)⁴¹, J. Collot [id](#)⁶⁰,
 P. Conde Muiño [id](#)^{130a,130g}, M.P. Connell [id](#)^{33c}, S.H. Connell [id](#)^{33c}, I.A. Connelly [id](#)⁵⁹, E.I. Conroy [id](#)¹²⁶,
 F. Conventi [id](#)^{72a,ag}, H.G. Cooke [id](#)²⁰, A.M. Cooper-Sarkar [id](#)¹²⁶, A. Cordeiro Oudot Choi [id](#)¹²⁷,
 L.D. Corpe [id](#)⁴⁰, M. Corradi [id](#)^{75a,75b}, F. Corriveau [id](#)^{104,w}, A. Cortes-Gonzalez [id](#)¹⁸, M.J. Costa [id](#)¹⁶³,
 F. Costanza [id](#)⁴, D. Costanzo [id](#)¹³⁹, B.M. Cote [id](#)¹¹⁹, G. Cowan [id](#)⁹⁵, K. Cranmer [id](#)¹⁷⁰,
 D. Cremonini [id](#)^{23b,23a}, S. Crépe-Renaudin [id](#)⁶⁰, F. Crescioli [id](#)¹²⁷, M. Cristinziani [id](#)¹⁴¹,
 M. Cristoforetti [id](#)^{78a,78b}, V. Croft [id](#)¹¹⁴, J.E. Crosby [id](#)¹²¹, G. Crosetti [id](#)^{43b,43a}, A. Cueto [id](#)⁹⁹,
 T. Cuhadar Donszelmann [id](#)¹⁶⁰, H. Cui [id](#)^{14a,14e}, Z. Cui [id](#)⁷, W.R. Cunningham [id](#)⁵⁹, F. Curcio [id](#)^{43b,43a},
 P. Czodrowski [id](#)³⁶, M.M. Czurylo [id](#)^{63b}, M.J. Da Cunha Sargedas De Sousa [id](#)^{57b,57a},
 J.V. Da Fonseca Pinto [id](#)^{83b}, C. Da Via [id](#)¹⁰¹, W. Dabrowski [id](#)^{86a}, T. Dado [id](#)⁴⁹, S. Dahbi [id](#)^{33g},
 T. Dai [id](#)¹⁰⁶, D. Dal Santo [id](#)¹⁹, C. Dallapiccola [id](#)¹⁰³, M. Dam [id](#)⁴², G. D'amen [id](#)²⁹, V. D'Amico [id](#)¹⁰⁹,
 J. Damp [id](#)¹⁰⁰, J.R. Dandoy [id](#)³⁴, M.F. Daneri [id](#)³⁰, M. Danninger [id](#)¹⁴², V. Dao [id](#)³⁶, G. Darbo [id](#)^{57b},
 S. Darmora [id](#)⁶, S.J. Das [id](#)^{29,ai}, S. D'Auria [id](#)^{71a,71b}, C. David [id](#)^{156b}, T. Davidek [id](#)¹³³,
 B. Davis-Purcell [id](#)³⁴, I. Dawson [id](#)⁹⁴, H.A. Day-hall [id](#)¹³², K. De [id](#)⁸, R. De Asmundis [id](#)^{72a},
 N. De Biase [id](#)⁴⁸, S. De Castro [id](#)^{23b,23a}, N. De Groot [id](#)¹¹³, P. de Jong [id](#)¹¹⁴, H. De la Torre [id](#)¹¹⁵,
 A. De Maria [id](#)^{14c}, A. De Salvo [id](#)^{75a}, U. De Sanctis [id](#)^{76a,76b}, F. De Santis [id](#)^{70a,70b}, A. De Santo [id](#)¹⁴⁶,
 J.B. De Vivie De Regie [id](#)⁶⁰, D.V. Dedovich³⁸, J. Degens [id](#)¹¹⁴, A.M. Deiana [id](#)⁴⁴, F. Del Corso [id](#)^{23b,23a},
 J. Del Peso [id](#)⁹⁹, F. Del Rio [id](#)^{63a}, L. Delagrangé [id](#)¹²⁷, F. Deliot [id](#)¹³⁵, C.M. Delitzsch [id](#)⁴⁹,
 M. Della Pietra [id](#)^{72a,72b}, D. Della Volpe [id](#)⁵⁶, A. Dell'Acqua [id](#)³⁶, L. Dell'Asta [id](#)^{71a,71b}, M. Delmastro [id](#)⁴,
 P.A. Delsart [id](#)⁶⁰, S. Demers [id](#)¹⁷², M. Demichev [id](#)³⁸, S.P. Denisov [id](#)³⁷, L. D'Eramo [id](#)⁴⁰,
 D. Derendarz [id](#)⁸⁷, F. Derue [id](#)¹²⁷, P. Dervan [id](#)⁹², K. Desch [id](#)²⁴, C. Deutsch [id](#)²⁴, F.A. Di Bello [id](#)^{57b,57a},
 A. Di Ciaccio [id](#)^{76a,76b}, L. Di Ciaccio [id](#)⁴, A. Di Domenico [id](#)^{75a,75b}, C. Di Donato [id](#)^{72a,72b},
 A. Di Girolamo [id](#)³⁶, G. Di Gregorio [id](#)³⁶, A. Di Luca [id](#)^{78a,78b}, B. Di Micco [id](#)^{77a,77b}, R. Di Nardo [id](#)^{77a,77b},
 C. Diaconu [id](#)¹⁰², M. Diamantopoulou [id](#)³⁴, F.A. Dias [id](#)¹¹⁴, T. Dias Do Vale [id](#)¹⁴², M.A. Diaz [id](#)^{137a,137b},
 F.G. Diaz Capriles [id](#)²⁴, M. Didenko [id](#)¹⁶³, E.B. Diehl [id](#)¹⁰⁶, L. Diehl [id](#)⁵⁴, S. Díez Cornell [id](#)⁴⁸,
 C. Díez Pardos [id](#)¹⁴¹, C. Dimitriadi [id](#)^{161,24}, A. Dimitrievska [id](#)^{17a}, J. Dingfelder [id](#)²⁴, I-M. Dinu [id](#)^{27b},
 S.J. Dittmeier [id](#)^{63b}, F. Dittus [id](#)³⁶, F. Djama [id](#)¹⁰², T. Djobava [id](#)^{149b}, J.I. Djuvsland [id](#)¹⁶,
 C. Doglioni [id](#)^{101,98}, A. Dohnalova [id](#)^{28a}, J. Dolejsi [id](#)¹³³, Z. Dolezal [id](#)¹³³, K.M. Dona [id](#)³⁹,
 M. Donadelli [id](#)^{83c}, B. Dong [id](#)¹⁰⁷, J. Donini [id](#)⁴⁰, A. D'Onofrio [id](#)^{72a,72b}, M. D'Onofrio [id](#)⁹²,
 J. Dopke [id](#)¹³⁴, A. Doria [id](#)^{72a}, N. Dos Santos Fernandes [id](#)^{130a}, P. Dougan [id](#)¹⁰¹, M.T. Dova [id](#)⁹⁰,
 A.T. Doyle [id](#)⁵⁹, M.A. Draguet [id](#)¹²⁶, E. Dreyer [id](#)¹⁶⁹, I. Drivas-koulouris [id](#)¹⁰, M. Drnevich [id](#)¹¹⁷,
 A.S. Drobac [id](#)¹⁵⁸, M. Drozdova [id](#)⁵⁶, D. Du [id](#)^{62a}, T.A. du Pree [id](#)¹¹⁴, F. Dubinin [id](#)³⁷, M. Dubovsky [id](#)^{28a},
 E. Duchovni [id](#)¹⁶⁹, G. Duckeck [id](#)¹⁰⁹, O.A. Ducu [id](#)^{27b}, D. Duda [id](#)⁵², A. Dudarev [id](#)³⁶, E.R. Duden [id](#)²⁶,
 M. D'uffizi [id](#)¹⁰¹, L. Duflo [id](#)⁶⁶, M. Dührssen [id](#)³⁶, C. Dülsen [id](#)¹⁷¹, A.E. Dumitriu [id](#)^{27b}, M. Dunford [id](#)^{63a},
 S. Dungs [id](#)⁴⁹, K. Dunne [id](#)^{47a,47b}, A. Duperrin [id](#)¹⁰², H. Duran Yildiz [id](#)^{3a}, M. Düren [id](#)⁵⁸,
 A. Durglishvili [id](#)^{149b}, B.L. Dwyer [id](#)¹¹⁵, G.I. Dyckes [id](#)^{17a}, M. Dyndal [id](#)^{86a}, B.S. Dziedzic [id](#)⁸⁷,
 Z.O. Earnshaw [id](#)¹⁴⁶, G.H. Eberwein [id](#)¹²⁶, B. Eckerova [id](#)^{28a}, S. Eggebrecht [id](#)⁵⁵,
 E. Egidio Purcino De Souza [id](#)¹²⁷, L.F. Ehrke [id](#)⁵⁶, G. Eigen [id](#)¹⁶, K. Einsweiler [id](#)^{17a}, T. Ekelof [id](#)¹⁶¹,
 P.A. Ekman [id](#)⁹⁸, S. El Farkh [id](#)^{35b}, Y. El Ghazali [id](#)^{35b}, H. El Jarrari [id](#)³⁶, A. El Moussaouy [id](#)¹⁰⁸,
 V. Ellajosyula [id](#)¹⁶¹, M. Ellert [id](#)¹⁶¹, F. Ellinghaus [id](#)¹⁷¹, N. Ellis [id](#)³⁶, J. Elmsheuser [id](#)²⁹, M. Elsing [id](#)³⁶,
 D. Emelianov [id](#)¹³⁴, Y. Enari [id](#)¹⁵³, I. Ene [id](#)^{17a}, S. Epari [id](#)¹³, J. Erdmann [id](#)⁴⁹, P.A. Erland [id](#)⁸⁷,
 M. Errenst [id](#)¹⁷¹, M. Escalier [id](#)⁶⁶, C. Escobar [id](#)¹⁶³, E. Etzion [id](#)¹⁵¹, G. Evans [id](#)^{130a}, H. Evans [id](#)⁶⁸,

L.S. Evans ^{id}95, M.O. Evans ^{id}146, A. Ezhilov ^{id}37, S. Ezzarqtouni ^{id}35a, F. Fabbri ^{id}59, L. Fabbri ^{id}23b,23a, G. Facini ^{id}96, V. Fadeyev ^{id}136, R.M. Fakhrutdinov ^{id}37, D. Fakoudis ^{id}100, S. Falciano ^{id}75a, L.F. Falda Ulhoa Coelho ^{id}36, P.J. Falke ^{id}24, J. Faltova ^{id}133, C. Fan ^{id}162, Y. Fan ^{id}14a, Y. Fang ^{id}14a,14e, M. Fanti ^{id}71a,71b, M. Faraj ^{id}69a,69b, Z. Farazpay ^{id}97, A. Farbin ^{id}8, A. Farilla ^{id}77a, T. Farooque ^{id}107, S.M. Farrington ^{id}52, F. Fassi ^{id}35e, D. Fassouliotis ^{id}9, M. Faucci Giannelli ^{id}76a,76b, W.J. Fawcett ^{id}32, L. Fayard ^{id}66, P. Federic ^{id}133, P. Federicova ^{id}131, O.L. Fedin ^{id}37,a, G. Fedotov ^{id}37, M. Feickert ^{id}170, L. Feligioni ^{id}102, D.E. Fellers ^{id}123, C. Feng ^{id}62b, M. Feng ^{id}14b, Z. Feng ^{id}114, M.J. Fenton ^{id}160, A.B. Fenyuk ^{id}37, L. Ferencz ^{id}48, R.A.M. Ferguson ^{id}91, S.I. Fernandez Luengo ^{id}137f, P. Fernandez Martinez ^{id}13, M.J.V. Fernoux ^{id}102, J. Ferrando ^{id}48, A. Ferrari ^{id}161, P. Ferrari ^{id}114,113, R. Ferrari ^{id}73a, D. Ferrere ^{id}56, C. Ferretti ^{id}106, F. Fiedler ^{id}100, P. Fiedler ^{id}132, A. Filipčič ^{id}93, E.K. Filmer ^{id}1, F. Filthaut ^{id}113, M.C.N. Fiolhais ^{id}130a,130c,c, L. Fiorini ^{id}163, W.C. Fisher ^{id}107, T. Fitschen ^{id}101, P.M. Fitzhugh ^{id}135, I. Fleck ^{id}141, P. Fleischmann ^{id}106, T. Flick ^{id}171, M. Flores ^{id}33d,ac, L.R. Flores Castillo ^{id}64a, L. Flores Sanz De Acedo ^{id}36, F.M. Follega ^{id}78a,78b, N. Fomin ^{id}16, J.H. Foo ^{id}155, B.C. Forland ^{id}68, A. Formica ^{id}135, A.C. Forti ^{id}101, E. Fortin ^{id}36, A.W. Fortman ^{id}61, M.G. Foti ^{id}17a, L. Fountas ^{id}9,j, D. Fournier ^{id}66, H. Fox ^{id}91, P. Francavilla ^{id}74a,74b, S. Francescato ^{id}61, S. Franchellucci ^{id}56, M. Franchini ^{id}23b,23a, S. Franchino ^{id}63a, D. Francis ^{id}36, L. Franco ^{id}113, V. Franco Lima ^{id}36, L. Franconi ^{id}48, M. Franklin ^{id}61, G. Frattari ^{id}26, A.C. Freegard ^{id}94, W.S. Freund ^{id}83b, Y.Y. Frid ^{id}151, J. Friend ^{id}59, N. Fritzsche ^{id}50, A. Froch ^{id}54, D. Froidevaux ^{id}36, J.A. Frost ^{id}126, Y. Fu ^{id}62a, S. Fuenzalida Garrido ^{id}137f, M. Fujimoto ^{id}102, K.Y. Fung ^{id}64a, E. Furtado De Simas Filho ^{id}83b, M. Furukawa ^{id}153, J. Fuster ^{id}163, A. Gabrielli ^{id}23b,23a, A. Gabrielli ^{id}155, P. Gadow ^{id}36, G. Gagliardi ^{id}57b,57a, L.G. Gagnon ^{id}17a, E.J. Gallas ^{id}126, B.J. Gallop ^{id}134, K.K. Gan ^{id}119, S. Ganguly ^{id}153, Y. Gao ^{id}52, F.M. Garay Walls ^{id}137a,137b, B. Garcia ^{id}29, C. García ^{id}163, A. Garcia Alonso ^{id}114, A.G. Garcia Caffaro ^{id}172, J.E. García Navarro ^{id}163, M. Garcia-Sciveres ^{id}17a, G.L. Gardner ^{id}128, R.W. Gardner ^{id}39, N. Garelli ^{id}158, D. Garg ^{id}80, R.B. Garg ^{id}143,n, J.M. Gargan ^{id}52, C.A. Garner ^{id}155, C.M. Garvey ^{id}33a, P. Gaspar ^{id}83b, V.K. Gassmann ^{id}158, G. Gaudio ^{id}73a, V. Gautam ^{id}13, P. Gauzzi ^{id}75a,75b, I.L. Gavrilenko ^{id}37, A. Gavrilyuk ^{id}37, C. Gay ^{id}164, G. Gaycken ^{id}48, E.N. Gazis ^{id}10, A.A. Geanta ^{id}27b, C.M. Gee ^{id}136, A. Gekow ^{id}119, C. Gemme ^{id}57b, M.H. Genest ^{id}60, S. Gentile ^{id}75a,75b, A.D. Gentry ^{id}112, S. George ^{id}95, W.F. George ^{id}20, T. Geralis ^{id}46, P. Gessinger-Befurt ^{id}36, M.E. Geyik ^{id}171, M. Ghani ^{id}167, M. Ghneimat ^{id}141, K. Ghorbanian ^{id}94, A. Ghosal ^{id}141, A. Ghosh ^{id}160, A. Ghosh ^{id}7, B. Giacobbe ^{id}23b, S. Giagu ^{id}75a,75b, T. Giani ^{id}114, P. Giannetti ^{id}74a, A. Giannini ^{id}62a, S.M. Gibson ^{id}95, M. Gignac ^{id}136, D.T. Gil ^{id}86b, A.K. Gilbert ^{id}86a, B.J. Gilbert ^{id}41, D. Gillberg ^{id}34, G. Gilles ^{id}114, N.E.K. Gillwald ^{id}48, L. Ginabat ^{id}127, D.M. Gingrich ^{id}2,af, M.P. Giordani ^{id}69a,69c, P.F. Giraud ^{id}135, G. Giugliarelli ^{id}69a,69c, D. Giugni ^{id}71a, F. Giuli ^{id}36, I. Gkialas ^{id}9,j, L.K. Gladilin ^{id}37, C. Glasman ^{id}99, G.R. Gledhill ^{id}123, G. Glemža ^{id}48, M. Glisic ^{id}123, I. Gnesi ^{id}43b,f, Y. Go ^{id}29,ai, M. Goblirsch-Kolb ^{id}36, B. Gocke ^{id}49, D. Godin ^{id}108, B. Gokturk ^{id}21a, S. Goldfarb ^{id}105, T. Golling ^{id}56, M.G.D. Gololo ^{id}33g, D. Golubkov ^{id}37, J.P. Gombas ^{id}107, A. Gomes ^{id}130a,130b, G. Gomes Da Silva ^{id}141, A.J. Gomez Delegido ^{id}163, R. Gonçalves ^{id}130a,130c, G. Gonella ^{id}123, L. Gonella ^{id}20, A. Gongadze ^{id}149c, F. Gonnella ^{id}20, J.L. Gonski ^{id}41, R.Y. González Andana ^{id}52, S. González de la Hoz ^{id}163, S. Gonzalez Fernandez ^{id}13, R. Gonzalez Lopez ^{id}92, C. Gonzalez Renteria ^{id}17a, M.V. Gonzalez Rodrigues ^{id}48, R. Gonzalez Suarez ^{id}161, S. Gonzalez-Sevilla ^{id}56, G.R. Gonzalvo Rodriguez ^{id}163, L. Goossens ^{id}36, B. Gorini ^{id}36, E. Gorini ^{id}70a,70b, A. Gorišek ^{id}93, T.C. Gosart ^{id}128, A.T. Goshaw ^{id}51, M.I. Gostkin ^{id}38, S. Goswami ^{id}121, C.A. Gottardo ^{id}36, S.A. Gotz ^{id}109, M. Goughri ^{id}35b, V. Goumarre ^{id}48, A.G. Goussiou ^{id}138, N. Govender ^{id}33c, I. Grabowska-Bold ^{id}86a, K. Graham ^{id}34, E. Gramstad ^{id}125, S. Grancagnolo ^{id}70a,70b, M. Grandi ^{id}146, C.M. Grant ^{id}1,135, P.M. Gravila ^{id}27f, F.G. Gravili ^{id}70a,70b, H.M. Gray ^{id}17a, M. Greco ^{id}70a,70b, C. Grefe ^{id}24, I.M. Gregor ^{id}48, P. Grenier ^{id}143, S.G. Grewe ^{id}110, C. Grieco ^{id}13, A.A. Grillo ^{id}136, K. Grimm ^{id}31, S. Grinstein ^{id}13,s, J.-F. Grivaz ^{id}66, E. Gross ^{id}169,

J. Grosse-Knetter ⁵⁵, C. Grud ¹⁰⁶, J.C. Grundy ¹²⁶, L. Guan ¹⁰⁶, W. Guan ²⁹, C. Gubbels ¹⁶⁴, J.G.R. Guerrero Rojas ¹⁶³, G. Guerrieri ^{69a,69c}, F. Guescini ¹¹⁰, R. Gugel ¹⁰⁰, J.A.M. Guhit ¹⁰⁶, A. Guida ¹⁸, E. Guilloton ^{167,134}, S. Guindon ³⁶, F. Guo ^{14a,14e}, J. Guo ^{62c}, L. Guo ⁴⁸, Y. Guo ¹⁰⁶, R. Gupta ⁴⁸, R. Gupta ¹²⁹, S. Gurbuz ²⁴, S.S. Gurdasani ⁵⁴, G. Gustavino ³⁶, M. Guth ⁵⁶, P. Gutierrez ¹²⁰, L.F. Gutierrez Zagazeta ¹²⁸, M. Gutsche ⁵⁰, C. Gutschow ⁹⁶, C. Gwenlan ¹²⁶, C.B. Gwilliam ⁹², E.S. Haaland ¹²⁵, A. Haas ¹¹⁷, M. Habedank ⁴⁸, C. Haber ^{17a}, H.K. Hadavand ⁸, A. Hadeef ⁵⁰, S. Hadzic ¹¹⁰, A.I. Hagan ⁹¹, J.J. Hahn ¹⁴¹, E.H. Haines ⁹⁶, M. Haleem ¹⁶⁶, J. Haley ¹²¹, J.J. Hall ¹³⁹, G.D. Hallewell ¹⁰², L. Halser ¹⁹, K. Hamano ¹⁶⁵, M. Hamer ²⁴, G.N. Hamity ⁵², E.J. Hampshire ⁹⁵, J. Han ^{62b}, K. Han ^{62a}, L. Han ^{14c}, L. Han ^{62a}, S. Han ^{17a}, Y.F. Han ¹⁵⁵, K. Hanagaki ⁸⁴, M. Hance ¹³⁶, D.A. Hangal ^{41,ab}, H. Hanif ¹⁴², M.D. Hank ¹²⁸, R. Hankache ¹⁰¹, J.B. Hansen ⁴², J.D. Hansen ⁴², P.H. Hansen ⁴², K. Hara ¹⁵⁷, D. Harada ⁵⁶, T. Harenberg ¹⁷¹, S. Harkusha ³⁷, M.L. Harris ¹⁰³, Y.T. Harris ¹²⁶, J. Harrison ¹³, N.M. Harrison ¹¹⁹, P.F. Harrison ¹⁶⁷, N.M. Hartman ¹¹⁰, N.M. Hartmann ¹⁰⁹, Y. Hasegawa ¹⁴⁰, R. Hauser ¹⁰⁷, C.M. Hawkes ²⁰, R.J. Hawkings ³⁶, Y. Hayashi ¹⁵³, S. Hayashida ¹¹¹, D. Hayden ¹⁰⁷, C. Hayes ¹⁰⁶, R.L. Hayes ¹¹⁴, C.P. Hays ¹²⁶, J.M. Hays ⁹⁴, H.S. Hayward ⁹², F. He ^{62a}, M. He ^{14a,14e}, Y. He ¹⁵⁴, Y. He ⁴⁸, N.B. Heatley ⁹⁴, V. Hedberg ⁹⁸, A.L. Heggelund ¹²⁵, N.D. Hehir ^{94,*}, C. Heidegger ⁵⁴, K.K. Heidegger ⁵⁴, W.D. Heidorn ⁸¹, J. Heilman ³⁴, S. Heim ⁴⁸, T. Heim ^{17a}, J.G. Heinlein ¹²⁸, J.J. Heinrich ¹²³, L. Heinrich ^{110,ad}, J. Hejbal ¹³¹, L. Helary ⁴⁸, A. Held ¹⁷⁰, S. Hellesund ¹⁶, C.M. Helling ¹⁶⁴, S. Hellman ^{47a,47b}, R.C.W. Henderson ⁹¹, L. Henkelmann ³², A.M. Henriques Correia ³⁶, H. Herde ⁹⁸, Y. Hernández Jiménez ¹⁴⁵, L.M. Herrmann ²⁴, T. Herrmann ⁵⁰, G. Herten ⁵⁴, R. Hertenberger ¹⁰⁹, L. Hervas ³⁶, M.E. Hesping ¹⁰⁰, N.P. Hessey ^{156a}, H. Hibi ⁸⁵, E. Hill ¹⁵⁵, S.J. Hillier ²⁰, J.R. Hinds ¹⁰⁷, F. Hinterkeuser ²⁴, M. Hirose ¹²⁴, S. Hirose ¹⁵⁷, D. Hirschbuehl ¹⁷¹, T.G. Hitchings ¹⁰¹, B. Hiti ⁹³, J. Hobbs ¹⁴⁵, R. Hobincu ^{27e}, N. Hod ¹⁶⁹, M.C. Hodgkinson ¹³⁹, B.H. Hodgkinson ³², A. Hoecker ³⁶, D.D. Hofer ¹⁰⁶, J. Hofer ⁴⁸, T. Holm ²⁴, M. Holzbock ¹¹⁰, L.B.A.H. Hommels ³², B.P. Honan ¹⁰¹, J. Hong ^{62c}, T.M. Hong ¹²⁹, B.H. Hooberman ¹⁶², W.H. Hopkins ⁶, Y. Horii ¹¹¹, S. Hou ¹⁴⁸, A.S. Howard ⁹³, J. Howarth ⁵⁹, J. Hoya ⁶, M. Hrabovsky ¹²², A. Hrynevich ⁴⁸, T. Hryn'ova ⁴, P.J. Hsu ⁶⁵, S.-C. Hsu ¹³⁸, Q. Hu ^{62a}, Y.F. Hu ^{14a,14e}, S. Huang ^{64b}, X. Huang ^{14c}, X. Huang ^{14a,14e}, Y. Huang ¹³⁹, Y. Huang ^{14a}, Z. Huang ¹⁰¹, Z. Hubacek ¹³², M. Huebner ²⁴, F. Huegging ²⁴, T.B. Huffman ¹²⁶, C.A. Hugli ⁴⁸, M. Huhtinen ³⁶, S.K. Huiberts ¹⁶, R. Hulsken ¹⁰⁴, N. Huseynov ¹², J. Huston ¹⁰⁷, J. Huth ⁶¹, R. Hyneman ¹⁴³, G. Iacobucci ⁵⁶, G. Iakovidis ²⁹, I. Ibragimov ¹⁴¹, L. Iconomidou-Fayard ⁶⁶, P. Iengo ^{72a,72b}, R. Iguchi ¹⁵³, T. Iizawa ¹²⁶, Y. Ikegami ⁸⁴, A. Ilg ¹⁹, N. Ilic ¹⁵⁵, H. Imam ^{35a}, M. Ince Lezki ⁵⁶, T. Ingebretsen Carlson ^{47a,47b}, G. Introzzi ^{73a,73b}, M. Iodice ^{77a}, V. Ippolito ^{75a,75b}, R.K. Irwin ⁹², M. Ishino ¹⁵³, W. Islam ¹⁷⁰, C. Issever ^{18,48}, S. Istin ^{21a,ak}, H. Ito ¹⁶⁸, J.M. Iturbe Ponce ^{64a}, R. Iuppa ^{78a,78b}, A. Ivina ¹⁶⁹, J.M. Izen ⁴⁵, V. Izzo ^{72a}, P. Jacka ^{131,132}, P. Jackson ¹, R.M. Jacobs ⁴⁸, B.P. Jaeger ¹⁴², C.S. Jagfeld ¹⁰⁹, G. Jain ^{156a}, P. Jain ⁵⁴, K. Jakobs ⁵⁴, T. Jakoubek ¹⁶⁹, J. Jamieson ⁵⁹, K.W. Janas ^{86a}, M. Javurkova ¹⁰³, F. Jeanneau ¹³⁵, L. Jeanty ¹²³, J. Jejelava ^{149a,z}, P. Jenni ^{54,g}, C.E. Jessiman ³⁴, S. Jézéquel ⁴, C. Jia ^{62b}, J. Jia ¹⁴⁵, X. Jia ⁶¹, X. Jia ^{14a,14e}, Z. Jia ^{14c}, S. Jiggins ⁴⁸, J. Jimenez Pena ¹³, S. Jin ^{14c}, A. Jinaru ^{27b}, O. Jinnouchi ¹⁵⁴, P. Johansson ¹³⁹, K.A. Johns ⁷, J.W. Johnson ¹³⁶, D.M. Jones ³², E. Jones ⁴⁸, P. Jones ³², R.W.L. Jones ⁹¹, T.J. Jones ⁹², H.L. Joos ^{55,36}, R. Joshi ¹¹⁹, J. Jovicevic ¹⁵, X. Ju ^{17a}, J.J. Junggeburth ¹⁰³, T. Junkermann ^{63a}, A. Juste Rozas ^{13,s}, M.K. Juzek ⁸⁷, S. Kabana ^{137e}, A. Kaczmarska ⁸⁷, M. Kado ¹¹⁰, H. Kagan ¹¹⁹, M. Kagan ¹⁴³, A. Kahn ⁴¹, A. Kahn ¹²⁸, C. Kahra ¹⁰⁰, T. Kaji ¹⁵³, E. Kajomovitz ¹⁵⁰, N. Kakati ¹⁶⁹, I. Kalaitzidou ⁵⁴, C.W. Kalderon ²⁹, A. Kamenshchikov ¹⁵⁵, N.J. Kang ¹³⁶, D. Kar ^{33g}, K. Karava ¹²⁶,

M.J. Kareem ^{156b}, E. Karentzos ⁵⁴, I. Karkanias ¹⁵², O. Karkout ¹¹⁴, S.N. Karpov ³⁸,
Z.M. Karpova ³⁸, V. Kartvelishvili ⁹¹, A.N. Karyukhin ³⁷, E. Kasimi ¹⁵², J. Katzy ⁴⁸,
S. Kaur ³⁴, K. Kawade ¹⁴⁰, M.P. Kawale ¹²⁰, C. Kawamoto ⁸⁸, T. Kawamoto ^{62a}, E.F. Kay ³⁶,
F.I. Kaya ¹⁵⁸, S. Kazakos ¹⁰⁷, V.F. Kazanin ³⁷, Y. Ke ¹⁴⁵, J.M. Keaveney ^{33a}, R. Keeler ¹⁶⁵,
G.V. Kehris ⁶¹, J.S. Keller ³⁴, A.S. Kelly ⁹⁶, J.J. Kempster ¹⁴⁶, K.E. Kennedy ⁴¹,
P.D. Kennedy ¹⁰⁰, O. Kepka ¹³¹, B.P. Kerridge ¹⁶⁷, S. Kersten ¹⁷¹, B.P. Kerševan ⁹³,
S. Keshri ⁶⁶, L. Keszeghova ^{28a}, S. Ketabchi Haghighat ¹⁵⁵, R.A. Khan ¹²⁹, M. Khandoga ¹²⁷,
A. Khanov ¹²¹, A.G. Kharlamov ³⁷, T. Kharlamova ³⁷, E.E. Khoda ¹³⁸, M. Kholodenko ³⁷,
T.J. Khoo ¹⁸, G. Khoraiuli ¹⁶⁶, J. Khubua ^{149b}, Y.A.R. Khwaira ⁶⁶, A. Kilgallon ¹²³,
D.W. Kim ^{47a,47b}, Y.K. Kim ³⁹, N. Kimura ⁹⁶, M.K. Kingston ⁵⁵, A. Kirchhoff ⁵⁵, C. Kirfel ²⁴,
F. Kirfel ²⁴, J. Kirk ¹³⁴, A.E. Kiryunin ¹¹⁰, C. Kitsaki ¹⁰, O. Kivernyk ²⁴, M. Klassen ^{63a},
C. Klein ³⁴, L. Klein ¹⁶⁶, M.H. Klein ¹⁰⁶, M. Klein ⁹², S.B. Klein ⁵⁶, U. Klein ⁹²,
P. Klimek ³⁶, A. Klimentov ²⁹, T. Klioutchnikova ³⁶, P. Kluit ¹¹⁴, S. Kluth ¹¹⁰, E. Kneringer ⁷⁹,
T.M. Knight ¹⁵⁵, A. Knue ⁴⁹, R. Kobayashi ⁸⁸, D. Kobylanski ¹⁶⁹, S.F. Koch ¹²⁶,
M. Kocian ¹⁴³, P. Kodyš ¹³³, D.M. Koeck ¹²³, P.T. Koenig ²⁴, T. Koffas ³⁴, O. Kolay ⁵⁰,
I. Koletsou ⁴, T. Komarek ¹²², K. Köneke ⁵⁴, A.X.Y. Kong ¹, T. Kono ¹¹⁸, N. Konstantinidis ⁹⁶,
P. Kontaxakis ⁵⁶, B. Konya ⁹⁸, R. Kopeliansky ⁶⁸, S. Koperny ^{86a}, K. Korcyl ⁸⁷, K. Kordas ^{152,e},
G. Koren ¹⁵¹, A. Korn ⁹⁶, S. Korn ⁵⁵, I. Korolkov ¹³, N. Korotkova ³⁷, B. Kortman ¹¹⁴,
O. Kortner ¹¹⁰, S. Kortner ¹¹⁰, W.H. Kostecka ¹¹⁵, V.V. Kostyukhin ¹⁴¹, A. Kotsokechagia ¹³⁵,
A. Kotwal ⁵¹, A. Koulouris ³⁶, A. Kourkoumeli-Charalampidi ^{73a,73b}, C. Kourkoumelis ⁹,
E. Kourlitis ^{110,ad}, O. Kovanda ¹⁴⁶, R. Kowalewski ¹⁶⁵, W. Kozanecki ¹³⁵, A.S. Kozhin ³⁷,
V.A. Kramarenko ³⁷, G. Kramberger ⁹³, P. Kramer ¹⁰⁰, M.W. Krasny ¹²⁷, A. Krasznahorkay ³⁶,
J.W. Kraus ¹⁷¹, J.A. Kremer ⁴⁸, T. Kresse ⁵⁰, J. Kretschmar ⁹², K. Kreul ¹⁸, P. Krieger ¹⁵⁵,
S. Krishnamurthy ¹⁰³, M. Krivos ¹³³, K. Krizka ²⁰, K. Kroeninger ⁴⁹, H. Kroha ¹¹⁰, J. Kroll ¹³¹,
J. Kroll ¹²⁸, K.S. Krowpman ¹⁰⁷, U. Kruchonak ³⁸, H. Krüger ²⁴, N. Krumnack ⁸¹, M.C. Kruse ⁵¹,
O. Kuchinskaia ³⁷, S. Kuday ^{3a}, S. Kuehn ³⁶, R. Kuesters ⁵⁴, T. Kuhl ⁴⁸, V. Kukhtin ³⁸,
Y. Kulchitsky ^{37,a}, S. Kuleshov ^{137d,137b}, M. Kumar ^{33g}, N. Kumari ⁴⁸, P. Kumari ^{156b},
A. Kupco ¹³¹, T. Kupfer ⁴⁹, A. Kupich ³⁷, O. Kuprash ⁵⁴, H. Kurashige ⁸⁵, L.L. Kurchaninov ^{156a},
O. Kurdysh ⁶⁶, Y.A. Kurochkin ³⁷, A. Kurova ³⁷, M. Kuze ¹⁵⁴, A.K. Kvam ¹⁰³, J. Kvitá ¹²²,
T. Kwan ¹⁰⁴, N.G. Kyriacou ¹⁰⁶, L.A.O. Laatu ¹⁰², C. Lacasta ¹⁶³, F. Lacava ^{75a,75b},
H. Lacker ¹⁸, D. Lacour ¹²⁷, N.N. Lad ⁹⁶, E. Ladygin ³⁸, B. Laforge ¹²⁷, T. Lagouri ^{137e},
F.Z. Lahbabi ^{35a}, S. Lai ⁵⁵, I.K. Lakomic ^{86a}, N. Lalloue ⁶⁰, J.E. Lambert ¹⁶⁵, S. Lammers ⁶⁸,
W. Lampl ⁷, C. Lampoudis ^{152,e}, A.N. Lancaster ¹¹⁵, E. Lançon ²⁹, U. Landgraf ⁵⁴,
M.P.J. Landon ⁹⁴, V.S. Lang ⁵⁴, R.J. Langenberg ¹⁰³, O.K.B. Langrekken ¹²⁵, A.J. Lankford ¹⁶⁰,
F. Lanni ³⁶, K. Lantzs ²⁴, A. Lanza ^{73a}, A. Lapertosa ^{57b,57a}, J.F. Laporte ¹³⁵, T. Lari ^{71a},
F. Lasagni Manghi ^{23b}, M. Lassnig ³⁶, V. Latonova ¹³¹, A. Laudrain ¹⁰⁰, A. Laurier ¹⁵⁰,
S.D. Lawlor ¹³⁹, Z. Lawrence ¹⁰¹, R. Lazaridou ¹⁶⁷, M. Lazzaroni ^{71a,71b}, B. Le ¹⁰¹,
E.M. Le Boulicaut ⁵¹, B. Leban ⁹³, A. Lebedev ⁸¹, M. LeBlanc ¹⁰¹, F. Ledroit-Guillon ⁶⁰,
A.C.A. Lee ⁹⁶, S.C. Lee ¹⁴⁸, S. Lee ^{47a,47b}, T.F. Lee ⁹², L.L. Leeuw ^{33c}, H.P. Lefebvre ⁹⁵,
M. Lefebvre ¹⁶⁵, C. Leggett ^{17a}, G. Lehmann Miotto ³⁶, M. Leigh ⁵⁶, W.A. Leight ¹⁰³,
W. Leinonen ¹¹³, A. Leisos ^{152,r}, M.A.L. Leite ^{83c}, C.E. Leitgeb ⁴⁸, R. Leitner ¹³³,
K.J.C. Leney ⁴⁴, T. Lenz ²⁴, S. Leone ^{74a}, C. Leonidopoulos ⁵², A. Leopold ¹⁴⁴, C. Leroy ¹⁰⁸,
R. Les ¹⁰⁷, C.G. Lester ³², M. Levchenko ³⁷, J. Levêque ⁴, D. Levin ¹⁰⁶, L.J. Levinson ¹⁶⁹,
M.P. Lewicki ⁸⁷, D.J. Lewis ⁴, A. Li ⁵, B. Li ^{62b}, C. Li ^{62a}, C-Q. Li ¹¹⁰, H. Li ^{62a}, H. Li ^{62b},
H. Li ^{14c}, H. Li ^{14b}, H. Li ^{62b}, J. Li ^{62c}, K. Li ¹³⁸, L. Li ^{62c}, M. Li ^{14a,14e}, Q.Y. Li ^{62a},
S. Li ^{14a,14e}, S. Li ^{62d,62c,d}, T. Li ⁵, X. Li ¹⁰⁴, Z. Li ¹²⁶, Z. Li ¹⁰⁴, Z. Li ^{14a,14e}, S. Liang ^{14a,14e},
Z. Liang ^{14a}, M. Liberatore ¹³⁵, B. Liberti ^{76a}, K. Lie ^{64c}, J. Lieber Marin ^{83b}, H. Lien ⁶⁸,

K. Lin ¹⁰⁷, R.E. Lindley ⁷, J.H. Lindon ², E. Lipeles ¹²⁸, A. Lipniacka ¹⁶, A. Lister ¹⁶⁴,
 J.D. Little ⁴, B. Liu ^{14a}, B.X. Liu ¹⁴², D. Liu ^{62d,62c}, J.B. Liu ^{62a}, J.K.K. Liu ³², K. Liu ^{62d,62c},
 M. Liu ^{62a}, M.Y. Liu ^{62a}, P. Liu ^{14a}, Q. Liu ^{62d,138,62c}, X. Liu ^{62a}, X. Liu ^{62b}, Y. Liu ^{14d,14e},
 Y.L. Liu ^{62b}, Y.W. Liu ^{62a}, J. Llorente Merino ¹⁴², S.L. Lloyd ⁹⁴, E.M. Lobodzinska ⁴⁸,
 P. Loch ⁷, T. Lohse ¹⁸, K. Lohwasser ¹³⁹, E. Loiacono ⁴⁸, M. Lokajicek ^{131,*}, J.D. Lomas ²⁰,
 J.D. Long ¹⁶², I. Longarini ¹⁶⁰, L. Longo ^{70a,70b}, R. Longo ¹⁶², I. Lopez Paz ⁶⁷,
 A. Lopez Solis ⁴⁸, N. Lorenzo Martinez ⁴, A.M. Lory ¹⁰⁹, G. Löschcke Centeno ¹⁴⁶, O. Loseva ³⁷,
 X. Lou ^{47a,47b}, X. Lou ^{14a,14e}, A. Lounis ⁶⁶, J. Love ⁶, P.A. Love ⁹¹, G. Lu ^{14a,14e}, M. Lu ⁸⁰,
 S. Lu ¹²⁸, Y.J. Lu ⁶⁵, H.J. Lubatti ¹³⁸, C. Luci ^{75a,75b}, F.L. Lucio Alves ^{14c}, A. Lucotte ⁶⁰,
 F. Luehring ⁶⁸, I. Luise ¹⁴⁵, O. Lukianchuk ⁶⁶, O. Lundberg ¹⁴⁴, B. Lund-Jensen ¹⁴⁴,
 N.A. Luongo ⁶, M.S. Lutz ¹⁵¹, A.B. Lux ²⁵, D. Lynn ²⁹, H. Lyons ⁹², R. Lysak ¹³¹, E. Lytken ⁹⁸,
 V. Lyubushkin ³⁸, T. Lyubushkina ³⁸, M.M. Lyukova ¹⁴⁵, H. Ma ²⁹, K. Ma ^{62a}, L.L. Ma ^{62b},
 W. Ma ^{62a}, Y. Ma ¹²¹, D.M. Mac Donell ¹⁶⁵, G. Maccarrone ⁵³, J.C. MacDonald ¹⁰⁰,
 P.C. Machado De Abreu Farias ^{83b}, R. Madar ⁴⁰, W.F. Mader ⁵⁰, T. Madula ⁹⁶, J. Maeda ⁸⁵,
 T. Maeno ²⁹, H. Maguire ¹³⁹, V. Maiboroda ¹³⁵, A. Maio ^{130a,130b,130d}, K. Maj ^{86a},
 O. Majersky ⁴⁸, S. Majewski ¹²³, N. Makovec ⁶⁶, V. Maksimovic ¹⁵, B. Malaescu ¹²⁷,
 Pa. Malecki ⁸⁷, V.P. Maleev ³⁷, F. Malek ⁶⁰, M. Mali ⁹³, D. Malito ⁹⁵, U. Mallik ⁸⁰,
 S. Maltezos ¹⁰, S. Malyukov ³⁸, J. Mamuzic ¹³, G. Mancini ⁵³, G. Manco ^{73a,73b}, J.P. Mandalia ⁹⁴,
 I. Mandić ⁹³, L. Manhaes de Andrade Filho ^{83a}, I.M. Maniatis ¹⁶⁹, J. Manjarres Ramos ^{102,aa},
 D.C. Mankad ¹⁶⁹, A. Mann ¹⁰⁹, B. Mansoulié ¹³⁵, S. Manzoni ³⁶, L. Mao ^{62c}, X. Mapekula ^{33c},
 A. Marantis ^{152,r}, G. Marchiori ⁵, M. Marcisovsky ¹³¹, C. Marcon ^{71a}, M. Marinescu ²⁰,
 S. Marium ⁴⁸, M. Marjanovic ¹²⁰, E.J. Marshall ⁹¹, Z. Marshall ^{17a}, S. Marti-Garcia ¹⁶³,
 T.A. Martin ¹⁶⁷, V.J. Martin ⁵², B. Martin dit Latour ¹⁶, L. Martinelli ^{75a,75b}, M. Martinez ^{13,s},
 P. Martinez Agullo ¹⁶³, V.I. Martinez Outschoorn ¹⁰³, P. Martinez Suarez ¹³, S. Martin-Haugh ¹³⁴,
 V.S. Martoiu ^{27b}, A.C. Martyniuk ⁹⁶, A. Marzin ³⁶, D. Mascione ^{78a,78b}, L. Masetti ¹⁰⁰,
 T. Mashimo ¹⁵³, J. Masik ¹⁰¹, A.L. Maslennikov ³⁷, L. Massa ^{23b}, P. Massarotti ^{72a,72b},
 P. Mastrandrea ^{74a,74b}, A. Mastroberardino ^{43b,43a}, T. Masubuchi ¹⁵³, T. Mathisen ¹⁶¹,
 J. Matousek ¹³³, N. Matsuzawa ¹⁵³, J. Maurer ^{27b}, B. Maček ⁹³, D.A. Maximov ³⁷, R. Mazini ¹⁴⁸,
 I. Maznas ¹⁵², M. Mazza ¹⁰⁷, S.M. Mazza ¹³⁶, E. Mazzeo ^{71a,71b}, C. Mc Ginn ²⁹,
 J.P. Mc Gowan ¹⁰⁴, S.P. Mc Kee ¹⁰⁶, C.C. McCracken ¹⁶⁴, E.F. McDonald ¹⁰⁵,
 A.E. McDougall ¹¹⁴, J.A. Mcfayden ¹⁴⁶, R.P. McGovern ¹²⁸, G. Mchedlidze ^{149b},
 R.P. Mckenzie ^{33g}, T.C. Mclachlan ⁴⁸, D.J. McLaughlin ⁹⁶, S.J. McMahon ¹³⁴,
 C.M. Mcpartland ⁹², R.A. McPherson ^{165,w}, S. Mehlhase ¹⁰⁹, A. Mehta ⁹², D. Melini ¹⁵⁰,
 B.R. Mellado Garcia ^{33g}, A.H. Melo ⁵⁵, F. Meloni ⁴⁸, A.M. Mendes Jacques Da Costa ¹⁰¹,
 H.Y. Meng ¹⁵⁵, L. Meng ⁹¹, S. Menke ¹¹⁰, M. Mentink ³⁶, E. Meoni ^{43b,43a}, G. Mercado ¹¹⁵,
 C. Merlassino ^{69a,69c}, L. Merola ^{72a,72b}, C. Meroni ^{71a,71b}, G. Merz ¹⁰⁶, J. Metcalfe ⁶, A.S. Mete ⁶,
 C. Meyer ⁶⁸, J-P. Meyer ¹³⁵, R.P. Middleton ¹³⁴, L. Mijović ⁵², G. Mikenberg ¹⁶⁹,
 M. Mikestikova ¹³¹, M. Mikuž ⁹³, H. Mildner ¹⁰⁰, A. Milic ³⁶, C.D. Milke ⁴⁴, D.W. Miller ³⁹,
 L.S. Miller ³⁴, A. Milov ¹⁶⁹, D.A. Milstead ^{47a,47b}, T. Min ^{14c}, A.A. Minaenko ³⁷,
 I.A. Minashvili ^{149b}, L. Mince ⁵⁹, A.I. Mincer ¹¹⁷, B. Mindur ^{86a}, M. Mineev ³⁸, Y. Mino ⁸⁸,
 L.M. Mir ¹³, M. Miralles Lopez ¹⁶³, M. Mironova ^{17a}, A. Mishima ¹⁵³, M.C. Missio ¹¹³,
 A. Mitra ¹⁶⁷, V.A. Mitsou ¹⁶³, Y. Mitsumori ¹¹¹, O. Miu ¹⁵⁵, P.S. Miyagawa ⁹⁴,
 T. Mkrtchyan ^{63a}, M. Mlinarevic ⁹⁶, T. Mlinarevic ⁹⁶, M. Mlynarikova ³⁶, S. Mobius ¹⁹,
 P. Moder ⁴⁸, P. Mogg ¹⁰⁹, M.H. Mohamed Farook ¹¹², A.F. Mohammed ^{14a,14e}, S. Mohapatra ⁴¹,
 G. Mokgatitswane ^{33g}, L. Moleri ¹⁶⁹, B. Mondal ¹⁴¹, S. Mondal ¹³², K. Mönig ⁴⁸,
 E. Monnier ¹⁰², L. Monsonis Romero ¹⁶³, J. Montejo Berlingen ¹³, M. Montella ¹¹⁹,
 F. Montereali ^{77a,77b}, F. Monticelli ⁹⁰, S. Monzani ^{69a,69c}, N. Morange ⁶⁶,

A.L. Moreira De Carvalho [ID130a](#), M. Moreno Llácer [ID163](#), C. Moreno Martinez [ID56](#), P. Morettini [ID57b](#),
 S. Morgenstern [ID36](#), M. Morii [ID61](#), M. Morinaga [ID153](#), A.K. Morley [ID36](#), F. Morodei [ID75a,75b](#),
 L. Morvaj [ID36](#), P. Moschovakos [ID36](#), B. Moser [ID36](#), M. Mosidze [ID149b](#), T. Moskalets [ID54](#),
 P. Moskvitina [ID113](#), J. Moss [ID31.1](#), E.J.W. Moyse [ID103](#), O. Mtintsilana [ID33g](#), S. Muanza [ID102](#),
 J. Mueller [ID129](#), D. Muenstermann [ID91](#), R. Müller [ID19](#), G.A. Mullier [ID161](#), A.J. Mullin³², J.J. Mullin¹²⁸,
 D.P. Mungo [ID155](#), D. Munoz Perez [ID163](#), F.J. Munoz Sanchez [ID101](#), M. Murin [ID101](#), W.J. Murray [ID167,134](#),
 A. Murrone [ID71a,71b](#), M. Muškinja [ID17a](#), C. Mwewa [ID29](#), A.G. Myagkov [ID37,a](#), A.J. Myers [ID8](#),
 G. Myers [ID68](#), M. Myska [ID132](#), B.P. Nachman [ID17a](#), O. Nackenhorst [ID49](#), A. Nag [ID50](#), K. Nagai [ID126](#),
 K. Nagano [ID84](#), J.L. Nagle [ID29,ai](#), E. Nagy [ID102](#), A.M. Nairz [ID36](#), Y. Nakahama [ID84](#), K. Nakamura [ID84](#),
 K. Nakkalil [ID5](#), H. Nanjo [ID124](#), R. Narayan [ID44](#), E.A. Narayanan [ID112](#), I. Naryshkin [ID37](#), M. Naseri [ID34](#),
 S. Nasri [ID159](#), C. Nass [ID24](#), G. Navarro [ID22a](#), J. Navarro-Gonzalez [ID163](#), R. Nayak [ID151](#), A. Nayaz [ID18](#),
 P.Y. Nechaeva [ID37](#), F. Nechansky [ID48](#), L. Nedic [ID126](#), T.J. Neep [ID20](#), A. Negri [ID73a,73b](#), M. Negrini [ID23b](#),
 C. Nellist [ID114](#), C. Nelson [ID104](#), K. Nelson [ID106](#), S. Nemecek [ID131](#), M. Nessi [ID36,h](#), M.S. Neubauer [ID162](#),
 F. Neuhaus [ID100](#), J. Neundorf [ID48](#), R. Newhouse [ID164](#), P.R. Newman [ID20](#), C.W. Ng [ID129](#), Y.W.Y. Ng [ID48](#),
 B. Ngair [ID35e](#), H.D.N. Nguyen [ID108](#), R.B. Nickerson [ID126](#), R. Nicolaidou [ID135](#), J. Nielsen [ID136](#),
 M. Niemeyer [ID55](#), J. Niermann [ID55,36](#), N. Nikiforou [ID36](#), V. Nikolaenko [ID37,a](#), I. Nikolic-Audit [ID127](#),
 K. Nikolopoulos [ID20](#), P. Nilsson [ID29](#), I. Ninca [ID48](#), H.R. Nindhito [ID56](#), G. Ninio [ID151](#), A. Nisati [ID75a](#),
 N. Nishu [ID2](#), R. Nisius [ID110](#), J-E. Nitschke [ID50](#), E.K. Nkadimeng [ID33g](#), T. Nobe [ID153](#), D.L. Noel [ID32](#),
 T. Nommensen [ID147](#), M.B. Norfolk [ID139](#), R.R.B. Norisam [ID96](#), B.J. Norman [ID34](#), M. Noury [ID35a](#),
 J. Novak [ID93](#), T. Novak [ID48](#), L. Novotny [ID132](#), R. Novotny [ID112](#), L. Nozka [ID122](#), K. Ntekas [ID160](#),
 N.M.J. Nunes De Moura Junior [ID83b](#), E. Nurse⁹⁶, J. Ocariz [ID127](#), A. Ochi [ID85](#), I. Ochoa [ID130a](#),
 S. Oerdek [ID48,t](#), J.T. Offermann [ID39](#), A. Ogrodnik [ID133](#), A. Oh [ID101](#), C.C. Ohm [ID144](#), H. Oide [ID84](#),
 R. Oishi [ID153](#), M.L. Ojeda [ID48](#), M.W. O’Keefe⁹², Y. Okumura [ID153](#), L.F. Oleiro Seabra [ID130a](#),
 S.A. Olivares Pino [ID137d](#), D. Oliveira Damazio [ID29](#), D. Oliveira Goncalves [ID83a](#), J.L. Oliver [ID160](#),
 Ö.O. Öncel [ID54](#), A.P. O’Neill [ID19](#), A. Onofre [ID130a,130e](#), P.U.E. Onyisi [ID11](#), M.J. Oreglia [ID39](#),
 G.E. Orellana [ID90](#), D. Orestano [ID77a,77b](#), N. Orlando [ID13](#), R.S. Orr [ID155](#), V. O’Shea [ID59](#),
 L.M. Osojnak [ID128](#), R. Ospanov [ID62a](#), G. Otero y Garzon [ID30](#), H. Otono [ID89](#), P.S. Ott [ID63a](#),
 G.J. Ottino [ID17a](#), M. Ouchrif [ID35d](#), J. Ouellette [ID29](#), F. Ould-Saada [ID125](#), M. Owen [ID59](#), R.E. Owen [ID134](#),
 K.Y. Oyulmaz [ID21a](#), V.E. Ozcan [ID21a](#), F. Ozturk [ID87](#), N. Ozturk [ID8](#), S. Ozturk [ID82](#), H.A. Pacey [ID126](#),
 A. Pacheco Pages [ID13](#), C. Padilla Aranda [ID13](#), G. Padovano [ID75a,75b](#), S. Pagan Griso [ID17a](#),
 G. Palacino [ID68](#), A. Palazzo [ID70a,70b](#), S. Palestini [ID36](#), J. Pan [ID172](#), T. Pan [ID64a](#), D.K. Panchal [ID11](#),
 C.E. Pandini [ID114](#), J.G. Panduro Vazquez [ID95](#), H.D. Pandya [ID1](#), H. Pang [ID14b](#), P. Pani [ID48](#),
 G. Panizzo [ID69a,69c](#), L. Paolozzi [ID56](#), C. Papadatos [ID108](#), S. Parajuli [ID44](#), A. Paramonov [ID6](#),
 C. Paraskevopoulos [ID10](#), D. Paredes Hernandez [ID64b](#), K.R. Park [ID41](#), T.H. Park [ID155](#), M.A. Parker [ID32](#),
 F. Parodi [ID57b,57a](#), E.W. Parrish [ID115](#), V.A. Parrish [ID52](#), J.A. Parsons [ID41](#), U. Parzefall [ID54](#),
 B. Pascual Dias [ID108](#), L. Pascual Dominguez [ID151](#), E. Pasqualucci [ID75a](#), S. Passaggio [ID57b](#), F. Pastore [ID95](#),
 P. Pasuwan [ID47a,47b](#), P. Patel [ID87](#), U.M. Patel [ID51](#), J.R. Pater [ID101](#), T. Pauly [ID36](#), J. Pearkes [ID143](#),
 M. Pedersen [ID125](#), R. Pedro [ID130a](#), S.V. Peleganchuk [ID37](#), O. Penc [ID36](#), E.A. Pender [ID52](#),
 K.E. Penski [ID109](#), M. Penzin [ID37](#), B.S. Peralva [ID83d](#), A.P. Pereira Peixoto [ID60](#), L. Pereira Sanchez [ID47a,47b](#),
 D.V. Perepelitsa [ID29,ai](#), E. Perez Codina [ID156a](#), M. Perganti [ID10](#), L. Perini [ID71a,71b,*](#), H. Pernegger [ID36](#),
 O. Perrin [ID40](#), K. Peters [ID48](#), R.F.Y. Peters [ID101](#), B.A. Petersen [ID36](#), T.C. Petersen [ID42](#), E. Petit [ID102](#),
 V. Petousis [ID132](#), C. Petridou [ID152,e](#), A. Petrukhin [ID141](#), M. Pettee [ID17a](#), N.E. Pettersson [ID36](#),
 A. Petukhov [ID37](#), K. Petukhova [ID133](#), R. Pezoa [ID137f](#), L. Pezzotti [ID36](#), G. Pezzullo [ID172](#), T.M. Pham [ID170](#),
 T. Pham [ID105](#), P.W. Phillips [ID134](#), G. Piacquadio [ID145](#), E. Pianori [ID17a](#), F. Piazza [ID123](#), R. Piegai [ID30](#),
 D. Pietreanu [ID27b](#), A.D. Pilkington [ID101](#), M. Pinamonti [ID69a,69c](#), J.L. Pinfeld [ID2](#),
 B.C. Pinheiro Pereira [ID130a](#), A.E. Pinto Pinoargote [ID100,135](#), L. Pintucci [ID69a,69c](#), K.M. Piper [ID146](#),
 A. Pirttikoski [ID56](#), D.A. Pizzi [ID34](#), L. Pizzimento [ID64b](#), A. Pizzini [ID114](#), M.-A. Pleier [ID29](#), V. Plesanovs⁵⁴,

V. Pleskot ¹³³, E. Plotnikova³⁸, G. Poddar ⁴, R. Poettgen ⁹⁸, L. Poggioli ¹²⁷, I. Pokharel ⁵⁵, S. Polacek ¹³³, G. Polesello ^{73a}, A. Poley ^{142,156a}, R. Polifka ¹³², A. Polini ^{23b}, C.S. Pollard ¹⁶⁷, Z.B. Pollock ¹¹⁹, V. Polychronakos ²⁹, E. Pompa Pacchi ^{75a,75b}, D. Ponomarenko ¹¹³, L. Pontecorvo ³⁶, S. Popa ^{27a}, G.A. Popeneciu ^{27d}, A. Poreba ³⁶, D.M. Portillo Quintero ^{156a}, S. Pospisil ¹³², M.A. Postill ¹³⁹, P. Postolache ^{27c}, K. Potamianos ¹⁶⁷, P.A. Potepa ^{86a}, I.N. Potrap ³⁸, C.J. Potter ³², H. Potti ¹, T. Poulsen ⁴⁸, J. Poveda ¹⁶³, M.E. Pozo Astigarraga ³⁶, A. Prades Ibanez ¹⁶³, J. Pretel ⁵⁴, D. Price ¹⁰¹, M. Primavera ^{70a}, M.A. Principe Martin ⁹⁹, R. Privara ¹²², T. Procter ⁵⁹, M.L. Proffitt ¹³⁸, N. Proklova ¹²⁸, K. Prokofiev ^{64c}, G. Proto ¹¹⁰, S. Protopopescu ²⁹, J. Proudfoot ⁶, M. Przybycien ^{86a}, W.W. Przygoda ^{86b}, J.E. Puddefoot ¹³⁹, D. Pudzha ³⁷, D. Pyatiizbyantseva ³⁷, J. Qian ¹⁰⁶, D. Qichen ¹⁰¹, Y. Qin ¹⁰¹, T. Qiu ⁵², A. Quadt ⁵⁵, M. Queitsch-Maitland ¹⁰¹, G. Quetant ⁵⁶, R.P. Quinn ¹⁶⁴, G. Rabanal Bolanos ⁶¹, D. Rafanoharana ⁵⁴, F. Ragusa ^{71a,71b}, J.L. Rainbolt ³⁹, J.A. Raine ⁵⁶, S. Rajagopalan ²⁹, E. Ramakoti ³⁷, I.A. Ramirez-Berend ³⁴, K. Ran ^{48,14e}, N.P. Rapheeha ^{33g}, H. Rasheed ^{27b}, V. Raskina ¹²⁷, D.F. Rassloff ^{63a}, A. Rastogi ^{17a}, S. Rave ¹⁰⁰, B. Ravina ⁵⁵, I. Ravinovich ¹⁶⁹, M. Raymond ³⁶, A.L. Read ¹²⁵, N.P. Readioff ¹³⁹, D.M. Rebuzzi ^{73a,73b}, G. Redlinger ²⁹, A.S. Reed ¹¹⁰, K. Reeves ²⁶, J.A. Reidelsturz ¹⁷¹, D. Reikher ¹⁵¹, A. Rej ⁴⁹, C. Rembser ³⁶, A. Renardi ⁴⁸, M. Renda ^{27b}, M.B. Rendel¹¹⁰, F. Renner ⁴⁸, A.G. Rennie ¹⁶⁰, A.L. Rescia ⁴⁸, S. Resconi ^{71a}, M. Ressegotti ^{57b,57a}, S. Rettie ³⁶, J.G. Reyes Rivera ¹⁰⁷, E. Reynolds ^{17a}, O.L. Rezanova ³⁷, P. Reznicek ¹³³, N. Ribaric ⁹¹, E. Ricci ^{78a,78b}, R. Richter ¹¹⁰, S. Richter ^{47a,47b}, E. Richter-Was ^{86b}, M. Ridel ¹²⁷, S. Ridouani ^{35d}, P. Rieck ¹¹⁷, P. Riedler ³⁶, E.M. Riefel ^{47a,47b}, J.O. Rieger ¹¹⁴, M. Rijssenbeek ¹⁴⁵, A. Rimoldi ^{73a,73b}, M. Rimoldi ³⁶, L. Rinaldi ^{23b,23a}, T.T. Rinn ²⁹, M.P. Rinnagel ¹⁰⁹, G. Ripellino ¹⁶¹, I. Riu ¹³, P. Rivadeneira ⁴⁸, J.C. Rivera Vergara ¹⁶⁵, F. Rizatdinova ¹²¹, E. Rizvi ⁹⁴, B.A. Roberts ¹⁶⁷, B.R. Roberts ^{17a}, S.H. Robertson ^{104,w}, D. Robinson ³², C.M. Robles Gajardo^{137f}, M. Robles Manzano ¹⁰⁰, A. Robson ⁵⁹, A. Rocchi ^{76a,76b}, C. Roda ^{74a,74b}, S. Rodriguez Bosca ^{63a}, Y. Rodriguez Garcia ^{22a}, A. Rodriguez Rodriguez ⁵⁴, A.M. Rodríguez Vera ^{156b}, S. Roe³⁶, J.T. Roemer ¹⁶⁰, A.R. Roepe-Gier ¹³⁶, J. Roggel ¹⁷¹, O. Røhne ¹²⁵, R.A. Rojas ¹⁰³, C.P.A. Roland ¹²⁷, J. Roloff ²⁹, A. Romaniouk ³⁷, E. Romano ^{73a,73b}, M. Romano ^{23b}, A.C. Romero Hernandez ¹⁶², N. Rompotis ⁹², L. Roos ¹²⁷, S. Rosati ^{75a}, B.J. Rosser ³⁹, E. Rossi ¹²⁶, E. Rossi ^{72a,72b}, L.P. Rossi ^{57b}, L. Rossini ⁵⁴, R. Rosten ¹¹⁹, M. Rotaru ^{27b}, B. Rottler ⁵⁴, C. Rougier ^{102,aa}, D. Rousseau ⁶⁶, D. Rousso ³², A. Roy ¹⁶², S. Roy-Garand ¹⁵⁵, A. Rozanov ¹⁰², Z.M.A. Rozario ⁵⁹, Y. Rozen ¹⁵⁰, X. Ruan ^{33g}, A. Rubio Jimenez ¹⁶³, A.J. Ruby ⁹², V.H. Ruelas Rivera ¹⁸, T.A. Ruggeri ¹, A. Ruggiero ¹²⁶, A. Ruiz-Martinez ¹⁶³, A. Rummeler ³⁶, Z. Rurikova ⁵⁴, N.A. Rusakovich ³⁸, H.L. Russell ¹⁶⁵, G. Russo ^{75a,75b}, J.P. Rutherford ⁷, S. Rutherford Colmenares ³², K. Rybacki⁹¹, M. Rybar ¹³³, E.B. Rye ¹²⁵, A. Ryzhov ⁴⁴, J.A. Sabater Iglesias ⁵⁶, P. Sabatini ¹⁶³, H.F-W. Sadrozinski ¹³⁶, F. Safai Tehrani ^{75a}, B. Safarzadeh Samani ¹³⁴, M. Safdari ¹⁴³, S. Saha ¹⁶⁵, M. Sahinsoy ¹¹⁰, A. Saibel ¹⁶³, M. Saimpert ¹³⁵, M. Saito ¹⁵³, T. Saito ¹⁵³, D. Salamani ³⁶, A. Salnikov ¹⁴³, J. Salt ¹⁶³, A. Salvador Salas ¹⁵¹, D. Salvatore ^{43b,43a}, F. Salvatore ¹⁴⁶, A. Salzburger ³⁶, D. Sammel ⁵⁴, D. Sampsonidis ^{152,e}, D. Sampsonidou ¹²³, J. Sánchez ¹⁶³, A. Sanchez Pineda ⁴, V. Sanchez Sebastian ¹⁶³, H. Sandaker ¹²⁵, C.O. Sander ⁴⁸, J.A. Sandesara ¹⁰³, M. Sandhoff ¹⁷¹, C. Sandoval ^{22b}, D.P.C. Sankey ¹³⁴, T. Sano ⁸⁸, A. Sansoni ⁵³, L. Santi ^{75a,75b}, C. Santoni ⁴⁰, H. Santos ^{130a,130b}, S.N. Santpur ^{17a}, A. Santra ¹⁶⁹, K.A. Saoucha ^{116b}, J.G. Saraiva ^{130a,130d}, J. Sardain ⁷, O. Sasaki ⁸⁴, K. Sato ¹⁵⁷, C. Sauer^{63b}, F. Sauerburger ⁵⁴, E. Sauvan ⁴, P. Savard ^{155,af}, R. Sawada ¹⁵³, C. Sawyer ¹³⁴, L. Sawyer ⁹⁷, I. Sayago Galvan¹⁶³, C. Sbarra ^{23b}, A. Sbrizzi ^{23b,23a}, T. Scanlon ⁹⁶, J. Schaarschmidt ¹³⁸, P. Schacht ¹¹⁰, U. Schäfer ¹⁰⁰, A.C. Schaffer ^{66,44}, D. Schaile ¹⁰⁹, R.D. Schamberger ¹⁴⁵, C. Scharf ¹⁸, M.M. Schefer ¹⁹,

V.A. Schegelsky [ID37](#), D. Scheirich [ID133](#), F. Schenck [ID18](#), M. Schernau [ID160](#), C. Scheulen [ID55](#), C. Schiavi [ID57b,57a](#), E.J. Schioppa [ID70a,70b](#), M. Schioppa [ID43b,43a](#), B. Schlag [ID143,n](#), K.E. Schleicher [ID54](#), S. Schlenker [ID36](#), J. Schmeing [ID171](#), M.A. Schmidt [ID171](#), K. Schmieden [ID100](#), C. Schmitt [ID100](#), N. Schmitt [ID100](#), S. Schmitt [ID48](#), L. Schoeffel [ID135](#), A. Schoening [ID63b](#), P.G. Scholer [ID54](#), E. Schopf [ID126](#), M. Schott [ID100](#), J. Schovancova [ID36](#), S. Schramm [ID56](#), F. Schroeder [ID171](#), T. Schroer [ID56](#), H-C. Schultz-Coulon [ID63a](#), M. Schumacher [ID54](#), B.A. Schumm [ID136](#), Ph. Schune [ID135](#), A.J. Schuy [ID138](#), H.R. Schwartz [ID136](#), A. Schwartzman [ID143](#), T.A. Schwarz [ID106](#), Ph. Schwemling [ID135](#), R. Schwienhorst [ID107](#), A. Sciandra [ID136](#), G. Sciolla [ID26](#), F. Scuri [ID74a](#), C.D. Sebastiani [ID92](#), K. Sedlaczek [ID115](#), P. Seema [ID18](#), S.C. Seidel [ID112](#), A. Seiden [ID136](#), B.D. Seidlitz [ID41](#), C. Seitz [ID48](#), J.M. Seixas [ID83b](#), G. Sekhniaidze [ID72a](#), S.J. Sekula [ID44](#), L. Selem [ID60](#), N. Semprini-Cesari [ID23b,23a](#), D. Sengupta [ID56](#), V. Senthilkumar [ID163](#), L. Serin [ID66](#), L. Serkin [ID69a,69b](#), M. Sessa [ID76a,76b](#), H. Severini [ID120](#), F. Sforza [ID57b,57a](#), A. Sfyrta [ID56](#), E. Shabalina [ID55](#), R. Shaheen [ID144](#), J.D. Shahinian [ID128](#), D. Shaked Renous [ID169](#), L.Y. Shan [ID14a](#), M. Shapiro [ID17a](#), A. Sharma [ID36](#), A.S. Sharma [ID164](#), P. Sharma [ID80](#), S. Sharma [ID48](#), P.B. Shatalov [ID37](#), K. Shaw [ID146](#), S.M. Shaw [ID101](#), A. Shcherbakova [ID37](#), Q. Shen [ID62c,5](#), D.J. Sheppard [ID142](#), P. Sherwood [ID96](#), L. Shi [ID96](#), X. Shi [ID14a](#), C.O. Shimmin [ID172](#), J.D. Shinner [ID95](#), I.P.J. Shipsey [ID126](#), S. Shirabe [ID56,h](#), M. Shiyakova [ID38,u](#), J. Shlomi [ID169](#), M.J. Shochet [ID39](#), J. Shojaii [ID105](#), D.R. Shope [ID125](#), B. Shrestha [ID120](#), S. Shrestha [ID119,aj](#), E.M. Shrif [ID33g](#), M.J. Shroff [ID165](#), P. Sicho [ID131](#), A.M. Sickles [ID162](#), E. Sideras Haddad [ID33g](#), A. Sidoti [ID23b](#), F. Siegert [ID50](#), Dj. Sijacki [ID15](#), F. Sili [ID90](#), J.M. Silva [ID20](#), M.V. Silva Oliveira [ID29](#), S.B. Silverstein [ID47a](#), S. Simion [ID66](#), R. Simoniello [ID36](#), E.L. Simpson [ID59](#), H. Simpson [ID146](#), L.R. Simpson [ID106](#), N.D. Simpson [ID98](#), S. Simsek [ID82](#), S. Sindhu [ID55](#), P. Sinervo [ID155](#), S. Singh [ID155](#), S. Sinha [ID48](#), S. Sinha [ID101](#), M. Sioli [ID23b,23a](#), I. Siral [ID36](#), E. Sitnikova [ID48](#), S.Yu. Sivoklov [ID37,*](#), J. Sjölin [ID47a,47b](#), A. Skaf [ID55](#), E. Skorda [ID20](#), P. Skubic [ID120](#), M. Slawinska [ID87](#), V. Smakhtin [ID169](#), B.H. Smart [ID134](#), J. Smiesko [ID36](#), S.Yu. Smirnov [ID37](#), Y. Smirnov [ID37](#), L.N. Smirnova [ID37,a](#), O. Smirnova [ID98](#), A.C. Smith [ID41](#), E.A. Smith [ID39](#), H.A. Smith [ID126](#), J.L. Smith [ID92](#), R. Smith [ID143](#), M. Smizanska [ID91](#), K. Smolek [ID132](#), A.A. Snesev [ID37](#), S.R. Snider [ID155](#), H.L. Snoek [ID114](#), S. Snyder [ID29](#), R. Sobie [ID165,w](#), A. Soffer [ID151](#), C.A. Solans Sanchez [ID36](#), E.Yu. Soldatov [ID37](#), U. Soldevila [ID163](#), A.A. Solodkov [ID37](#), S. Solomon [ID26](#), A. Soloshenko [ID38](#), K. Solovieva [ID54](#), O.V. Solovyanov [ID40](#), V. Solovyev [ID37](#), P. Sommer [ID36](#), A. Sonay [ID13](#), W.Y. Song [ID156b](#), J.M. Sonneveld [ID114](#), A. Sopczak [ID132](#), A.L. Soppio [ID96](#), F. Sopkova [ID28b](#), I.R. Sotarriva Alvarez [ID154](#), V. Sothilingam [ID63a](#), O.J. Soto Sandoval [ID137c,137b](#), S. Sottocornola [ID68](#), R. Soualah [ID116b](#), Z. Soumami [ID35e](#), D. South [ID48](#), N. Soybelman [ID169](#), S. Spagnolo [ID70a,70b](#), M. Spalla [ID110](#), D. Sperlich [ID54](#), G. Spigo [ID36](#), S. Spinali [ID91](#), D.P. Spiteri [ID59](#), M. Spousta [ID133](#), E.J. Staats [ID34](#), A. Stabile [ID71a,71b](#), R. Stamen [ID63a](#), A. Stampekis [ID20](#), M. Standke [ID24](#), E. Stanecka [ID87](#), M.V. Stange [ID50](#), B. Stanislaus [ID17a](#), M.M. Stanitzki [ID48](#), B. Stapf [ID48](#), E.A. Starchenko [ID37](#), G.H. Stark [ID136](#), J. Stark [ID102,aa](#), D.M. Starke [ID156b](#), P. Staroba [ID131](#), P. Starovoitov [ID63a](#), S. Stärz [ID104](#), R. Staszewski [ID87](#), G. Stavropoulos [ID46](#), J. Steentoft [ID161](#), P. Steinberg [ID29](#), B. Stelzer [ID142,156a](#), H.J. Stelzer [ID129](#), O. Stelzer-Chilton [ID156a](#), H. Stenzel [ID58](#), T.J. Stevenson [ID146](#), G.A. Stewart [ID36](#), J.R. Stewart [ID121](#), M.C. Stockton [ID36](#), G. Stoicea [ID27b](#), M. Stolarski [ID130a](#), S. Stonjek [ID110](#), A. Straessner [ID50](#), J. Strandberg [ID144](#), S. Strandberg [ID47a,47b](#), M. Stratmann [ID171](#), M. Strauss [ID120](#), T. Streblner [ID102](#), P. Strizenc [ID28b](#), R. Ströhmer [ID166](#), D.M. Strom [ID123](#), R. Stroynowski [ID44](#), A. Strubig [ID47a,47b](#), S.A. Stucci [ID29](#), B. Stugu [ID16](#), J. Stupak [ID120](#), N.A. Styles [ID48](#), D. Su [ID143](#), S. Su [ID62a](#), W. Su [ID62d](#), X. Su [ID62a,66](#), K. Sugizaki [ID153](#), V.V. Sulim [ID37](#), M.J. Sullivan [ID92](#), D.M.S. Sultan [ID78a,78b](#), L. Sultanaliev [ID37](#), S. Sultansoy [ID3b](#), T. Sumida [ID88](#), S. Sun [ID106](#), S. Sun [ID170](#), O. Sunneborn Gudnadottir [ID161](#), N. Sur [ID102](#), M.R. Sutton [ID146](#), H. Suzuki [ID157](#), M. Svatos [ID131](#), M. Swiatlowski [ID156a](#), T. Swirski [ID166](#), I. Sykora [ID28a](#), M. Sykora [ID133](#), T. Sykora [ID133](#), D. Ta [ID100](#), K. Tackmann [ID48,t](#), A. Taffard [ID160](#), R. Tafirout [ID156a](#), J.S. Tafoya Vargas [ID66](#), E.P. Takeva [ID52](#),

Y. Takubo ⁸⁴, M. Talby ¹⁰², A.A. Talyshev ³⁷, K.C. Tam ^{64b}, N.M. Tamir ¹⁵¹, A. Tanaka ¹⁵³,
 J. Tanaka ¹⁵³, R. Tanaka ⁶⁶, M. Tanasini ^{57b,57a}, Z. Tao ¹⁶⁴, S. Tapia Araya ^{137f},
 S. Tapprogge ¹⁰⁰, A. Tarek Abouelfadl Mohamed ¹⁰⁷, S. Tarem ¹⁵⁰, K. Tariq ^{14a}, G. Tarna ^{102,27b},
 G.F. Tartarelli ^{71a}, P. Tas ¹³³, M. Tasevsky ¹³¹, E. Tassi ^{43b,43a}, A.C. Tate ¹⁶², G. Tateno ¹⁵³,
 Y. Tayalati ^{35e,v}, G.N. Taylor ¹⁰⁵, W. Taylor ^{156b}, A.S. Tee ¹⁷⁰, R. Teixeira De Lima ¹⁴³,
 P. Teixeira-Dias ⁹⁵, J.J. Teoh ¹⁵⁵, K. Terashi ¹⁵³, J. Terron ⁹⁹, S. Terzo ¹³, M. Testa ⁵³,
 R.J. Teuscher ^{155,w}, A. Thaler ⁷⁹, O. Theiner ⁵⁶, N. Themistokleous ⁵², T. Theveneaux-Pelzer ¹⁰²,
 O. Thielmann ¹⁷¹, D.W. Thomas ⁹⁵, J.P. Thomas ²⁰, E.A. Thompson ^{17a}, P.D. Thompson ²⁰,
 E. Thomson ¹²⁸, Y. Tian ⁵⁵, V. Tikhomirov ^{37,a}, Yu.A. Tikhonov ³⁷, S. Timoshenko ³⁷,
 D. Timoshyn ¹³³, E.X.L. Ting ¹, P. Tipton ¹⁷², S.H. Tlou ^{33g}, A. Tnourji ⁴⁰, K. Todome ¹⁵⁴,
 S. Todorova-Nova ¹³³, S. Todt ⁵⁰, M. Togawa ⁸⁴, J. Tojo ⁸⁹, S. Tokár ^{28a}, K. Tokushuku ⁸⁴,
 O. Toldaiev ⁶⁸, R. Tombs ³², M. Tomoto ^{84,111}, L. Tompkins ^{143,n}, K.W. Topolnicki ^{86b},
 E. Torrence ¹²³, H. Torres ^{102,aa}, E. Torró Pastor ¹⁶³, M. Toscani ³⁰, C. Tosciri ³⁹, M. Tost ¹¹,
 D.R. Tovey ¹³⁹, A. Traeet ¹⁶, I.S. Trandafir ^{27b}, T. Trefzger ¹⁶⁶, A. Tricoli ²⁹, I.M. Trigger ^{156a},
 S. Trincaz-Duvoid ¹²⁷, D.A. Trischuk ²⁶, B. Trocmé ⁶⁰, C. Troncon ^{71a}, L. Truong ^{33c},
 M. Trzebinski ⁸⁷, A. Trzuppek ⁸⁷, F. Tsai ¹⁴⁵, M. Tsai ¹⁰⁶, A. Tsiamis ^{152,e}, P.V. Tsiareshka ³⁷,
 S. Tsigaridas ^{156a}, A. Tsigotis ^{152,r}, V. Tsiskaridze ¹⁵⁵, E.G. Tskhadadze ^{149a},
 M. Tsopoulou ^{152,e}, Y. Tsujikawa ⁸⁸, I.I. Tsukerman ³⁷, V. Tsulaia ^{17a}, S. Tsuno ⁸⁴, K. Tsuru ¹¹⁸,
 D. Tsybychev ¹⁴⁵, Y. Tu ^{64b}, A. Tudorache ^{27b}, V. Tudorache ^{27b}, A.N. Tuna ⁶¹,
 S. Turchikhin ^{57b,57a}, I. Turk Cakir ^{3a}, R. Turra ^{71a}, T. Turtuvshin ^{38,x}, P.M. Tuts ⁴¹,
 S. Tzamarias ^{152,e}, P. Tzanis ¹⁰, E. Tzovara ¹⁰⁰, F. Ukegawa ¹⁵⁷, P.A. Ulloa Poblete ^{137c,137b},
 E.N. Umaka ²⁹, G. Unal ³⁶, M. Unal ¹¹, A. Undrus ²⁹, G. Unel ¹⁶⁰, J. Urban ^{28b},
 P. Urquijo ¹⁰⁵, P. Urrejola ^{137a}, G. Usai ⁸, R. Ushioda ¹⁵⁴, M. Usman ¹⁰⁸, Z. Uysal ^{21b},
 V. Vacek ¹³², B. Vachon ¹⁰⁴, K.O.H. Vadla ¹²⁵, T. Vafeiadis ³⁶, A. Vaitkus ⁹⁶, C. Valderanis ¹⁰⁹,
 E. Valdes Santurio ^{47a,47b}, M. Valente ^{156a}, S. Valentinetti ^{23b,23a}, A. Valero ¹⁶³,
 E. Valiente Moreno ¹⁶³, A. Vallier ^{102,aa}, J.A. Valls Ferrer ¹⁶³, D.R. Van Arneman ¹¹⁴,
 T.R. Van Daalen ¹³⁸, A. Van Der Graaf ⁴⁹, P. Van Gemmeren ⁶, M. Van Rijnbach ^{125,36},
 S. Van Stroud ⁹⁶, I. Van Vulpen ¹¹⁴, M. Vanadia ^{76a,76b}, W. Vandelli ³⁶, M. Vandenbroucke ¹³⁵,
 E.R. Vandewall ¹²¹, D. Vannicola ¹⁵¹, L. Vannoli ^{57b,57a}, R. Vari ^{75a}, E.W. Varnes ⁷,
 C. Varni ^{17b}, T. Varol ¹⁴⁸, D. Varouchas ⁶⁶, L. Varriale ¹⁶³, K.E. Varvell ¹⁴⁷, M.E. Vasile ^{27b},
 L. Vaslin ⁸⁴, G.A. Vasquez ¹⁶⁵, A. Vasyukov ³⁸, F. Vazeille ⁴⁰, T. Vazquez Schroeder ³⁶,
 J. Veatch ³¹, V. Vecchio ¹⁰¹, M.J. Veen ¹⁰³, I. Veliscek ¹²⁶, L.M. Veloce ¹⁵⁵, F. Veloso ^{130a,130c},
 S. Veneziano ^{75a}, A. Ventura ^{70a,70b}, S. Ventura Gonzalez ¹³⁵, A. Verbytskyi ¹¹⁰,
 M. Verducci ^{74a,74b}, C. Vergis ²⁴, M. Verissimo De Araujo ^{83b}, W. Verkerke ¹¹⁴,
 J.C. Vermeulen ¹¹⁴, C. Vernieri ¹⁴³, M. Vessella ¹⁰³, M.C. Vetterli ^{142,af}, A. Vgenopoulos ^{152,e},
 N. Viaux Maira ^{137f}, T. Vickey ¹³⁹, O.E. Vickey Boeriu ¹³⁹, G.H.A. Viehhauser ¹²⁶, L. Vigani ^{63b},
 M. Villa ^{23b,23a}, M. Villaplana Perez ¹⁶³, E.M. Villhauer ⁵², E. Vilucchi ⁵³, M.G. Vinciter ³⁴,
 G.S. Virdee ²⁰, A. Vishwakarma ⁵², A. Visibile ¹¹⁴, C. Vittori ³⁶, I. Vivarelli ¹⁴⁶,
 E. Voevodina ¹¹⁰, F. Vogel ¹⁰⁹, J.C. Voigt ⁵⁰, P. Vokac ¹³², Yu. Volkotrub ^{86a}, J. Von Ahnen ⁴⁸,
 E. Von Toerne ²⁴, B. Vormwald ³⁶, V. Vorobel ¹³³, K. Vorobev ³⁷, M. Vos ¹⁶³, K. Voss ¹⁴¹,
 J.H. Vossebeld ⁹², M. Vozak ¹¹⁴, L. Vozdecky ⁹⁴, N. Vranjes ¹⁵, M. Vranjes Milosavljevic ¹⁵,
 M. Vreeswijk ¹¹⁴, R. Vuillermet ³⁶, O. Vujanovic ¹⁰⁰, I. Vukotic ³⁹, S. Wada ¹⁵⁷, C. Wagner ¹⁰³,
 J.M. Wagner ^{17a}, W. Wagner ¹⁷¹, S. Wahdan ¹⁷¹, H. Wahlberg ⁹⁰, M. Wakida ¹¹¹, J. Walder ¹³⁴,
 R. Walker ¹⁰⁹, W. Walkowiak ¹⁴¹, A. Wall ¹²⁸, T. Wamorkar ⁶, A.Z. Wang ¹³⁶, C. Wang ¹⁰⁰,
 C. Wang ^{62c}, H. Wang ^{17a}, J. Wang ^{64a}, R.-J. Wang ¹⁰⁰, R. Wang ⁶¹, R. Wang ⁶,
 S.M. Wang ¹⁴⁸, S. Wang ^{62b}, T. Wang ^{62a}, W.T. Wang ⁸⁰, W. Wang ^{14a}, X. Wang ^{14c},
 X. Wang ¹⁶², X. Wang ^{62c}, Y. Wang ^{62d}, Y. Wang ^{14c}, Z. Wang ¹⁰⁶, Z. Wang ^{62d,51,62c},

Z. Wang ¹⁰⁶, A. Warburton ¹⁰⁴, R.J. Ward ²⁰, N. Warrack ⁵⁹, A.T. Watson ²⁰, H. Watson ⁵⁹, M.F. Watson ²⁰, E. Watton ^{59,134}, G. Watts ¹³⁸, B.M. Waugh ⁹⁶, C. Weber ²⁹, H.A. Weber ¹⁸, M.S. Weber ¹⁹, S.M. Weber ^{63a}, C. Wei ^{62a}, Y. Wei ¹²⁶, A.R. Weidberg ¹²⁶, E.J. Weik ¹¹⁷, J. Weingarten ⁴⁹, M. Weirich ¹⁰⁰, C. Weiser ⁵⁴, C.J. Wells ⁴⁸, T. Wenaus ²⁹, B. Wendland ⁴⁹, T. Wengler ³⁶, N.S. Wenke ¹¹⁰, N. Wermes ²⁴, M. Wessels ^{63a}, A.M. Wharton ⁹¹, A.S. White ⁶¹, A. White ⁸, M.J. White ¹, D. Whiteson ¹⁶⁰, L. Wickremasinghe ¹²⁴, W. Wiedenmann ¹⁷⁰, C. Wiel ⁵⁰, M. Wielers ¹³⁴, C. Wiglesworth ⁴², D.J. Wilbern ¹²⁰, H.G. Wilkens ³⁶, D.M. Williams ⁴¹, H.H. Williams ¹²⁸, S. Williams ³², S. Willocq ¹⁰³, B.J. Wilson ¹⁰¹, P.J. Windischhofer ³⁹, F.I. Winkel ³⁰, F. Winklmeier ¹²³, B.T. Winter ⁵⁴, J.K. Winter ¹⁰¹, M. Wittgen ¹⁴³, M. Wobisch ⁹⁷, Z. Wolffs ¹¹⁴, J. Wollrath ¹⁶⁰, M.W. Wolter ⁸⁷, H. Wolters ^{130a,130c}, A.F. Wongel ⁴⁸, E.L. Woodward ⁴¹, S.D. Worm ⁴⁸, B.K. Wosiek ⁸⁷, K.W. Woźniak ⁸⁷, S. Wozniowski ⁵⁵, K. Wraight ⁵⁹, C. Wu ²⁰, J. Wu ^{14a,14e}, M. Wu ^{64a}, M. Wu ¹¹³, S.L. Wu ¹⁷⁰, X. Wu ⁵⁶, Y. Wu ^{62a}, Z. Wu ¹³⁵, J. Wuerzinger ^{110,ad}, T.R. Wyatt ¹⁰¹, B.M. Wynne ⁵², S. Xella ⁴², L. Xia ^{14c}, M. Xia ^{14b}, J. Xiang ^{64c}, M. Xie ^{62a}, X. Xie ^{62a}, S. Xin ^{14a,14e}, A. Xiong ¹²³, J. Xiong ^{17a}, D. Xu ^{14a}, H. Xu ^{62a}, L. Xu ^{62a}, R. Xu ¹²⁸, T. Xu ¹⁰⁶, Y. Xu ^{14b}, Z. Xu ⁵², Z. Xu ^{14c}, B. Yabsley ¹⁴⁷, S. Yacoob ^{33a}, Y. Yamaguchi ¹⁵⁴, E. Yamashita ¹⁵³, H. Yamauchi ¹⁵⁷, T. Yamazaki ^{17a}, Y. Yamazaki ⁸⁵, J. Yan ^{62c}, S. Yan ¹²⁶, Z. Yan ²⁵, H.J. Yang ^{62c,62d}, H.T. Yang ^{62a}, S. Yang ^{62a}, T. Yang ^{64c}, X. Yang ³⁶, X. Yang ^{14a}, Y. Yang ⁴⁴, Y. Yang ^{62a}, Z. Yang ^{62a}, W.-M. Yao ^{17a}, Y.C. Yap ⁴⁸, H. Ye ^{14c}, H. Ye ⁵⁵, J. Ye ^{14a}, S. Ye ²⁹, X. Ye ^{62a}, Y. Yeh ⁹⁶, I. Yeletsikh ³⁸, B.K. Yeo ^{17b}, M.R. Yexley ⁹⁶, P. Yin ⁴¹, K. Yorita ¹⁶⁸, S. Younas ^{27b}, C.J.S. Young ³⁶, C. Young ¹⁴³, C. Yu ^{14a,14e,ah}, Y. Yu ^{62a}, M. Yuan ¹⁰⁶, R. Yuan ^{62b}, L. Yue ⁹⁶, M. Zaazoua ^{62a}, B. Zabinski ⁸⁷, E. Zaid ⁵², Z.K. Zak ⁸⁷, T. Zakareishvili ^{149b}, N. Zakharchuk ³⁴, S. Zambito ⁵⁶, J.A. Zamora Saa ^{137d,137b}, J. Zang ¹⁵³, D. Zanzi ⁵⁴, O. Zaplatilek ¹³², C. Zeitnitz ¹⁷¹, H. Zeng ^{14a}, J.C. Zeng ¹⁶², D.T. Zenger Jr ²⁶, O. Zenin ³⁷, T. Ženiš ^{28a}, S. Zenz ⁹⁴, S. Zerradi ^{35a}, D. Zerwas ⁶⁶, M. Zhai ^{14a,14e}, B. Zhang ^{14c}, D.F. Zhang ¹³⁹, J. Zhang ^{62b}, J. Zhang ⁶, K. Zhang ^{14a,14e}, L. Zhang ^{14c}, P. Zhang ^{14a,14e}, R. Zhang ¹⁷⁰, S. Zhang ¹⁰⁶, S. Zhang ⁴⁴, T. Zhang ¹⁵³, X. Zhang ^{62c}, X. Zhang ^{62b}, Y. Zhang ^{62c,5}, Y. Zhang ⁹⁶, Y. Zhang ^{14c}, Z. Zhang ^{17a}, Z. Zhang ⁶⁶, H. Zhao ¹³⁸, T. Zhao ^{62b}, Y. Zhao ¹³⁶, Z. Zhao ^{62a}, A. Zhemchugov ³⁸, J. Zheng ^{14c}, K. Zheng ¹⁶², X. Zheng ^{62a}, Z. Zheng ¹⁴³, D. Zhong ¹⁶², B. Zhou ¹⁰⁶, H. Zhou ⁷, N. Zhou ^{62c}, Y. Zhou ⁷, C.G. Zhu ^{62b}, J. Zhu ¹⁰⁶, Y. Zhu ^{62c}, Y. Zhu ^{62a}, X. Zhuang ^{14a}, K. Zhukov ³⁷, V. Zhulanov ³⁷, N.I. Zimine ³⁸, J. Zinsser ^{63b}, M. Ziolkowski ¹⁴¹, L. Živković ¹⁵, A. Zoccoli ^{23b,23a}, K. Zoch ⁶¹, T.G. Zorbas ¹³⁹, O. Zormpa ⁴⁶, W. Zou ⁴¹, L. Zwalinski ³⁶.

¹Department of Physics, University of Adelaide, Adelaide; Australia.

²Department of Physics, University of Alberta, Edmonton AB; Canada.

^{3(a)}Department of Physics, Ankara University, Ankara; ^(b)Division of Physics, TOBB University of Economics and Technology, Ankara; Türkiye.

⁴LAPP, Université Savoie Mont Blanc, CNRS/IN2P3, Annecy; France.

⁵APC, Université Paris Cité, CNRS/IN2P3, Paris; France.

⁶High Energy Physics Division, Argonne National Laboratory, Argonne IL; United States of America.

⁷Department of Physics, University of Arizona, Tucson AZ; United States of America.

⁸Department of Physics, University of Texas at Arlington, Arlington TX; United States of America.

⁹Physics Department, National and Kapodistrian University of Athens, Athens; Greece.

¹⁰Physics Department, National Technical University of Athens, Zografou; Greece.

¹¹Department of Physics, University of Texas at Austin, Austin TX; United States of America.

¹²Institute of Physics, Azerbaijan Academy of Sciences, Baku; Azerbaijan.

- ¹³Institut de Física d'Altes Energies (IFAE), Barcelona Institute of Science and Technology, Barcelona; Spain.
- ¹⁴(^a)Institute of High Energy Physics, Chinese Academy of Sciences, Beijing; (^b)Physics Department, Tsinghua University, Beijing; (^c)Department of Physics, Nanjing University, Nanjing; (^d)School of Science, Shenzhen Campus of Sun Yat-sen University; (^e)University of Chinese Academy of Science (UCAS), Beijing; China.
- ¹⁵Institute of Physics, University of Belgrade, Belgrade; Serbia.
- ¹⁶Department for Physics and Technology, University of Bergen, Bergen; Norway.
- ¹⁷(^a)Physics Division, Lawrence Berkeley National Laboratory, Berkeley CA; (^b)University of California, Berkeley CA; United States of America.
- ¹⁸Institut für Physik, Humboldt Universität zu Berlin, Berlin; Germany.
- ¹⁹Albert Einstein Center for Fundamental Physics and Laboratory for High Energy Physics, University of Bern, Bern; Switzerland.
- ²⁰School of Physics and Astronomy, University of Birmingham, Birmingham; United Kingdom.
- ²¹(^a)Department of Physics, Bogazici University, Istanbul; (^b)Department of Physics Engineering, Gaziantep University, Gaziantep; (^c)Department of Physics, Istanbul University, Istanbul; Türkiye.
- ²²(^a)Facultad de Ciencias y Centro de Investigaciones, Universidad Antonio Nariño, Bogotá; (^b)Departamento de Física, Universidad Nacional de Colombia, Bogotá; Colombia.
- ²³(^a)Dipartimento di Fisica e Astronomia A. Righi, Università di Bologna, Bologna; (^b)INFN Sezione di Bologna; Italy.
- ²⁴Physikalisches Institut, Universität Bonn, Bonn; Germany.
- ²⁵Department of Physics, Boston University, Boston MA; United States of America.
- ²⁶Department of Physics, Brandeis University, Waltham MA; United States of America.
- ²⁷(^a)Transilvania University of Brasov, Brasov; (^b)Horia Hulubei National Institute of Physics and Nuclear Engineering, Bucharest; (^c)Department of Physics, Alexandru Ioan Cuza University of Iasi, Iasi; (^d)National Institute for Research and Development of Isotopic and Molecular Technologies, Physics Department, Cluj-Napoca; (^e)National University of Science and Technology Politehnica, Bucharest; (^f)West University in Timisoara, Timisoara; (^g)Faculty of Physics, University of Bucharest, Bucharest; Romania.
- ²⁸(^a)Faculty of Mathematics, Physics and Informatics, Comenius University, Bratislava; (^b)Department of Subnuclear Physics, Institute of Experimental Physics of the Slovak Academy of Sciences, Kosice; Slovak Republic.
- ²⁹Physics Department, Brookhaven National Laboratory, Upton NY; United States of America.
- ³⁰Universidad de Buenos Aires, Facultad de Ciencias Exactas y Naturales, Departamento de Física, y CONICET, Instituto de Física de Buenos Aires (IFIBA), Buenos Aires; Argentina.
- ³¹California State University, CA; United States of America.
- ³²Cavendish Laboratory, University of Cambridge, Cambridge; United Kingdom.
- ³³(^a)Department of Physics, University of Cape Town, Cape Town; (^b)iThemba Labs, Western Cape; (^c)Department of Mechanical Engineering Science, University of Johannesburg, Johannesburg; (^d)National Institute of Physics, University of the Philippines Diliman (Philippines); (^e)University of South Africa, Department of Physics, Pretoria; (^f)University of Zululand, KwaDlangezwa; (^g)School of Physics, University of the Witwatersrand, Johannesburg; South Africa.
- ³⁴Department of Physics, Carleton University, Ottawa ON; Canada.
- ³⁵(^a)Faculté des Sciences Ain Chock, Réseau Universitaire de Physique des Hautes Energies - Université Hassan II, Casablanca; (^b)Faculté des Sciences, Université Ibn-Tofail, Kénitra; (^c)Faculté des Sciences Semlalia, Université Cadi Ayyad, LPHEA-Marrakech; (^d)LPMR, Faculté des Sciences, Université Mohamed Premier, Oujda; (^e)Faculté des sciences, Université Mohammed V, Rabat; (^f)Institute of Applied Physics, Mohammed VI Polytechnic University, Ben Guerir; Morocco.

- ³⁶CERN, Geneva; Switzerland.
- ³⁷Affiliated with an institute covered by a cooperation agreement with CERN.
- ³⁸Affiliated with an international laboratory covered by a cooperation agreement with CERN.
- ³⁹Enrico Fermi Institute, University of Chicago, Chicago IL; United States of America.
- ⁴⁰LPC, Université Clermont Auvergne, CNRS/IN2P3, Clermont-Ferrand; France.
- ⁴¹Nevis Laboratory, Columbia University, Irvington NY; United States of America.
- ⁴²Niels Bohr Institute, University of Copenhagen, Copenhagen; Denmark.
- ⁴³(^a)Dipartimento di Fisica, Università della Calabria, Rende;(^b)INFN Gruppo Collegato di Cosenza, Laboratori Nazionali di Frascati; Italy.
- ⁴⁴Physics Department, Southern Methodist University, Dallas TX; United States of America.
- ⁴⁵Physics Department, University of Texas at Dallas, Richardson TX; United States of America.
- ⁴⁶National Centre for Scientific Research "Demokritos", Agia Paraskevi; Greece.
- ⁴⁷(^a)Department of Physics, Stockholm University;(^b)Oskar Klein Centre, Stockholm; Sweden.
- ⁴⁸Deutsches Elektronen-Synchrotron DESY, Hamburg and Zeuthen; Germany.
- ⁴⁹Fakultät Physik , Technische Universität Dortmund, Dortmund; Germany.
- ⁵⁰Institut für Kern- und Teilchenphysik, Technische Universität Dresden, Dresden; Germany.
- ⁵¹Department of Physics, Duke University, Durham NC; United States of America.
- ⁵²SUPA - School of Physics and Astronomy, University of Edinburgh, Edinburgh; United Kingdom.
- ⁵³INFN e Laboratori Nazionali di Frascati, Frascati; Italy.
- ⁵⁴Physikalisches Institut, Albert-Ludwigs-Universität Freiburg, Freiburg; Germany.
- ⁵⁵II. Physikalisches Institut, Georg-August-Universität Göttingen, Göttingen; Germany.
- ⁵⁶Département de Physique Nucléaire et Corpusculaire, Université de Genève, Genève; Switzerland.
- ⁵⁷(^a)Dipartimento di Fisica, Università di Genova, Genova;(^b)INFN Sezione di Genova; Italy.
- ⁵⁸II. Physikalisches Institut, Justus-Liebig-Universität Giessen, Giessen; Germany.
- ⁵⁹SUPA - School of Physics and Astronomy, University of Glasgow, Glasgow; United Kingdom.
- ⁶⁰LPSC, Université Grenoble Alpes, CNRS/IN2P3, Grenoble INP, Grenoble; France.
- ⁶¹Laboratory for Particle Physics and Cosmology, Harvard University, Cambridge MA; United States of America.
- ⁶²(^a)Department of Modern Physics and State Key Laboratory of Particle Detection and Electronics, University of Science and Technology of China, Hefei;(^b)Institute of Frontier and Interdisciplinary Science and Key Laboratory of Particle Physics and Particle Irradiation (MOE), Shandong University, Qingdao;(^c)School of Physics and Astronomy, Shanghai Jiao Tong University, Key Laboratory for Particle Astrophysics and Cosmology (MOE), SKLPPC, Shanghai;(^d)Tsung-Dao Lee Institute, Shanghai;(^e)School of Physics and Microelectronics, Zhengzhou University; China.
- ⁶³(^a)Kirchhoff-Institut für Physik, Ruprecht-Karls-Universität Heidelberg, Heidelberg;(^b)Physikalisches Institut, Ruprecht-Karls-Universität Heidelberg, Heidelberg; Germany.
- ⁶⁴(^a)Department of Physics, Chinese University of Hong Kong, Shatin, N.T., Hong Kong;(^b)Department of Physics, University of Hong Kong, Hong Kong;(^c)Department of Physics and Institute for Advanced Study, Hong Kong University of Science and Technology, Clear Water Bay, Kowloon, Hong Kong; China.
- ⁶⁵Department of Physics, National Tsing Hua University, Hsinchu; Taiwan.
- ⁶⁶IJCLab, Université Paris-Saclay, CNRS/IN2P3, 91405, Orsay; France.
- ⁶⁷Centro Nacional de Microelectrónica (IMB-CNM-CSIC), Barcelona; Spain.
- ⁶⁸Department of Physics, Indiana University, Bloomington IN; United States of America.
- ⁶⁹(^a)INFN Gruppo Collegato di Udine, Sezione di Trieste, Udine;(^b)ICTP, Trieste;(^c)Dipartimento Politecnico di Ingegneria e Architettura, Università di Udine, Udine; Italy.
- ⁷⁰(^a)INFN Sezione di Lecce;(^b)Dipartimento di Matematica e Fisica, Università del Salento, Lecce; Italy.
- ⁷¹(^a)INFN Sezione di Milano;(^b)Dipartimento di Fisica, Università di Milano, Milano; Italy.

- 72^(a) INFN Sezione di Napoli; ^(b) Dipartimento di Fisica, Università di Napoli, Napoli; Italy.
- 73^(a) INFN Sezione di Pavia; ^(b) Dipartimento di Fisica, Università di Pavia, Pavia; Italy.
- 74^(a) INFN Sezione di Pisa; ^(b) Dipartimento di Fisica E. Fermi, Università di Pisa, Pisa; Italy.
- 75^(a) INFN Sezione di Roma; ^(b) Dipartimento di Fisica, Sapienza Università di Roma, Roma; Italy.
- 76^(a) INFN Sezione di Roma Tor Vergata; ^(b) Dipartimento di Fisica, Università di Roma Tor Vergata, Roma; Italy.
- 77^(a) INFN Sezione di Roma Tre; ^(b) Dipartimento di Matematica e Fisica, Università Roma Tre, Roma; Italy.
- 78^(a) INFN-TIFPA; ^(b) Università degli Studi di Trento, Trento; Italy.
- 79 Universität Innsbruck, Department of Astro and Particle Physics, Innsbruck; Austria.
- 80 University of Iowa, Iowa City IA; United States of America.
- 81 Department of Physics and Astronomy, Iowa State University, Ames IA; United States of America.
- 82 İstinye University, Sarıyer, Istanbul; Türkiye.
- 83^(a) Departamento de Engenharia Elétrica, Universidade Federal de Juiz de Fora (UFJF), Juiz de Fora; ^(b) Universidade Federal do Rio De Janeiro COPPE/EE/IF, Rio de Janeiro; ^(c) Instituto de Física, Universidade de São Paulo, São Paulo; ^(d) Rio de Janeiro State University, Rio de Janeiro; Brazil.
- 84 KEK, High Energy Accelerator Research Organization, Tsukuba; Japan.
- 85 Graduate School of Science, Kobe University, Kobe; Japan.
- 86^(a) AGH University of Krakow, Faculty of Physics and Applied Computer Science, Krakow; ^(b) Marian Smoluchowski Institute of Physics, Jagiellonian University, Krakow; Poland.
- 87 Institute of Nuclear Physics Polish Academy of Sciences, Krakow; Poland.
- 88 Faculty of Science, Kyoto University, Kyoto; Japan.
- 89 Research Center for Advanced Particle Physics and Department of Physics, Kyushu University, Fukuoka ; Japan.
- 90 Instituto de Física La Plata, Universidad Nacional de La Plata and CONICET, La Plata; Argentina.
- 91 Physics Department, Lancaster University, Lancaster; United Kingdom.
- 92 Oliver Lodge Laboratory, University of Liverpool, Liverpool; United Kingdom.
- 93 Department of Experimental Particle Physics, Jožef Stefan Institute and Department of Physics, University of Ljubljana, Ljubljana; Slovenia.
- 94 School of Physics and Astronomy, Queen Mary University of London, London; United Kingdom.
- 95 Department of Physics, Royal Holloway University of London, Egham; United Kingdom.
- 96 Department of Physics and Astronomy, University College London, London; United Kingdom.
- 97 Louisiana Tech University, Ruston LA; United States of America.
- 98 Fysiska institutionen, Lunds universitet, Lund; Sweden.
- 99 Departamento de Física Teórica C-15 and CIAFF, Universidad Autónoma de Madrid, Madrid; Spain.
- 100 Institut für Physik, Universität Mainz, Mainz; Germany.
- 101 School of Physics and Astronomy, University of Manchester, Manchester; United Kingdom.
- 102 CPPM, Aix-Marseille Université, CNRS/IN2P3, Marseille; France.
- 103 Department of Physics, University of Massachusetts, Amherst MA; United States of America.
- 104 Department of Physics, McGill University, Montreal QC; Canada.
- 105 School of Physics, University of Melbourne, Victoria; Australia.
- 106 Department of Physics, University of Michigan, Ann Arbor MI; United States of America.
- 107 Department of Physics and Astronomy, Michigan State University, East Lansing MI; United States of America.
- 108 Group of Particle Physics, University of Montreal, Montreal QC; Canada.
- 109 Fakultät für Physik, Ludwig-Maximilians-Universität München, München; Germany.
- 110 Max-Planck-Institut für Physik (Werner-Heisenberg-Institut), München; Germany.

- ¹¹¹Graduate School of Science and Kobayashi-Maskawa Institute, Nagoya University, Nagoya; Japan.
- ¹¹²Department of Physics and Astronomy, University of New Mexico, Albuquerque NM; United States of America.
- ¹¹³Institute for Mathematics, Astrophysics and Particle Physics, Radboud University/Nikhef, Nijmegen; Netherlands.
- ¹¹⁴Nikhef National Institute for Subatomic Physics and University of Amsterdam, Amsterdam; Netherlands.
- ¹¹⁵Department of Physics, Northern Illinois University, DeKalb IL; United States of America.
- ¹¹⁶^(a)New York University Abu Dhabi, Abu Dhabi;^(b)University of Sharjah, Sharjah; United Arab Emirates.
- ¹¹⁷Department of Physics, New York University, New York NY; United States of America.
- ¹¹⁸Ochanomizu University, Otsuka, Bunkyo-ku, Tokyo; Japan.
- ¹¹⁹Ohio State University, Columbus OH; United States of America.
- ¹²⁰Homer L. Dodge Department of Physics and Astronomy, University of Oklahoma, Norman OK; United States of America.
- ¹²¹Department of Physics, Oklahoma State University, Stillwater OK; United States of America.
- ¹²²Palacký University, Joint Laboratory of Optics, Olomouc; Czech Republic.
- ¹²³Institute for Fundamental Science, University of Oregon, Eugene, OR; United States of America.
- ¹²⁴Graduate School of Science, Osaka University, Osaka; Japan.
- ¹²⁵Department of Physics, University of Oslo, Oslo; Norway.
- ¹²⁶Department of Physics, Oxford University, Oxford; United Kingdom.
- ¹²⁷LPNHE, Sorbonne Université, Université Paris Cité, CNRS/IN2P3, Paris; France.
- ¹²⁸Department of Physics, University of Pennsylvania, Philadelphia PA; United States of America.
- ¹²⁹Department of Physics and Astronomy, University of Pittsburgh, Pittsburgh PA; United States of America.
- ¹³⁰^(a)Laboratório de Instrumentação e Física Experimental de Partículas - LIP, Lisboa;^(b)Departamento de Física, Faculdade de Ciências, Universidade de Lisboa, Lisboa;^(c)Departamento de Física, Universidade de Coimbra, Coimbra;^(d)Centro de Física Nuclear da Universidade de Lisboa, Lisboa;^(e)Departamento de Física, Universidade do Minho, Braga;^(f)Departamento de Física Teórica y del Cosmos, Universidad de Granada, Granada (Spain);^(g)Departamento de Física, Instituto Superior Técnico, Universidade de Lisboa, Lisboa; Portugal.
- ¹³¹Institute of Physics of the Czech Academy of Sciences, Prague; Czech Republic.
- ¹³²Czech Technical University in Prague, Prague; Czech Republic.
- ¹³³Charles University, Faculty of Mathematics and Physics, Prague; Czech Republic.
- ¹³⁴Particle Physics Department, Rutherford Appleton Laboratory, Didcot; United Kingdom.
- ¹³⁵IRFU, CEA, Université Paris-Saclay, Gif-sur-Yvette; France.
- ¹³⁶Santa Cruz Institute for Particle Physics, University of California Santa Cruz, Santa Cruz CA; United States of America.
- ¹³⁷^(a)Departamento de Física, Pontificia Universidad Católica de Chile, Santiago;^(b)Millennium Institute for Subatomic physics at high energy frontier (SAPHIR), Santiago;^(c)Instituto de Investigación Multidisciplinario en Ciencia y Tecnología, y Departamento de Física, Universidad de La Serena;^(d)Universidad Andres Bello, Department of Physics, Santiago;^(e)Instituto de Alta Investigación, Universidad de Tarapacá, Arica;^(f)Departamento de Física, Universidad Técnica Federico Santa María, Valparaíso; Chile.
- ¹³⁸Department of Physics, University of Washington, Seattle WA; United States of America.
- ¹³⁹Department of Physics and Astronomy, University of Sheffield, Sheffield; United Kingdom.
- ¹⁴⁰Department of Physics, Shinshu University, Nagano; Japan.

- ¹⁴¹Department Physik, Universität Siegen, Siegen; Germany.
- ¹⁴²Department of Physics, Simon Fraser University, Burnaby BC; Canada.
- ¹⁴³SLAC National Accelerator Laboratory, Stanford CA; United States of America.
- ¹⁴⁴Department of Physics, Royal Institute of Technology, Stockholm; Sweden.
- ¹⁴⁵Departments of Physics and Astronomy, Stony Brook University, Stony Brook NY; United States of America.
- ¹⁴⁶Department of Physics and Astronomy, University of Sussex, Brighton; United Kingdom.
- ¹⁴⁷School of Physics, University of Sydney, Sydney; Australia.
- ¹⁴⁸Institute of Physics, Academia Sinica, Taipei; Taiwan.
- ¹⁴⁹^(a)E. Andronikashvili Institute of Physics, Iv. Javakhishvili Tbilisi State University, Tbilisi;^(b)High Energy Physics Institute, Tbilisi State University, Tbilisi;^(c)University of Georgia, Tbilisi; Georgia.
- ¹⁵⁰Department of Physics, Technion, Israel Institute of Technology, Haifa; Israel.
- ¹⁵¹Raymond and Beverly Sackler School of Physics and Astronomy, Tel Aviv University, Tel Aviv; Israel.
- ¹⁵²Department of Physics, Aristotle University of Thessaloniki, Thessaloniki; Greece.
- ¹⁵³International Center for Elementary Particle Physics and Department of Physics, University of Tokyo, Tokyo; Japan.
- ¹⁵⁴Department of Physics, Tokyo Institute of Technology, Tokyo; Japan.
- ¹⁵⁵Department of Physics, University of Toronto, Toronto ON; Canada.
- ¹⁵⁶^(a)TRIUMF, Vancouver BC;^(b)Department of Physics and Astronomy, York University, Toronto ON; Canada.
- ¹⁵⁷Division of Physics and Tomonaga Center for the History of the Universe, Faculty of Pure and Applied Sciences, University of Tsukuba, Tsukuba; Japan.
- ¹⁵⁸Department of Physics and Astronomy, Tufts University, Medford MA; United States of America.
- ¹⁵⁹United Arab Emirates University, Al Ain; United Arab Emirates.
- ¹⁶⁰Department of Physics and Astronomy, University of California Irvine, Irvine CA; United States of America.
- ¹⁶¹Department of Physics and Astronomy, University of Uppsala, Uppsala; Sweden.
- ¹⁶²Department of Physics, University of Illinois, Urbana IL; United States of America.
- ¹⁶³Instituto de Física Corpuscular (IFIC), Centro Mixto Universidad de Valencia - CSIC, Valencia; Spain.
- ¹⁶⁴Department of Physics, University of British Columbia, Vancouver BC; Canada.
- ¹⁶⁵Department of Physics and Astronomy, University of Victoria, Victoria BC; Canada.
- ¹⁶⁶Fakultät für Physik und Astronomie, Julius-Maximilians-Universität Würzburg, Würzburg; Germany.
- ¹⁶⁷Department of Physics, University of Warwick, Coventry; United Kingdom.
- ¹⁶⁸Waseda University, Tokyo; Japan.
- ¹⁶⁹Department of Particle Physics and Astrophysics, Weizmann Institute of Science, Rehovot; Israel.
- ¹⁷⁰Department of Physics, University of Wisconsin, Madison WI; United States of America.
- ¹⁷¹Fakultät für Mathematik und Naturwissenschaften, Fachgruppe Physik, Bergische Universität Wuppertal, Wuppertal; Germany.
- ¹⁷²Department of Physics, Yale University, New Haven CT; United States of America.
- ^a Also Affiliated with an institute covered by a cooperation agreement with CERN.
- ^b Also at An-Najah National University, Nablus; Palestine.
- ^c Also at Borough of Manhattan Community College, City University of New York, New York NY; United States of America.
- ^d Also at Center for High Energy Physics, Peking University; China.
- ^e Also at Center for Interdisciplinary Research and Innovation (CIRI-AUTH), Thessaloniki; Greece.
- ^f Also at Centro Studi e Ricerche Enrico Fermi; Italy.
- ^g Also at CERN, Geneva; Switzerland.

^h Also at Département de Physique Nucléaire et Corpusculaire, Université de Genève, Genève; Switzerland.

ⁱ Also at Departament de Física de la Universitat Autònoma de Barcelona, Barcelona; Spain.

^j Also at Department of Financial and Management Engineering, University of the Aegean, Chios; Greece.

^k Also at Department of Physics, Ben Gurion University of the Negev, Beer Sheva; Israel.

^l Also at Department of Physics, California State University, Sacramento; United States of America.

^m Also at Department of Physics, King's College London, London; United Kingdom.

ⁿ Also at Department of Physics, Stanford University, Stanford CA; United States of America.

^o Also at Department of Physics, University of Fribourg, Fribourg; Switzerland.

^p Also at Department of Physics, University of Thessaly; Greece.

^q Also at Department of Physics, Westmont College, Santa Barbara; United States of America.

^r Also at Hellenic Open University, Patras; Greece.

^s Also at Institutio Catalana de Recerca i Estudis Avancats, ICREA, Barcelona; Spain.

^t Also at Institut für Experimentalphysik, Universität Hamburg, Hamburg; Germany.

^u Also at Institute for Nuclear Research and Nuclear Energy (INRNE) of the Bulgarian Academy of Sciences, Sofia; Bulgaria.

^v Also at Institute of Applied Physics, Mohammed VI Polytechnic University, Ben Guerir; Morocco.

^w Also at Institute of Particle Physics (IPP); Canada.

^x Also at Institute of Physics and Technology, Mongolian Academy of Sciences, Ulaanbaatar; Mongolia.

^y Also at Institute of Physics, Azerbaijan Academy of Sciences, Baku; Azerbaijan.

^z Also at Institute of Theoretical Physics, Ilia State University, Tbilisi; Georgia.

^{aa} Also at L2IT, Université de Toulouse, CNRS/IN2P3, UPS, Toulouse; France.

^{ab} Also at Lawrence Livermore National Laboratory, Livermore; United States of America.

^{ac} Also at National Institute of Physics, University of the Philippines Diliman (Philippines); Philippines.

^{ad} Also at Technical University of Munich, Munich; Germany.

^{ae} Also at The Collaborative Innovation Center of Quantum Matter (CICQM), Beijing; China.

^{af} Also at TRIUMF, Vancouver BC; Canada.

^{ag} Also at Università di Napoli Parthenope, Napoli; Italy.

^{ah} Also at University of Chinese Academy of Sciences (UCAS), Beijing; China.

^{ai} Also at University of Colorado Boulder, Department of Physics, Colorado; United States of America.

^{aj} Also at Washington College, Chestertown, MD; United States of America.

^{ak} Also at Yeditepe University, Physics Department, Istanbul; Türkiye.

* Deceased